DIPLOMARBEIT

Advanced Numerical Methods for Fluid Structure Interaction

Ausgeführt am Institut für

Analysis und Scientific Computing

der Technischen Universität Wien

unter der Anleitung von

Univ.Prof. Dipl.-Ing. Dr.techn. Joachim SCHÖBERL

durch

Michael NEUNTEUFEL BSc

Dr.-Schober-Straße 85, 1130 Wien

September 3, 2017

Abstract

This thesis deals with the coupling of fluid dynamics with elastic solid structure, namely the Navier-Stokes equations and the nonlinear elastic wave equation, which is due to the different types of these PDEs a challenging problem.
Two different discretizations for the Navier-Stokes equations are discussed: the popular Taylor-Hood elements and the H(div)-conforming Hybrid Discontinuous Galerkin method, which ensures exact divergence-freeness.
For the elastic wave equation a standard Newmark method is used and a new H(curl)-conforming method is introduced. Therefore, an additional variable is needed: the time derivative of the momentum, which is in the dual space of H(curl).
The Arbitrary Lagrangian Eulerian description is well understood for H1-conforming methods, where the mesh velocity appears in the Navier-Stokes equations. For H(div)-conforming schemes, however, the ALE method is more involved and an additional term appears, which plays a crucial role.
The methods are implemented in NGS-Py, which is based on the finite element library Netgen/NGSolve and tested with proper examples.

Acknowledgements

First of all, I want to use this opportunity to thank Prof. Dr. Joachim Schöberl for supervising and supporting this thesis. Many time-intense discussions during the last year enhanced my knowledge of this topic and led me finding solutions for arising problems.

I also want to thank Georg Hofstätter for his comments and proof-reading this work, which led to an improvement of this thesis.

Furthermore, I want to thank my family for supporting me during my studies.

Contents

1 Introduction

Fluid-structure interaction (FSI) describes the interaction between an elastic, deformable, solid structure and a fluid which flows internally or surrounding the elastic body. The coupling of these completely different materials is of great interest in research and real-life, because it can be observed often in nature and also in technology. Examples in nature are the flow in blood vessels or surrounding the heart valves, while in technology FSI has to be taken into account in aerodynamics, e.g. when constructing wings. One of the most infamous example, where the effects of fluid-structure interaction were not considered enough, is the Tacoma Narrows Bridge.

The problems arising from fluid-structure interaction are often very complex and cannot be solved analytically. Thus, numerical simulations are important in this field. For solving such problems two completely different kinds of partial differential equations (PDEs) have to be coupled. On the one side solid structures are described by the nonlinear elastic wave equation and on the other side fluids by the Navier-Stokes equations.

It is common to use the Lagrangian (material) description for elasticity problems, while in fluid dynamics the Eulerian (spatial) description is used more often. This will lead to the so-called Arbitrary Lagrangian Eulerian description (ALE), where additional nonlinear terms appear. At a mathematical point of view the unsteady Navier-Stokes equation is of parabolic type, while the equation for describing elastic waves is of hyperbolic type.

One important thing both equations have in common is their nonlinearity, which makes each one alone already interesting and not easy to handle. Thus, before combining them, we have to understand both independently and study how to discretize them correctly to obtain an accurate, stable and efficient method.

Outline of this thesis

The first chapter gives a short introduction in the Eulerian and Lagrangian form of describing the change of position of particles at a domain and brings out the differences and how these can be transformed into each other. In the following two sections the Navier-Stokes equations and the elastic wave equation are going to be derived. After that we discretize the Navier-Stokes equations in space and time where two different types of spatial discretization are considered, one guaranteeing only discrete divergence freeness, while the other ensures exact divergence freeness. In section 4 the discretization of the elastic wave equation is treated. There, two completely different approaches for the time discretization are introduced which affect the spatial discretization. Then, we generalize section 2 by introducing the ALE method as preliminary work for coupling the Navier-Stokes with the elastic wave equation. In section 8 a monolithic approach for solving FSI problems with two different discretizations is given and in section 9 numerical examples are discussed.

Implementations

For all numerical examples the open source software packages Netgen[1] and NGSolve[2], see [Sch97] and [Sch14], are used.

Notation

u	velocity
p	pressure/time derivative of the momentum
ρ	density
σ^f	fluid stress tensor
Φ	deformation
d	displacement
F	deformation gradient
J	determinant of the deformation gradient ($J = \det(F)$)
C	Cauchy-Green strain tensor
E	Green strain tensor
v, w, q	test functions
σ^s	1st Piola-Kirchhoff stress tensor
Σ	2nd Piola-Kirchhoff stress tensor
$\mathbb{M}(n)$	set of all $n \times n$ matrices
$\mathbb{M}_+(n)$	set of all $n \times n$ matrices with positive determinant
$\mathrm{GL}(n)$	set of all invertible $n \times n$ matrices
$\mathbb{O}(n)$	set of all orthogonal $n \times n$ matrices
$SO(n)$	set of all special orthogonal $n \times n$ matrices ($SO(n) = \mathbb{O}_+(n)$)
$\mathbb{S}(n)$	set of all symmetric $n \times n$ matrices
S^2	unit sphere in $\mathbb{R}^3$
I	identity matrix
$P[\sigma]$	Piola transformation of σ
$\mathcal{T}_h$	Triangulation of a domain
$\Pi^k(\mathcal{T}_h)$	Space of all polynomials on $\mathcal{T}_h$ up to degree k
$\mathrm{tr}(\cdot)$	trace of a matrix A: $\mathrm{tr}(A) := \sum_{i=0}^{n} A_{ii}$
$\mathrm{sym}(\cdot)$	symmetric part of a matrix A, $\mathrm{sym}(A) := \frac{1}{2}\left(A + A^T\right)$
$\mathrm{skew}(\cdot)$	skew symmetric part of a matrix A, $\mathrm{skew}(A) := \frac{1}{2}\left(A - A^T\right)$
$\mathrm{rot}(\cdot)$	rotation of a vector v in $\mathbb{R}^2$, $\mathrm{rot}(v) := \begin{pmatrix} v_2 \\ -v_1 \end{pmatrix}$
$A(d)u$	an operator nonlinear in d and linear in u

[1] https://sourceforge.net/projects/netgen-mesher/
[2] https://sourceforge.net/projects/ngsolve/

2 Eulerian and Lagrangian description

This section gives a brief introduction into two different types of describing the change of position of particles. In section 7 we generalize these approaches by the ALE description and is therefore a motivation. The results are already used in the next section.

Let $\Omega \subset \mathbb{R}^n$ be a (bounded) domain, which means that it is open and connected. The parameter for describing the movement of the particles is going to be identified with the time t and an arbitrary choice of $t = 0$ defines an initial state.

We start by fixing an arbitrary particle, which has the coordinate $X \in \mathbb{R}^n$ at time $t = 0$ and at $t > 0$ another position x. Let ϕ be the function describing the evolution of the particle:

$$\begin{aligned} &\phi : \Omega \times [0, T] \to \Omega \\ &(X, t) \mapsto \phi(X, t) = x. \end{aligned} \tag{2.1}$$

We assume that for a fixed t the function $\phi(\cdot, t)$ is invertible, which means in physical sense that only one particle is allowed to be at one position

$$X = \phi^{-1}(x, t). \tag{2.2}$$

The Lagrangian formulation uses the material coordinates X, where a particle is fixed and we follow its trajectory. The Eulerian description, however, uses the spatial x coordinates, so we sit at a fixed point at the domain and look at the particles moving through it.

For both types of description PDEs can be formulated. It is important to mention that each form can be transformed into the other one, which will be discussed below.

An arbitrary quantity b can be defined using material or spatial coordinates

$$\hat{b}(X, t) \qquad b(x, t), \tag{2.3}$$

where $\hat{\cdot}$ is often neglected. Under the assumption that ϕ is "smooth enough" we define the material (time) derivative for b as

$$\frac{Db}{Dt} := \frac{\partial b}{\partial t}(\phi(X, t), t) = \frac{\partial \hat{b}}{\partial t}(X, t)\big|_{X=\text{const}}, \tag{2.4}$$

which describes the change of the quantity with respect to time following the particles. The spatial time derivative

$$\frac{\partial b}{\partial t} := \frac{\partial b}{\partial t}(x, t)\big|_{x=\text{const}}, \tag{2.5}$$

gives the change of the quantity at a fixed position x. As an important example we look at the velocity of a particle named X, which is defined as

$$u(X, t) := \frac{\partial \phi}{\partial t}(X, t) = \frac{\partial x}{\partial t}\big|_{X=\text{const}}, \tag{2.6}$$

and the velocity at a point x denoted by

$$u = u(x,t). \tag{2.7}$$

To compute the acceleration a in Eulerian description we use the relation $u(X,t) = u \circ (\phi \times \mathrm{id})$ and the chain rule

$$\frac{Du}{Dt} = a(x,t) = \frac{d}{dt}(u(x,t)) = \nabla u \underbrace{\frac{\partial \phi}{\partial t}}_{=u} + \frac{\partial u}{\partial t} = \frac{\partial u}{\partial t} + (u \cdot \nabla)u, \tag{2.8}$$

where the components of the vector $(u \cdot \nabla)u$ are given by $\sum_i u_i \frac{\partial u_j}{\partial x_i}$.

More general, the following relation holds between the material and spatial time derivative:

$$\frac{Db}{Dt} = \frac{\partial b}{\partial t} + (u \cdot \nabla)b. \tag{2.9}$$

3 Derivation of the Navier-Stokes equations

This section treats the derivation of the unsteady, incompressible, Newtonian Navier-Stokes equations, which describe the flow of an incompressible fluid e.g. water or gas.

As mentioned before, the Eulerian description suits better for fluids than the Lagrangian formulation, as we consider a fixed and bounded reference domain $\Omega \subset \mathbb{R}^3$ where the fluid flows through. At $\partial\Omega = \Gamma_D \dot{\cup} \Gamma_N$ we consider Dirichlet data on Γ_D, where the velocity u_D is prescribed and Neumann data on Γ_N, which defines the stresses on the fluid.

One possible way to derive the Navier-Stokes equations is by starting at the Boltzmann equation, the most general transport equation (see Chapman-Enskog Expansion). In this thesis, however, we use physical conservation laws, e.g. the conservation of mass and momentum to model the equations and go ahead similarly like in [Bra16]. A good introduction can also be found in [CM13].

We start by introducing some physical quantities used later on. Note that the velocity and volume forces are vector fields, whereas the density and pressure are scalar fields. The SI-Units used here are length [m] in meters, time [s] in seconds and mass [kg] in kilogramme.

Quantity	Description	Unit
$u(x,t)$	velocity	m s^{-1}
$\rho(x,t)$	density field	kg m^{-3}
$p(x,t)$	pressure field	kg $m^{-1}s^{-2}$
$f(x,t)$	external volume forces	m s^{-2}
ν	kinematic viscosity	m^2 s^{-1}

Table 3.1: Physical quantities used in the Navier-Stokes equations

3.1 Conservation of mass

Let $V_0 \subset \Omega$ be an arbitrary control volume, which is mass fixed, i.e. whose evolution $V(t)$ of V_0 follows the movement of the particles

$$V(t) := \{\phi(X,t) : X \in V_0\}, \tag{3.1}$$

with ϕ defined as in (2.1). Then the total mass at time t is

$$m(t) := \int_{V(t)} \rho(x,t)\, dx \tag{3.2}$$

and the conservation of mass reads

$$\frac{Dm}{Dt} = \frac{D}{Dt} \int_{V(t)} \rho(x,t)\, dx = 0\,. \tag{3.3}$$

We have to be careful when interchanging the integral with the derivative, because the control volume $V(t)$ itself depends on time t. The so-called Reynolds transport theorem shows how this can be done.

3.1 Theorem (Reynolds transport theorem). *Let $V(t) \subset \Omega$ be an arbitrary mass fixed volume in a fluid transported with velocity u and $b \in C^1(\Omega \times (0,T))$ an arbitrary function. Then there holds*

$$\frac{D}{Dt}\int_{V(t)} b(x,t)\,dx = \int_{V(t)} \frac{\partial b}{\partial t}(x,t)\,dx + \int_{\partial V(t)} n \cdot ub\,ds. \tag{3.4}$$

Using (3.4) and Gauß' theorem for (3.3) yields

$$0 \overset{(3.3)}{=} \frac{D}{Dt}\int_{V(t)} \rho\,dx = \int_{V(t)} \frac{\partial \rho}{\partial t}\,dx + \int_{V(t)} \operatorname{div}(u\rho)\,dx, \tag{3.5}$$

which holds for all control volumes V. Thus, we can rewrite it in differential form

$$\frac{\partial \rho}{\partial t} + \operatorname{div}(u\rho) = 0. \tag{3.6}$$

In this thesis we always assume that the density ρ is constant in space and time and so we can deduce the incompressibility constraint for the velocity

$$\operatorname{div}(u) = 0. \tag{3.7}$$

3.2 Conservation of momentum

The conservation of momentum equation follows from Newton's second law

$$ma = \hat{f}, \tag{3.8}$$

which claims that the change of momentum is caused by the sum of the external forces $\hat{f}$, where m denotes the mass and a the acceleration. We use (3.4) on each component of u which yields the vector-valued equation

$$\begin{aligned}
\frac{D}{Dt}\int_{V(t)} \rho u\,dx &\overset{(3.4)}{=} \int_{V(t)} \rho\frac{\partial u}{\partial t} + \rho(u\cdot\nabla)u + \rho u \operatorname{div}(u)\,dx \\
&\overset{(2.9)}{=} \int_{V(t)} \rho\frac{D}{Dt}u + \rho u \operatorname{div}(u)\,dx \\
&\overset{(3.7)}{=} \int_{V(t)} \rho\frac{D}{Dt}u\,dx \\
&\overset{(3.8)}{=} \hat{f}.
\end{aligned} \tag{3.9}$$

The external forces are going to be split into external volume forces acting on the control volume $V(t)$

$$\int_{V(t)} \rho f \, dx \tag{3.10}$$

and surface forces described by the stress vector $\tau = \tau(x, n)$, where n denotes the outer normal vector.
One can show that:

1. τ depends linearly on n and thus there exists a tensor σ such that $\tau(x, n) = \sigma(x) \cdot n$
2. σ is symmetric ($\sigma = \sigma^T$)

The first point follows directly from conservation of momentum and the second from conservation of angular momentum. σ is called the stress tensor. Using σ the surface forces can be written in divergence form

$$\int_{\partial V(t)} \tau(x, n) \, ds = \int_{\partial V(t)} \sigma \cdot n \, ds = \int_{V(t)} \operatorname{div}(\sigma) \, dx. \tag{3.11}$$

The conservation of momentum in differential form now reads

$$\rho \frac{D}{Dt} u = \rho f + \operatorname{div}(\sigma). \tag{3.12}$$

Exploiting the identity

$$(u \cdot \nabla) u \overset{(3.7)}{=} (u \cdot \nabla) u + u \operatorname{div}(u) = u \otimes u, \tag{3.13}$$

and using (2.9) yields

$$\rho \frac{\partial u}{\partial t} + \operatorname{div}(\rho(u \otimes u) - \sigma) = \rho f. \tag{3.14}$$

Here, $u \otimes u$ denotes the outer (dyadic) product of two vectors

$$u \otimes u := \begin{pmatrix} u_1 u_1 & u_1 u_2 & u_1 u_3 \\ u_2 u_1 & u_2 u_2 & u_2 u_3 \\ u_3 u_1 & u_3 u_2 & u_3 u_3 \end{pmatrix} = u u^T \tag{3.15}$$

and the divergence of a matrix A is taken row-wise

$$\operatorname{div}(A) = \begin{pmatrix} \operatorname{div}(A_{1,:}) \\ \operatorname{div}(A_{2,:}) \\ \operatorname{div}(A_{3,:}) \end{pmatrix}. \tag{3.16}$$

3.3 Stokes fluid

The stress tensor σ is often split into the stress deviator tensor σ', which is responsible for the friction of the fluid, and a pressure part p

$$\sigma = \sigma' - pI \tag{3.17}$$

where I denotes the identity matrix. For a so-called perfect fluid the friction is neglected and hence

$$\sigma = -pI \text{ and } \sigma' \equiv 0. \tag{3.18}$$

In this theses we assume that every appearing fluid is a Stokes fluid, i.e. it has the following properties:

1. $\sigma = f(\varepsilon(u))$ is a continuous function depending only on $\varepsilon(u) := \frac{1}{2}(\nabla u^T + \nabla u)$
2. σ is isotropic
3. σ is homogeneous
4. If $\varepsilon(u) = 0$ then there holds $\sigma = -pI$

The tensor $\varepsilon(u)$ is called the deformation tensor and is also sometimes denoted by $D(u)$. The mathematical translation of the second point reads

$$U\sigma U^{-1} = f(U\varepsilon(u)U^{-1}) \text{ for all orthogonal matrices } U \in \mathbb{O}^3, \tag{3.19}$$

which means that σ is invariant under rigid body rotations or in other words we have uniformity in all directions. A function is called homogeneous if it does not depend explicitly on the position x.

The Rivlin-Ericksen theorem (theorem 4.4), which is going to be treated in section 4, guarantees under these assumptions that σ can be rewritten in a form which depends only on three independent parameters.

By assuming additionally that we have a Newtonian fluid, i.e. the dependency $\sigma = f(\varepsilon(u))$ is linear, one can show that there holds

$$\sigma = (-p + \lambda \mathrm{div}(u))I + 2\mu\varepsilon(u) \overset{(3.7)}{=} -pI + 2\mu\varepsilon(u) = -pI + \mu(\nabla u + \nabla u^T), \tag{3.20}$$

where λ is called the volume viscosity and μ the dynamic or shear viscosity. Examples of Newtonian fluids are water and oil, while ketchup and blood are non-Newtonian.

Now, by plugging (3.20) into (3.14) we obtain

$$\rho\frac{\partial u}{\partial t} + \rho(u \cdot \nabla)u - \mu\,\mathrm{div}(\nabla u + \nabla u^T) + \nabla p = \rho f. \tag{3.21}$$

We divide the equation by ρ and define $\nu := \frac{\mu}{\rho}$ as the kinematic viscosity and the scaled pressure $\tilde{p} := \frac{p}{\rho}$. Thus, we finally obtain the unsteady, incompressible, Newtonian Navier-Stokes equations

$$\frac{\partial u}{\partial t} + (u \cdot \nabla)u - \nu \operatorname{div}(\nabla u + \nabla u^T) + \nabla \tilde{p} = f \tag{3.22a}$$

$$\operatorname{div}(u) = 0 \tag{3.22b}$$

3.2 Remark. *To simplify notation we will always write p for $\tilde{p}$. Another often used scaling is by defining the negative pressure $\tilde{p} := -\frac{p}{\rho}$ to improve the solvability for numerical solvers.*

Often, instead of the symmetric gradient of the velocity u, only the normal gradient is used and the constant 2 is neglected, which yields for the Navier-Stokes equation (3.22a)

$$\frac{\partial u}{\partial t} + (u \cdot \nabla)u - \frac{1}{Re}\Delta u + \nabla p = f. \tag{3.23}$$

These formulations (beside the factor 2) are equivalent if only Dirichlet data is prescribed on the whole boundary. For simplicity we will use (3.23) for the analysis and derivations.

3.4 Boundary and initial conditions

As mentioned at the beginning of the section, the boundary is split into the Dirichlet and Neumann boundary $\partial\Omega = \Gamma_D \dot{\cup} \Gamma_N$. On Γ_D the velocity is prescribed $u = u_D$, which is also called the no-slip condition if $u_D \equiv 0$. The natural boundary conditions for the Navier-Stokes equations are to prescribe the normal component of the stress tensor $\sigma_n = g$.

As the Navier-Stokes equations are of parabolic type, initial data for the velocity have to be prescribed as $u(0) = u_0$, where u_0 is divergence free. Note that the pressure p is not prescribed directly, as it can be interpreted as a Lagrange parameter for the divergence freeness of the velocity and must therefore be calculated, e.g. by the Stokes problem (3.26).

By choosing characteristic (reference) parameters for the length and velocity, denoted by L and U, (3.22) can be transformed into dimensionless form with the dimensionless parameter

$$Re := \frac{LU}{\nu} \tag{3.24}$$

called Reynolds number, which is a measure for the turbulences of a fluid. The complete (dimensionless) Navier-Stokes problem in strong form reads:

3.3 Problem (Navier-Stokes). *For given* $f \in C(\Omega, \mathbb{R}^3)$, $g \in C(\Gamma_N, \mathbb{R}^3)$, $u_D \in C(\Gamma_D, \mathbb{R}^3)$ *and* $u_0 \in C^2(\Omega, \mathbb{R}^3)$ *find* $u \in C^1((0,T); C^2(\Omega, \mathbb{R}^3))$ *and* $p \in C((0,T); C^1(\Omega))$ *such that*

$$\frac{\partial u}{\partial t} + (u \cdot \nabla)u - \frac{1}{Re}\Delta u + \nabla p = f \quad \text{in } \Omega \times [0,T], \tag{3.25a}$$
$$\operatorname{div}(u) = 0 \quad \text{in } \Omega \times [0,T], \tag{3.25b}$$
$$\sigma_n = g, \quad \text{on } \Gamma_N \times [0,T], \tag{3.25c}$$
$$u = u_D \quad \text{on } \Gamma_D \times [0,T], \tag{3.25d}$$
$$u = u_0 \quad \text{in } \Omega, t = 0. \tag{3.25e}$$

If we neglect the convection term $(u \cdot \nabla)u$ and only look for steady solutions, $\frac{\partial u}{\partial t} = 0$, we obtain the Stokes problem.

3.4 Problem (Stokes). *For given* $f \in C(\Omega, \mathbb{R}^3)$, $g \in C(\Gamma_N, \mathbb{R}^3)$ *and* $u_D \in C(\Gamma_D, \mathbb{R}^3)$ *find* $u \in C^2(\Omega, \mathbb{R}^3)$ *and* $p \in C^1(\Omega)$ *such that*

$$-\frac{1}{Re}\Delta u + \nabla p = f \quad \text{in } \Omega, \tag{3.26a}$$
$$\operatorname{div}(u) = 0 \quad \text{in } \Omega, \tag{3.26b}$$
$$\sigma_n = g, \quad \text{on } \Gamma_N, \tag{3.26c}$$
$$u = u_D \quad \text{on } \Gamma_D. \tag{3.26d}$$

As we will see in section 5 the Stokes problem has the structure of a saddle-point problem, which brings some difficulties in finding a stable discretization.

4 Derivation of the elastic wave equation

To derive the equation for elastic waves we start with the elasticity equation. First, we use the Eulerian description, but then transform it to the Lagrangian form, which is more common for elasticity problems.

The main quantities in elasticity are the deformation Φ and the displacement d. Furthermore we will use the density ρ and two important parameters, namely Young's modulus and Poisson's ratio describing the material's properties, which will be discussed in the following sections.

Quantity	Description	Unit
$\Phi(x,t)$	deformation	m
$d(x,t)$	displacement	m
$\rho(x,t)$	density	kg m^{-3}
$F(x,t)$	deformation gradient	-
E	Young's modulus	kg $\mathrm{m}^{-1}\mathrm{s}^{-2}$
ν	Poisson's ratio	-

Table 4.1: Physical quantities used in the elastic wave equation

4.1 Derivation of the elasticity equation

In this subsection we proceed as in [Bra13, Kapitel VI]. For an introduction in continuum mechanics we refer to [Wri13, Kapitel 3] and [MH12].

4.1.1 Strain tensors

Let $\Omega \subset \mathbb{R}^3$ be an open and bounded domain and let the boundary $\partial\Omega$ of Ω be sufficiently smooth. Then $\overline{\Omega}$ describes a body, which is in a relaxed, undeformed state, called the reference configuration. If some forces act on the body, it gets deformed. The current configuration is described by the deformation

$$\Phi : \overline{\Omega} \times [0,T] \to \mathbb{R}^3. \tag{4.1}$$

For ease of presentation we will neglect the time dependency in this subsection. We define

$$d(x) := \Phi(x) - x \quad \forall x \in \overline{\Omega} \tag{4.2}$$

as the displacement of the body. Often it is assumed that the displacement is small ($\Phi \approx \mathrm{id}$), hence higher order terms are neglected which leads to linear elasticity.

We assume that Φ is smooth enough. Then we can define

$$F := \nabla\Phi := \begin{pmatrix} \frac{\partial\Phi_1}{\partial x_1} & \frac{\partial\Phi_1}{\partial x_2} & \frac{\partial\Phi_1}{\partial x_3} \\ \frac{\partial\Phi_2}{\partial x_1} & \frac{\partial\Phi_2}{\partial x_2} & \frac{\partial\Phi_2}{\partial x_3} \\ \frac{\partial\Phi_3}{\partial x_1} & \frac{\partial\Phi_3}{\partial x_2} & \frac{\partial\Phi_3}{\partial x_3} \end{pmatrix} = \left(\frac{\partial\Phi_i}{\partial x_j}\right)_{i,j=1}^{3} \tag{4.3}$$

which is called the deformation gradient of Φ.

A deformation is called permissible if $\det F > 0$, which means that the orientation is preserved and the range of volume elements with positive measure have also positive measure afterwards. The power of the deformation is measured by the ratio of $\Phi(x + \Delta x) - \Phi(x)$ to Δx.

4.1 Lemma. *Assume that x, $x + \Delta x \in \Omega$. Then under the assumption of $\Phi \in C^2(\Omega, \mathbb{R}^3)$ there holds*

$$\frac{||\Phi(x + \Delta x) - \Phi(x)||^2}{||\Delta x||^2} = \frac{\Delta x^T F^T F \Delta x}{||\Delta x||^2} + \mathcal{O}(||\Delta x||) \text{ as } ||\Delta x|| \to 0.$$

Proof. Taylor. □

The local, quadratic change of length at a point x in direction Δx is described by the the Cauchy Green strain tensor

$$C := F^T F. \tag{4.4}$$

If $C = I$ then the body will not be deformed. This is called a rigid body motion. One can expect that a body, which just rotates or gets translated, will not be deformed.

4.2 Theorem. *Let Ω be a connected domain and $\Phi \in C^1(\Omega, \mathbb{R}^3)$. Then a deformation is a rigid body motion if and only if*

$$\Phi(x) = a + Qx$$

for all vectors $a \in \mathbb{R}^3$ and special orthogonal matrices $Q \in \mathrm{SO}(3)$.

Proof. See [Bra13, p. 277 f]. □

We define the Green strain tensor

$$E := \frac{1}{2}(C - I) \tag{4.5}$$

as the deviation from the rigid body motion, which is symmetric. Plugging (4.4) and (4.2) into (4.5) yields

$$E = \frac{1}{2}(\nabla(d + \mathrm{id})^T \nabla(d + \mathrm{id}) - I) = \frac{1}{2}(\nabla d^T \nabla d + \nabla d^T + \nabla d). \tag{4.6}$$

Discarding higher order terms, we obtain in first approximation the linearised strain tensor

$$\varepsilon(d) = \frac{1}{2}(\nabla d^T + \nabla d). \tag{4.7}$$

4.1.2 Stress tensors

In the following we assume that all forces which act on the body are volume or surface forces. A typical volume force is gravity, while a truck driving over a bridge produces a surface force on it. The volume forces can be described by a function $f : \Omega \to \mathbb{R}^3$ and the surface forces by $t : \Omega \times S^2 \to \mathbb{R}^3$, where S^2 denotes the unit sphere in $\mathbb{R}^3$.

Let $V \subset \Omega$ be a subdomain with sufficiently smooth boundary and dA an according surface element with the outer normal vector n. Hence, the element generates the force $t(x, n)dA$. The vector $t(x, n)$ is called the Cauchy stress vector.

The axiom of static equilibrium claims that all forces and moments at a point sum up to zero if the body is in equilibrium.

Axiom of the static equilibrium: Assume that the body Ω is in equilibrium under the volume forces f. Then there exists a vector field t on $\Omega \times S^2$, such that for all subsets $V \subset \Omega$ there holds

$$\int_V f(x)\,dx + \int_{\partial V} t(x, n(x))\,ds \qquad = 0, \tag{4.8a}$$

$$\int_V x \times f(x)\,dx + \int_{\partial V} x \times t(x, n)\,ds = 0, \tag{4.8b}$$

where $\times$ denotes the vector product in $\mathbb{R}^3$.

The following theorem says that the Cauchy stress vector depends linearly on the outer normal vector n.

4.3 Theorem (of Cauchy). *Let $t(\cdot, n) \in C^1(\Omega, \mathbb{R}^3)$, $t(x, \cdot) \in C(S^2, \mathbb{R}^3)$ for all $x \in \Omega$ and $n \in S^2$. Further assume that $f \in C(\Omega, \mathbb{R}^3)$ and the body Ω fulfils the axiom of static equilibrium. Then there exists a symmetric tensor $T \in C^1(\Omega, \mathbb{S}^3)$ such that*

$$t(x, n) \qquad = T(x)n, \tag{4.9a}$$

$$\operatorname{div}(T(x)) + f(x) = 0, \tag{4.9b}$$

$$T(x) \qquad = T^T(x). \tag{4.9c}$$

The tensor T is called the Cauchy stress tensor.

The equations above are given in Eulerian form. Often the range $\Phi(\Omega) = B$ is identified with Ω, due to the assumption of small displacement. Nevertheless, it is better

to transform the equation in Lagrangian form at a fixed reference domain. During the transformation the quantities on the reference configuration are signed with the subscript R.

The transformation of the volume forces follows directly from the integral transformation theorem

$$\int_{\phi(U)} f(v)\,dv = \int_U f(\phi(u))|\det(\nabla\phi)|\,du \tag{4.10}$$

and the conservation of mass:

$$f_R = \det(F)f. \tag{4.11}$$

The transformation for the stress tensor is a bit more demanding but can be calculated elementarily (see e.g. [Cia94]).

With the first Piola-Kirchhoff stress tensor (see Piola transformation (5.34))

$$\sigma := \det(F)TF^{-T} \tag{4.12}$$

we obtain

$$\mathrm{div}_R(\sigma) \overset{(5.35)}{=} \det(F)\mathrm{div}(T) \tag{4.13}$$

and thus

$$\mathrm{div}_R(\sigma) + f_R = \det(F)\mathrm{div}(T) + \det(F)f \overset{\det(F)>0}{=} 0. \tag{4.14}$$

Note that the first Piola-Kirchhoff stress tensor is not symmetric. Thus, we define the second Piola-Kirchhoff stress tensor which is symmetric again

$$\Sigma := F^{-1}\sigma = \det(F)F^{-1}TF^{-T}. \tag{4.15}$$

4.1.3 Material properties and material laws

Until now only the equilibrium conditions for a body have been mentioned. The material laws also have to be considered as the deformation can depend heavily on the material properties.
We call a material elastic, if the Cauchy stress tensor T is a function depending only on the deformation gradient

$$T(x) = \hat{T}(F(x)), \tag{4.16}$$

where the function $\hat{T}$ is called the response function.

Further we demand that a material has the following properties:

1. The material is homogeneous.
2. The material is objective (frame indifferent), $\hat{T}(QF) = Q\hat{T}(F)Q^T \quad \forall Q \in \mathrm{SO}(3)$.
3. The material is isotropic.

With this assumptions we can formulate an important and famous theorem in mechanics.

4.4 Theorem (Rivlin-Ericksen Theorem). *A response function $\hat{T} : \mathbb{M}^3_+ \to \mathbb{S}^3$ is isotropic and objective, if and only if it is of the form*

$$\hat{T} = \overline{T}(FF^T), \tag{4.17}$$

where the mapping $\overline{T} : \mathbb{S}^3_+ \to \mathbb{S}^3$ has the following form

$$\overline{T}(A) = \gamma(i_A)I + \gamma_1(i_A)A + \gamma_2(i_A)A^2 \tag{4.18}$$

for all $A \in \mathbb{S}^3_+$, where $\gamma_0, \gamma_1, \gamma_2$ are real-valued functions of the invariants $i_A = (i_1(A), i_2(A), i_3(A))$ with

- $i_1(A) = \lambda_1 + \lambda_2 + \lambda_3$
- $i_2(A) = \lambda_1\lambda_2 + \lambda_2\lambda_3 + \lambda_1\lambda_3$
- $i_3(A) = \lambda_1\lambda_2\lambda_3$

and $\lambda_1, \lambda_2, \lambda_3$ the eigenvalues of A.

Proof. See [Bra13, p. 283 f]. □

For the second Piola-Kirchhoff tensor we obtain the following result.

4.5 Theorem. *Assume an isotropic and objective material is given and let γ_0, γ_1 and γ_2 be differentiable functions of $i_1(E), i_2(E)$ and $i_3(E)$ with E denoting the Green strain tensor. Then there exist constants π, λ, μ with*

$$\tilde{\Sigma}(I + 2E) = -\pi + \mathrm{tr}(E)\lambda I + 2\mu E + \mathcal{O}(||E||^2) \text{ as } ||E|| \to 0. \tag{4.19}$$

Proof. See [Bra13, p. 285]. □

If there holds $C = I$, then the body is in a relaxed state and thus $\pi = 0$. The other two parameters are called Lamé-constants.

Neglecting higher order terms, we obtain the so-called linearised material law of Hooke

$$\tilde{\Sigma}(C) = \tilde{\Sigma}(I + 2E) = \lambda \mathrm{tr}(E)I + 2\mu E. \tag{4.20}$$

4.6 Remark. *If Hook's law holds also for large deformations for a material, it is called a St. Venant-Kirchhoff material. Hence,* (4.20) *is also often called the material law of St. Venant-Kirchhoff.*

4.7 Remark. *Another material law, which describes the behaviour well for large deformations, is the material law of Neo-Hook*

$$N(C) := \frac{\mu}{2}\left(\mathrm{tr}(C-I) + \frac{2\mu}{\lambda}(\det(C))^{-\frac{\lambda}{2\mu}} - 1\right) \tag{4.21}$$

where big compressions of the elements get penalized.

4.1.4 Hyperelastic materials and boundary conditions

In solid mechanics hyperelastic materials are often used, where an energy function can be introduced. Namely for a hyperelastic material it holds that a function $W : \Omega \times \mathbb{M}^3_+ \to \mathbb{R}$ exists such that

$$\hat{T} = \frac{\partial W}{\partial F}(x, F). \tag{4.22}$$

If the material is objective and isotropic, similar results hold for energy functions as for response functions. These are listed in the following lemma.

4.8 Lemma. *For an objective material $W(x,\cdot)$ is a function of $C = F^T F$*

$$W(x, F) = \tilde{W}(x, F^T F)$$

and especially for the second Piola-Kirchhoff tensor there holds

$$\tilde{\Sigma}(x, C) = 2\frac{\partial \tilde{W}}{\partial C}(x, C). \tag{4.23}$$

Further, $\tilde{W}$ depends only on the invariants of C and for small deformations there holds

$$\tilde{W}(x, C) = \frac{\lambda}{2}(\mathrm{tr}(E))^2 + \mu E : E + o(E^2) \text{ as } ||E|| \to 0.$$

The inner product $A : B$ of two matrices is defined as

$$A : B := \sum_{i,j=0}^{n} A_{ij}B_{ij} = \mathrm{tr}(AB^T). \tag{4.24}$$

Again, the boundary of the domain Ω is split into the Dirichlet and Neumann boundary. On Γ_D the displacement (deformation) is prescribed $d = d_D$, while on Γ_N the

normal component of the stress is given $\sigma_n = (F\Sigma)_n = g$.

All together by combining the results from this section, we can formulate the elasticity problem:

4.9 Problem (Elasticity). *For given $f \in C(\Omega, \mathbb{R}^3)$, $g \in C(\Gamma_N, \mathbb{R}^3)$ and $d_D \in C(\Gamma_D, \mathbb{R}^3)$ find $d \in C^2(\Omega, \mathbb{R}^3)$ with $F = I + \nabla d$, $C = F^T F$, $\Sigma = 2\frac{\partial W}{\partial C}$ and $\sigma = F\Sigma$ such that*

$$-\operatorname{div}(\sigma) = f \quad \text{in } \Omega, \tag{4.25a}$$
$$(F\Sigma)_n = g \quad \text{on } \Gamma_N, \tag{4.25b}$$
$$d = d_D \quad \text{on } \Gamma_D. \tag{4.25c}$$

The material law (4.20) uses the Lamé coefficients λ and μ. Other parameters to describe the elasticity of a material are the Poisson's ratio ν and Young's modulus E. The Young's modulus describes the relation between the strain and the stress during the deformation of a body, while Poisson's ratio models the change of the signed ratio of the transverse strain to the axial strain of the body.

Due to physical reasons there holds $\lambda > 0$, $\mu > 0$ and $E > 0$, $0 < \nu < \frac{1}{2}$. The formulae for the conversion read

$$\nu = \frac{\lambda}{2(\lambda+\mu)}, \qquad E = \frac{\mu(3\lambda+2\mu)}{\lambda+\mu}, \tag{4.26a}$$
$$\lambda = \frac{E\nu}{(1+\nu)(1-2\nu)}, \qquad \mu = \frac{E}{2(1+\nu)}. \tag{4.26b}$$

4.2 The elastic wave equation

While the elasticity equation can be interpreted as a (nonlinear) elliptic PDE, the elastic wave equation, as the name suggests, is of hyperbolic type.

We consider the hyperelastic elastic energy functional

$$J(d) := \int_\Omega W(C(d))\,dx - \int_\Omega f \cdot d\,dx - \int_{\Gamma_N} g \cdot d\,ds, \tag{4.27}$$

on the space V of all permissible displacements. On the Dirichlet boundary Γ_D we prescribe the deformation, whereas g describes the surface forces on the Neumann boundary Γ_N and f denotes the external volume forces.

If a body is in equilibrium, then $J'(d) = 0$. Otherwise, $J'(d)$ acts as an accelerating force according to Newton's second law

$$\rho\frac{D^2 d}{Dt^2} = -J'(d). \tag{4.28}$$

We calculate the directional derivative in direction v, such that $d + v \in V$,

$$\langle J'(d), v\rangle = \int_\Omega \frac{dW}{dC}(C(d))\langle\frac{\partial C}{\partial d}(d), v\rangle\, dx - \int_\Omega f \cdot v\, dx - \int_{\Gamma_N} g \cdot v\, ds \tag{4.29}$$

and therefore the directional derivative $\langle\frac{\partial C}{\partial d}(d), v\rangle$ of C in direction v. We remember that C is the Cauchy-Green tensor with $C(d) = (I + \nabla d)^T(I + \nabla d)$,

$$\begin{aligned}
\langle\frac{\partial C}{\partial d}(d), v\rangle &= \lim_{t\to 0}\frac{1}{t}(C(d + tv) - C(d)) \\
&= \lim_{t\to 0}\frac{1}{t}((I + \nabla d + t\nabla v)^T(I + \nabla d + t\nabla v) - (I + \nabla d)^T(I + \nabla d)) \\
&= (I + \nabla d)^T\nabla v + \nabla v^T(I + \nabla d) \\
&= F^T\nabla v + \nabla v^T F \\
&= 2\,\mathrm{sym}(F^T\nabla v).
\end{aligned}$$

4.10 Remark. *More precisely, $\langle J'(d), v\rangle$ is the first variation $\delta J(d, v)$ in direction v, which coincides with the Gâteaux derivative and the Fréchet derivative if the function is smooth enough.*

We plug (4.23) and the directional derivative in (4.29) yielding

$$\begin{aligned}
\langle J'(d), v\rangle &= \int_\Omega \Sigma : \mathrm{sym}(F^T\nabla v)\, dx - \int_\Omega f \cdot v\, dx - \int_{\Gamma_N} g \cdot v\, ds \\
&\overset{\Sigma=\Sigma^T}{=} \int_\Omega F\Sigma : \nabla v\, dx - \int_\Omega f \cdot v\, dx - \int_{\Gamma_N} g \cdot v\, ds,
\end{aligned} \tag{4.30}$$

where the symmetry of the 2nd Piola-Kirchhoff tensor Σ has been used.

With integration by parts and using (4.15) we obtain the elastic wave equation in weak form. As relation (4.30) holds for all arbitrary directions v we can write it in differential form

$$\rho\frac{D^2 d}{Dt^2} = \mathrm{div}(\sigma) + f. \tag{4.31}$$

The boundary conditions on Γ_D and Γ_N are the same as for the elasticity equation (4.25), but now additional initial conditions for the displacement $d = d_0$ and the velocity $\frac{Dd}{Dt} = d_1$ have to be prescribed. With them the elastic wave problem reads:

4.11 Problem (Elastic wave). *For given $f \in C(\Omega, \mathbb{R}^3)$, $g \in C(\Gamma_N, \mathbb{R}^3)$, $d_D \in C(\Gamma_D, \mathbb{R}^3)$, $d_0 \in C^2(\Omega, \mathbb{R}^3)$ and $d_1 \in C^1(\Omega, \mathbb{R}^3)$ find $d \in C^2((0,T), C^2(\Omega, \mathbb{R}^3))$ with $F = I + \nabla d$, $C = F^T F$, $\Sigma = 2\frac{\partial W}{\partial C}$ and $\sigma = F\Sigma$ such that*

$$\rho \frac{D^2 d}{Dt^2} - \operatorname{div}(\sigma) = f \quad \text{in } \Omega \times [0,T], \tag{4.32a}$$
$$(F\Sigma)_n = g \quad \text{on } \Gamma_N \times [0,T], \tag{4.32b}$$
$$d = d_D \quad \text{on } \Gamma_D \times [0,T], \tag{4.32c}$$
$$d = d_0 \quad \text{on } \Omega, t = 0, \tag{4.32d}$$
$$\frac{Dd}{Dt} = d_1 \quad \text{on } \Omega, t = 0. \tag{4.32e}$$

4.12 Remark. *This is another possibility of deriving the elasticity equation, if we consider only hyperelastic materials. In nature the deformation d with the minimal energy is taken*

$$\min_d J(d). \tag{4.33}$$

Thus, by calculating the first variation and setting it zero in all permissible directions v, a candidate for the minimum can be found.

4.13 Remark. *As the elastic wave equation is in Lagrangian form no additional terms appear due to the time derivative, and derivatives and integrals can be changed without Reynold's transport theorem.*

4.14 Remark. *For ease of presentation we will write -not absolutely correct- $\frac{\partial \cdot}{\partial t}$ instead of $\frac{D \cdot}{Dt}$ if there are no possible misunderstandings.*

5 Discretization of the Navier-Stokes equation

In this section we look for a satisfactory discretization in space and time of the Navier-Stokes equations. At first we consider the weak formulation and look for a condition to find the appropriate spaces to obtain a stable method. Then we derive two different (stable) discretizations and discuss them.

In the whole section we assume a bounded domain Ω with a sufficient smooth boundary $\partial\Omega = \Gamma_N \dot\cup \Gamma_D$, which is split into the Dirichlet boundary Γ_D and the Neumann boundary Γ_N. We assume a (quasi-uniform) triangulation $\mathcal{T}_h$ of the domain Ω where h denotes the maximal mesh size. The space of all polynomials on the triangulation $\mathcal{T}_h$ up to degree k is denoted by $\Pi^k(\mathcal{T}_h)$.

5.1 Weak formulation of the Navier-Stokes equation

Before finite element spaces are considered we discuss the continuous problem. First, we look at the Stokes problem (3.26), where we set $\frac{1}{Re} = \nu$, e.g. the characteristic velocity and length is 1.

$$-\nu\Delta u + \nabla p = f \tag{5.1a}$$
$$\operatorname{div}(u) \qquad = 0. \tag{5.1b}$$

It consists of two different physical quantities, the velocity and the pressure. Thus, we have two different spaces for the solution and the test functions, where the space V is going to represents the velocity, while the pressure will be in the space Q, which will be specified later. For ease of presentation we assume in this subsection that homogeneous Dirichlet boundary conditions, $u_D = 0$, are prescribed on the whole boundary $\partial\Omega$.

To obtain a weak formulation we multiply the Stokes equations (5.1) with test functions $v \in V$ and $q \in Q$, respectively, integrate over the whole domain Ω and integrate by parts:

$$\int_\Omega \nu\nabla u\nabla v\,dx - \int_\Omega \operatorname{div}(v)p\,dx = \int_\Omega fv\,dx\,, \tag{5.2a}$$
$$-\int_\Omega \operatorname{div}(u)q \qquad = 0\,. \tag{5.2b}$$

As preparation for the abstract theory we define the following (bi-)linear forms

$$a(u,v) := \int_\Omega \nu\nabla u\nabla v\,dx \qquad b(u,q) := -\int_\Omega \operatorname{div}(u)q\,dx \qquad f(v) := \int_\Omega fv\,dx. \tag{5.3}$$

Equation (5.2) should hold for all $v \in V$ and $q \in Q$ and thus, the variational problem for the Stokes equations reads:

5.1 Problem. *Find $u \in V$ and $p \in Q$ such that*

$$a(u,v) + b(v,p) = f(v) \quad \forall v \in V\,, \tag{5.4a}$$
$$b(u,q) \qquad\quad = 0 \qquad \forall q \in Q\,. \tag{5.4b}$$

We define a huge bilinear form $B(\cdot,\cdot)$ by adding both equations

$$B((u,p),(v,q)) := a(u,v) + b(v,p) + b(u,q), \tag{5.5}$$

hence the problem reads:

5.2 Problem. *Find $(u,p) \in V \times Q$ such that*

$$B((u,p),(v,q)) = f(v) \quad \forall (v,q) \in V \times Q. \tag{5.6}$$

To prove the existence, uniqueness and stability we could prove the coercivity and continuity for the huge bilinear form $B(\cdot,\cdot)$. Then the lemma of Lax-Milgram would guarantee the unique solvability for all right-hand sides. Unfortunately, the coercivity holds not for this kind of problems. Thus, we use the abstract theory for saddle-point problems, namely Brezzi's theorem for mixed methods.

A general mixed variational problem involves two Hilbert spaces V and Q, the bilinear forms

$$a : V \times V \to \mathbb{R},$$
$$b : V \times Q \to \mathbb{R},$$

and the continuous linear forms

$$f : V \to \mathbb{R},$$
$$g : Q \to \mathbb{R}.$$

With these forms we define the following mixed problem:

5.3 Problem. *Find $u \in V$ and $p \in Q$ such that*

$$a(u,v) + b(v,p) = f(v) \quad \forall v \in V, \tag{5.7a}$$
$$b(u,q) \qquad\quad = g(q) \quad \forall q \in Q. \tag{5.7b}$$

We denote with V_0 the kernel of the bilinear form $b(\cdot,\cdot)$ in the first component

$$V_0 := \{v :\ b(v,q) = 0\,, \forall q \in Q\}. \tag{5.8}$$

5.4 Theorem (Brezzi's theorem). *Assume that $a(\cdot,\cdot)$ and $b(\cdot,\cdot)$ are continuous bilinear forms, i.e.*

$$a(u,v) \leq \alpha_2 ||u||_V ||v||_V \quad \forall u,v \in V, \tag{5.9}$$
$$b(u,q) \leq \beta_2 ||u||_V ||q||_Q \quad \forall u \in V, \forall q \in Q. \tag{5.10}$$

Assume there holds coercivity of $a(\cdot,\cdot)$ on the kernel, i.e.

$$a(u,u) \geq \alpha_1 ||u||_V^2 \quad \forall u \in V_0, \tag{5.11}$$

and there holds the LBB (Ladyzhenskaya-Babuška-Brezzi) condition

$$\sup_{u \in V} \frac{b(u,q)}{||u||_V} \geq \beta_1 ||q||_Q \quad \forall q \in Q. \tag{5.12}$$

Then, the mixed problem is uniquely solvable. The solution fulfils the stability estimate

$$||u||_V + ||q||_Q \leq c\{||f||_{V^*} + ||g||_{Q^*}\} \tag{5.13}$$

with the constant c depending on $\alpha_1, \alpha_2, \beta_1, \beta_2$.

Proof. See [Sch14, p. 98 f]. □

Here, V^* denotes the topological dual space to V and $||\cdot||_{V^*}$ the according dual norm

$$||f||_{V^*} = \sup_{0 \neq x \in V} \frac{|f(x)|}{||x||_V}. \tag{5.14}$$

To apply Brezzi's theorem to problem 5.1, it has to fulfil the assumptions. We only mention that the continuity of the discrete bilinear forms follows directly from the continuous case, but the LBB condition has to be proven again, as the discrete forms do not inherit this property.

For the full Navier-Stokes equations the convection term is added in a natural way

$$c(u,w,v) := \int_\Omega (w \cdot \nabla) u \cdot v \, dx. \tag{5.15}$$

Note that $c(\cdot,\cdot,\cdot)$ is a trilinear form, where w can be interpreted as the wind of the convection, which plays a crucial role for upwinding schemes. For the Navier-Stokes equations the solution is also its own wind and thus the final variational formulation is:

5.5 Problem. *Find $(u, p) \in V \times Q$ such that*

$$a(u, v) + b(v, p) + c(u, u, v) = f(v) \quad \forall v \in V, \tag{5.16a}$$
$$b(u, q) = 0 \quad \forall q \in Q. \tag{5.16b}$$

5.2 Taylor-Hood discretization

For the first discretization of the Navier-Stokes equations, polynomials of the same order for the velocity and the pressure were used, which gave "good looking" solutions. Nevertheless, rather soon it was discovered that this pair was not stable. The first stable pair was discovered by Taylor and Hood in [HT73] where they made the ansatz of using polynomials of one degree lower for the pressure than the velocity. These elements are quite easy to implement, as for both spaces H1-conforming finite elements can be used.

For ease of presentation we only consider the pair $P_2 - P_1$ in two dimensions, where quadratic polynomials are used for approximating the velocity and linear ones for the pressure, but we mention that pairs of the form $P_k - P_{k-1}$ are also stable. The finite element spaces can be chosen as follows:

$$V_h := [\Pi^2(\mathcal{T}_h)]^n \cap [C^0(\Omega)]^n \quad \text{and} \quad Q_h := \Pi^1(\mathcal{T}_h) \cap C^0(\Omega). \tag{5.17}$$

If only Dirichlet data is prescribed on the boundary, $\Gamma_N = \emptyset$, then the space Q_h must be chosen as

$$Q_h := \Pi^1(\mathcal{T}_h) \cap C^0(\Omega) \cap L^2_0(\Omega),$$

where $L^2_0(\Omega)$ denotes all functions with zero mean

$$L^2_0(\Omega) := \{q \in L^2(\Omega) : \int_\Omega q \, dx = 0\}.$$

The claim of zero mean value is needed to ensure an unique solution which can be seen as following. If we integrate by parts in the bilinear form $b(\cdot, \cdot)$ from (5.3) we get

$$b(v, p) = -\int_\Omega \operatorname{div}(v) p \, dx = \int_\Omega v \cdot \nabla p \, dx.$$

Due to the derivative one can add a constant to the pressure p without changing the solution.

As usual, the test functions for the velocity live in the space

$$V_{h,\Gamma_D} := \{u_h \in V_h : \, u_h = 0 \text{ on } \Gamma_D\}.$$

Due to the continuity of the velocity and pressure, system (5.16) has not to be changed a lot, only the Neumann boundary has to be considered, and we immediately obtain the

discrete variational formulation for the Navier-Stokes equations with Taylor-Hood elements:

5.6 Problem. *Find* $(u_h, p_h) \in V_h \times Q_h$ *such that*

$$a(u_h, v_h) + c(u_h, u_h, v_h) + b(v_h, p_h) = f(v_h) + \int_{\Gamma_N} \sigma_n \cdot v_h \, ds \quad \forall v_h \in V_{h,\Gamma_D}\,, \tag{5.18a}$$

$$b(u_h, q_h) = 0 \quad \forall q_h \in Q_h\,. \tag{5.18b}$$

As we will see in section 8, the boundary term $\int_{\Gamma_N} \sigma_n \cdot v_h \, ds$ will play a crucial role for fluid-structure interaction. We remember that σ represents the stress tensor of the fluid. To distinguish it from the first Piola-Kirchhoff tensor (4.12) we define

$$\sigma^f := \sigma. \tag{5.19}$$

The discrete LBB-condition for Taylor-Hood elements can be proven (e.g. in [MSW13]), but some assumptions on the mesh $\mathcal{T}_h$ of the domain have to be made.

The Taylor-Hood elements are quite popular and often used, but the method has the drawback that it only provides so-called discrete divergence-free solutions, as the solution for the velocity u_h fulfils

$$\int_\Omega \operatorname{div}(u_h) q_h \, dx = 0 \quad \forall q_h \in Q_h, \tag{5.20}$$

and thus we cannot conclude $\operatorname{div}(u_h) = 0$, because it does not hold in general.

If we could guarantee that the divergence of the velocity is an element in the pressure space Q_h

$$\operatorname{div}(V_h) \subset Q_h, \tag{5.21}$$

which does not hold for Taylor-Hood elements, then exact divergence-freeness follows directly from discrete divergence-freeness, i.e.

$$\int_\Omega \operatorname{div}(u_h) q_h \, dx = 0 \quad \forall q_h \in Q_h \Rightarrow \operatorname{div}(u_h) = 0. \tag{5.22}$$

Thus, the solution would also be exact divergence-free.

5.7 Remark. *The Taylor-Hood discretization has a quadratic convergence rate, assuming the solution is stable. Another type of pairing for the velocity and the pressure is to use a complete discontinuous pressure and two additional polynomial degrees for the velocity,* $P_3 - P_1^{dc}$*. For this pairing the LBB-condition can be proven in an easy way but the convergence rate is only linear.*

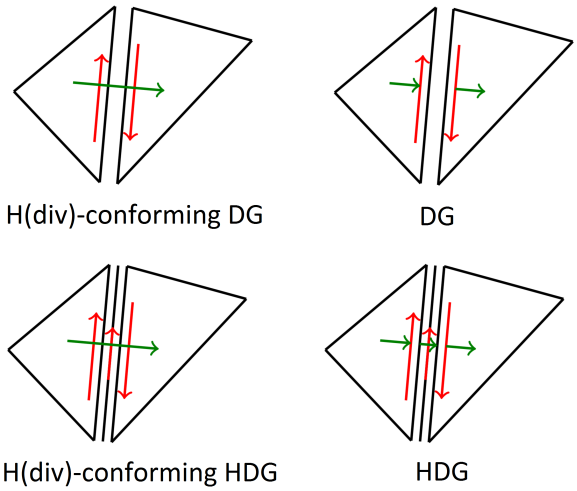

Figure 5.1: Normal and tangential continuity for different methods

5.3 Hybrid discontinuous Galerkin method for the Navier-Stokes equations

A big drawback of the Taylor-Hood discretization is the divergence-free constraint, which ensures only that the velocity is discrete divergence-free, but not exact. This leads to a variety of problems from slower convergence rates and bad looking solutions up to instability. One possible way to repair this is to use a reconstruction operator, see for detailed information [Led16] and [LLMS17], or to use another type of discretization where this problem does not appear at all.

The approach to use finite element spaces where the solution is locally exact divergence-free on each element overcomes this problems. For the Navier-Stokes equations Discontinuous Galerkin (DG) methods were developed as they provide good stability and conservation properties (see e.g. [CKS05], [CKS07]). A drawback of DG schemes is the high number of degree of freedoms. Thus, additional unknowns were added on the element interfaces to apply static condensation to reduce the size of the linear system, which yields to Hybrid Discontinuous Galerkin (HDG) methods (see e.g. [CCNP13]). The following method introduced by Joachim Schöberl and Christoph Lehrenfeld in [Leh10] and [LS16] uses a HDG approach, where only the tangential continuity of the velocity is broken and a completely discontinuous pressure is used. This yields to an H(div)-conforming discretization, which ensures the continuity of the normal component over element boundaries and the additional facet variables are introduced to approximate the tangential trace of the velocity. We will call this method H(div)-conforming HDG (see figure 5.1 for the different methods).

5.3.1 H(div)-conforming elements

The Sobolev space used for H(div)-conforming functions on Ω is defined as

$$H(\mathrm{div}, \Omega) := \{u \in [L^2(\Omega)]^n : \mathrm{div}(u) \in L^2(\Omega)\}. \tag{5.23}$$

As we work with piecewise polynomial functions on each element the normal continuity is trivially fulfilled on each triangle. To obtain a global function which lies in $H(\mathrm{div}, \Omega)$, a compatibility condition has to be fulfilled. Like in $H^1(\Omega)$, where the discrete functions have to be continuous over elements, the normal component has to be continuous.

We introduce the finite element space

$$W_h := \{u_h \in [\Pi^k(\mathcal{T}_h)]^2 : [\![u_h \cdot n]\!]_E = 0\,, \forall E \in \mathcal{F}_h\}, \tag{5.24}$$

where $\mathcal{F}_h$ denotes the skeleton of $\mathcal{T}_h$, or in other words, the set of all edges in two dimensions and faces in three dimensions of $\mathcal{T}_h$, and n the outer normal vector. The jump over the interface E of two neighboured elements T_1 and T_2 is defined as

$$[\![u_h \cdot n]\!]_E := (u_h|_{T_1} - u_h|_{T_2})\big|_E \cdot n_1, \tag{5.25}$$

which is also called the normal jump $[\![u]\!]_n$ of u.

The following lemma guarantees that W_h is a (finite dimensional) subspace of $H(\mathrm{div}, \Omega)$.

5.8 Lemma. *Let $\mathcal{T}_h$ be a triangulation of a domain Ω. A function u is in $H(\mathrm{div}, \Omega)$ if and only if $u \in H(\mathrm{div}, T)$ for all triangles $T \in \mathcal{T}_h$ and the normal jump $[\![u]\!]_n$ vanishes on all inner facets E.*

Proof. See [Sch09b, p. 103]. □

The facet variables, which are used to enforce the tangential continuity of the velocity weakly, can be interpreted as an interior penalty. To avoid full coupling between the elements they are introduced in a hybrid fashion. Thus, the facet variables live only on the skeleton of $\mathcal{T}_h$ in the vector-facet finite element space

$$F_h := \{\hat{u}_h \in [\Pi^k(\mathcal{F}_h)]^n : \hat{u}_h \cdot n = 0\}. \tag{5.26}$$

We define the velocity space as

$$V_h := W_h \times F_h \tag{5.27}$$

and write $\overline{u} := (u, \hat{u})$ for the velocity.

To ensure the exact divergence-free property of the velocity, $\mathrm{div}(W_h) = Q_h$, the pressure space has to be of a polynomial order less than the velocity

$$Q_h := \Pi^{k-1}(\mathcal{T}_h), \tag{5.28}$$

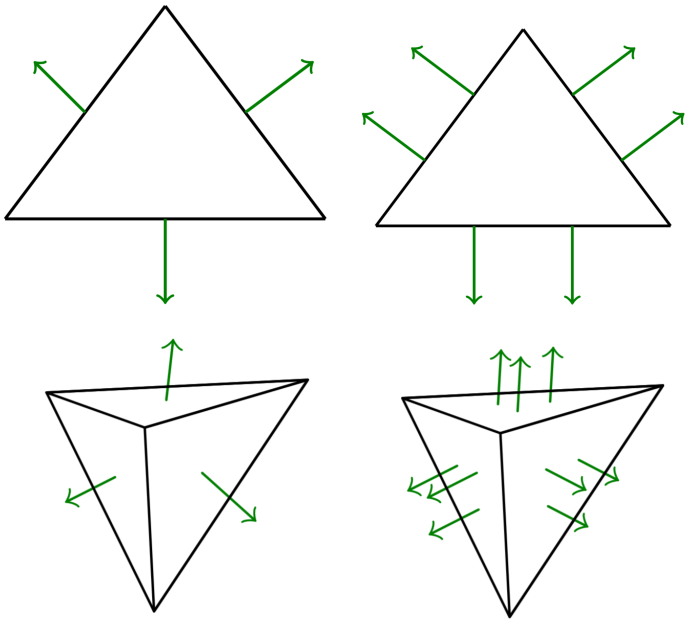

Figure 5.2: Lowest order Raviart-Thomas and BDM element in two and three dimensions

which is obviously a finite dimensional subspace of $L^2(\Omega)$.

Examples for H(div)-conforming elements are the Raviart-Thomas (RT), introduced in [RT77], and Brezzi-Douglas-Marini (BDM) elements, see [BDM85]. While BDM elements use polynomial spaces of complete order, i.e.

$$V_{\mathrm{BDM}_k} := \{\sigma \in [\Pi^k(\mathcal{T}_h)]^n : \sigma \cdot n \text{ continuous across edges}\}, \tag{5.29}$$

the RT elements of order k lie exactly between the polynomial spaces of order $k-1$ and k (see figure 5.2)

$$[\Pi^{k-1}(\mathcal{T}_h)]^n \subsetneq V_{\mathrm{RT}_k} \subsetneq [\Pi^k(\mathcal{T}_h)]^n, \tag{5.30}$$

$$V_{\mathrm{RT}_k(T)} = [\Pi^k(\mathcal{T}_h)]^n \oplus \vec{x} \cdot \Pi^{k,*}(\mathcal{T}_h), \tag{5.31}$$

where $\Pi^{k,*}$ denotes all polynomials of exactly degree k and $\vec{x} = (x_1, \cdots, x_n)^T$. For example the lowest order Raviart-Thomas elements RT_0 consist of all constant functions and some linear ones

$$V_{\mathrm{RT}_0} = \left\{ \begin{pmatrix} a \\ b \end{pmatrix} + c \begin{pmatrix} x \\ y \end{pmatrix} : a, b, c \in \mathbb{R} \right\}. \tag{5.32}$$

For the construction of higher order H(div)-conforming elements we refer to [Zag06].

To ensure the normal continuity also on physical elements and not only on the reference element the Piola transformation is used.

5.9 Theorem (Piola transformation). *Let $\Phi : \hat{T} \to T$ be a diffeomorphic mapping from the reference element $\hat{T}$ to the physical element T and Ψ a diffeomorphic mapping from T to another physical element $\tilde{T}$. Let $\hat{\sigma} \in H(\mathrm{div}, \hat{T})$. Then, the Piola transformation*

$$\sigma := P_\Phi[\hat{\sigma}] \tag{5.33}$$

defined by

$$\sigma = P_\Phi[\hat{\sigma}] := (J^{-1} F \hat{\sigma}) \circ \Phi^{-1}, \tag{5.34}$$

where F denotes the gradient of Φ, $F := \nabla\Phi$, and $J := \det(F)$ has the following properties:

1. *σ is in the space $H(\mathrm{div}, T)$ with*

$$\mathrm{div}(\sigma) = (J^{-1}\mathrm{div}(\hat{\sigma})) \circ \Phi^{-1}. \tag{5.35}$$

2. *Let furthermore $\hat{e}$ be an edge of the reference element and $e = \Phi(\hat{e})$. Then*

$$\int_e \sigma \cdot n_e \, ds = \int_{\hat{e}} \hat{\sigma} \cdot n_{\hat{e}} \, d\hat{s}. \tag{5.36}$$

3. *With $\varphi := \Psi \circ \Phi$ there holds*

$$P_{\Psi\circ\Phi}[\hat{\sigma}] = P_\varphi[\hat{\sigma}] = P_\Psi[P_\Phi[\hat{\sigma}]]. \tag{5.37}$$

Proof. 1. & 2. : See [Sch09b, p. 106].
3. : We start from the right-hand side:

$$\begin{aligned}
P_\Psi[P_\Phi[\hat{\sigma}]] = P_\Psi[\sigma] &= \left(\frac{1}{\det(\nabla\Psi)}\nabla\Psi\sigma\right) \circ \Psi^{-1} \\
&= \left(\frac{1}{\det(\nabla\Psi)}\nabla\Psi \left(\frac{1}{\det(\nabla\Phi)}\nabla\Phi\hat{\sigma}\right) \circ \Phi^{-1}\right) \circ \Psi^{-1} \\
&= \left(\frac{1}{\det((\nabla\Psi \circ \Phi)\nabla\Phi)}(\nabla\Psi \circ \Phi)\nabla\Phi\hat{\sigma}\right) \circ \Phi^{-1} \circ \Psi^{-1} \\
&= \left(\frac{1}{\det(\nabla\varphi)}\nabla\varphi\hat{\sigma}\right) \circ \varphi^{-1} \\
&= P_\varphi[\hat{\sigma}]
\end{aligned}$$

□

5.10 Remark. *If the mapping Φ is obvious we will neglect the subscript for the Piola transformation and only write $P[\sigma]$.*

5.3.2 Derivation of the discrete H(div)-conforming HDG Navier-Stokes equations

Due to the discontinuity of the velocity the discrete form of the variational problem 5.5 cannot be used without bigger changes. Thus, we quickly derive the formula, where we use a similar approach as for HDG methods like in [Leh10].

We start the derivation of the method with the viscous part. As usual we multiply with a test function and integrate over the domain, but now we integrate by parts on each triangle T, because of the broken continuity of the velocity u. We neglect the subscript h during the derivation.

$$\int_\Omega \operatorname{div}(-\nu\nabla u)v\,dx = \sum_{T\in\mathcal{T}_h}\left\{\int_T \nu\nabla u : \nabla v\,dx - \int_{\partial T}\nu\frac{\partial u}{\partial n}v\,ds\right\} \tag{5.38}$$

Now the facet variables $\hat{u}$ are introduced by adding the consistency term

$$\sum_{T\in\mathcal{T}_h}\int_{\partial T}\nu\frac{\partial u}{\partial n}\tilde{v}\,ds = \int_{\Gamma_N}\nu\frac{\partial u}{\partial n}\tilde{v}\,ds, \tag{5.39}$$

where $\tilde{v} := v_n + \hat{v}_\tau$ denotes the sum of the normal component of the $H(\operatorname{div},\Omega)$ function and the tangential component of the facet function which yields

$$\sum_{T\in\mathcal{T}_h}\int_T \nu\nabla u : \nabla v\,dx - \int_{\partial T}\nu\frac{\partial u}{\partial n}\underbrace{(v-\tilde{v})}_{=[\![v^\tau]\!]} - \int_{\Gamma_N}\nu\frac{\partial u}{\partial n}\tilde{v} \tag{5.40}$$

where we used

$$v - \tilde{v} = v_\tau - \hat{v}_\tau =: [\![v^\tau]\!].$$

The boundary integral over the Neumann boundary can be used for prescribing an outflow condition and will be neglected for now. We use the fact that $[\![u^\tau]\!]$ is zero for the true solution and add terms for symmetry and stability to define the following bilinear form

$$a_h(\bar{u},\bar{v}) := \sum_{T\in\mathcal{T}_h}\int_T \nu\nabla u : \nabla v\,dx - \int_{\partial T}\left(\nu\frac{\partial u}{\partial n}[\![v^\tau]\!] + \nu\frac{\partial v}{\partial n}[\![u^\tau]\!] - \nu\beta[\![u^\tau]\!][\![v^\tau]\!]\right)ds, \tag{5.41}$$

where β denotes the stability factor (see remark 5.13).

For the pressure part we also integrate by parts

$$\int_\Omega v\cdot\nabla p\,dx = \sum_{T\in\mathcal{T}_h}\int_T v\cdot\nabla p\,dx = -\sum_{T\in\mathcal{T}_h}\int_T \operatorname{div}(v)p\,dx + \int_{\Gamma_N} pv_n\,ds. \tag{5.42}$$

The boundary integral is part of the boundary conditions and will be neglected for the definition of the following bilinear form

$$b_h(\bar{v},p) := -\sum_{T\in\mathcal{T}_h}\int_T \operatorname{div}(v)p\,dx. \tag{5.43}$$

The Stokes problem with H(div)-conforming elements now reads:

5.11 Problem. *Find $\bar{u}_h \in V_h$ and $p_h \in Q_h$ such that*

$$a_h(\bar{u}_h, \bar{v}_h) + b_h(\bar{v}_h, p_h) = f(\bar{v}_h) \quad \forall \bar{v}_h \in V_h, \tag{5.44a}$$
$$b_h(\bar{u}_h, q_h) = 0 \quad \forall q_h \in Q_h. \tag{5.44b}$$

For the convection part we use a kind of upwinding technique. We only have to treat the tangential part in the upwind fashion because of the normal continuity of the velocity. The upwind function u^{up} is defined as

$$u^{up} := u_n + \begin{cases} \hat{u}_\tau, & w_n < 0 \\ u_\tau, & w_n \geq 0 \end{cases} \tag{5.45}$$

where w_n denotes the normal component of the wind of the convection in $\operatorname{div}(u \otimes w) = (w \cdot \nabla)u$.

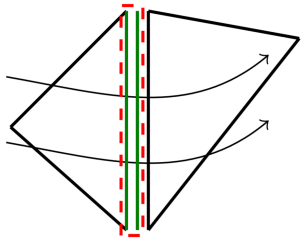

Figure 5.3: The facet is glued to the outflow boundary

The facet variables are glued to the upwind triangle in the following way

$$\int_{\partial T_{out}} w_n(\hat{u}_\tau - u_\tau)\hat{v}_\tau \, ds \,, \tag{5.46}$$

where ∂T_{out} denotes the element edges where the upwind value $w_n > 0$ is positive (see figure 5.3).
The convection trilinear form reads

$$c_h(w, \bar{u}, \bar{v}) = \sum_{T \in \mathcal{T}_h} \left\{ - \int_T u \otimes w : \nabla v \, dx + \int_{\partial T} w_n u^{up} v \, ds + \int_{\partial T_{out}} w_n (\hat{u} - u)_\tau \hat{v}_\tau \, ds \right\}. \tag{5.47}$$

Finally we obtain the spatial discretization of the Navier-Stokes equations by setting the wind as the velocity itself:

5.12 Problem. *Find $\bar{u}_h \in V_h$ and $p_h \in Q_h$ such that*

$$a_h(\bar{u}_h, \bar{v}_h) + c_h(\bar{u}_h, \bar{u}_h, \bar{v}_h) + b_h(\bar{v}_h, p_h) = f(\bar{v}_h) \quad \forall \bar{v}_h \in V_h, \tag{5.48a}$$
$$b_h(\bar{u}_h, q_h) = 0 \quad \forall q_h \in Q_h. \tag{5.48b}$$

5.13 Remark. *For a rigorous analysis of H(div)-conforming HDG we refer to [Leh10], but mention that it is stable if the stability parameter β is chosen sufficiently large. It depends quadratically on the polynomial order k and linearly on the mesh size h. The factor α depends heavily on the mesh. Numerical experiments showed that values between 5 and 10 are satisfactory for most situations:*

$$\beta = \frac{\alpha k^2}{h}.$$

5.4 Time discretization of the unsteady Navier-Stokes equation

After the spatial discretizations have been introduced, the time discretization has to be considered to derive the complete discretization. The methods discussed in this section can be applied to both, the Taylor-Hood and the H(div)-conforming HDG discretization. In this subsection we will assume homogeneous Dirichlet boundary conditions on the whole boundary for ease of presentation.

For the time discretization of the unsteady Navier-Stokes equation we will use the method of lines, where the spatial discretization is given and then the discretization in time is done at each mesh node. Another possibility would be to discretize first in time and so the spatial domain can be changed at each step (see figure 5.4). This approach, however, will not be discussed here.

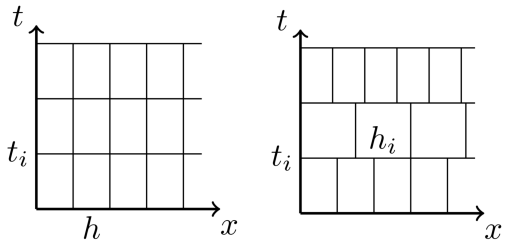

Figure 5.4: Method of lines and space-time discretization

For the method of lines we make the ansatz of time dependent constants for the velocity and the pressure

$$u_h(x,t) = \sum_{i=0}^{N_V} \alpha_i(t)\varphi_i(x) \qquad p_h(x,t) = \sum_{j=0}^{N_Q} \beta_j(t)\psi_j(x), \tag{5.49}$$

where $\{\varphi_i\}_{i=0}^{N_V}$ and $\{\psi_j\}_{j=0}^{N_Q}$ denote the shape functions of the finite element spaces V_h and Q_h, respectively.

After the spatial discretization we obtain with the matrices $M \in \mathbb{R}^{N_V \times N_V}$, $A \in \mathbb{R}^{N_V \times N_V}$ and $B \in \mathbb{R}^{N_V \times N_Q}$

$$\begin{aligned} M_{ij} &:= \int_\Omega \varphi_i \cdot \varphi_j \, dx && \forall i,j = 0,\dots,N_V, \\ A_{ij} &:= \int_\Omega \nu \nabla\varphi_i : \nabla\varphi_j \, dx && \forall i,j = 0,\cdots,N_V, \\ B_{ij} &:= -\int_\Omega \operatorname{div}(\varphi_i)\psi_j \, dx && \forall i = 0,\dots,N_V,\ \forall j = 0,\dots,N_Q, \end{aligned}$$

the vector $C(u_h)u_h$

$$C_i(u_h)u_h := \int_\Omega (u_h \cdot \nabla u_h)\varphi_i \, dx \quad \forall i = 0,\dots,N_V$$

and the following problem:

5.14 Problem. *Given the initial data u_0 find $(u,p) \in \mathbb{R}^{N_V \times N_Q}$ such that*

$$M\frac{\partial u}{\partial t} + Au + Bp + C(u)u = f \quad \text{in } [0,T], \tag{5.50a}$$
$$B^T u = 0 \quad \text{in } [0,T], \tag{5.50b}$$
$$u(0) = u_0. \tag{5.50c}$$

Next, the interval $[0,T]$ is divided in equidistant steps

$$0 = t_0 < \cdots < t_i < \cdots < t_N = T,$$

with the step size $\tau = t_{i+1} - t_i$ for all $i = 1,\dots,N-1$. We use the notation $u^n := u(t_n)$ and $p^n := p(t^n)$.

By integrating (5.50) over time and using some kind of integration schemes we obtain the complete discretization. Therefore we will use two different approaches: IMEX schemes and the Crank-Nicolson method.

5.4.1 Implicit-Explicit splitting schemes

For the Navier-Stokes equations we will first consider lowest order time integration schemes, namely the explicit and implicit Euler scheme.

Explicit schemes are very cheap and fast due to avoiding solving difficult nonlinear and nonsymmetric systems. Unfortunately the Navier-Stokes equations cannot be handled

completely in an explicit way, because it is not a pure differential equation, but has the type of a differential algebraic equation (DAE) due to the incompressible constraint. Thus, the pressure and the constraint have to be treated implicitly to guarantee that the solution is (discrete) divergence free after each step.

The drawback of explicit methods is that they are not unconditionally stable and so a time restriction must be kept. The convection step size restriction scales linearly with the spatial discretization parameter h, whereas the diffusion has a quadratic dependency. Such terms as the diffusion are therefore called to be stiff and should be handled implicitly.

Implicit schemes overcome this problem and are unconditionally stable. The disadvantage of them is that at each step a (nonlinear) system has to be solved, which can change at every new step and thus, are quite slow and inefficient.

The idea of so called semi-implicit methods is to try to mix both schemes and combine them in the following way:

- Nonlinear terms and external forces are treated explicitly to avoid difficult, non-symmetric equations which would be too expensive to solve at every time step.
- Linear and stiff parts are handled implicitly to avoid the quadratic dependency of the time step τ on the mesh size h.

The system involves not only the mass matrix, but due to the linearity of the additional terms, it has to be solved only once and can then be used in every time step.

Such additive decomposition methods are called Implicit-Explicit (short IMEX) splitting schemes. For the construction of IMEX schemes we refer to [ARS97].

By applying the first order IMEX method on (5.50) we obtain

$$M\frac{u^{n+1}-u^n}{\tau} + Au^{n+1} + Bp^{n+1} = f^n - C(u^n)u^n, \tag{5.51a}$$

$$B^T u^{n+1} = 0, \tag{5.51b}$$

which can be written compactly in matrix form

$$\begin{pmatrix} M+\tau A & \tau B^T \\ \tau B & 0 \end{pmatrix} \begin{pmatrix} u^{n+1}-u^n \\ p^{n+1} \end{pmatrix} = \tau \begin{pmatrix} f^n - Au^n - C(u^n) \\ 0 \end{pmatrix}. \tag{5.52}$$

Note that there holds $Bu^n = 0$ because the constraint $Bu = 0$ is treated implicitly. We would like to rewrite the equations in residual (update) form, so by adding $\pm p^n$ we obtain the following system

$$\begin{pmatrix} M+\tau A & \tau B^T \\ \tau B & 0 \end{pmatrix} \begin{pmatrix} u^{n+1}-u^n \\ p^{n+1}-p^n \end{pmatrix} = \tau \begin{pmatrix} f^n - Au^n - C(u^n) - Bu^n \\ -B^T p^n \end{pmatrix}. \tag{5.53}$$

By defining the left matrix as $M^\star$ and putting A, B^T and B together as the Stokes operator D, $\tilde{f} := \begin{pmatrix} f \\ 0 \end{pmatrix}$ and $\tilde{C} := \begin{pmatrix} C \\ 0 \end{pmatrix}$, (5.53) transforms to

$$\begin{pmatrix} u^{n+1} \\ p^{n+1} \end{pmatrix} = \begin{pmatrix} u^n \\ p^n \end{pmatrix} - \tau (M^\star)^{-1} \left(D(u^n, p^n) + \tilde{C}(u^n) - \tilde{f}^n \right) . \tag{5.54}$$

One disadvantage of an IMEX splitting is that the same time step τ is used for the explicit and implicit part. With more advanced splitting methods this restriction can be overcome so that a small step size τ_c for the convection and a larger one τ_D for the stiff part, which is again stable, but faster as the linear system must be solved less often. In this thesis, however, we will not use such splitting techniques.

5.4.2 Crank-Nicolson method for the Navier-Stokes equations

A different approach to splitting methods is to discretize everything with an appropriate integration scheme and then solve the arising nonlinear system with Newton's method:

Algorithm 5.1 Newton(x_0, ε, *maxit*, F)

```
for i = 0 to maxit do
    r = F(x_0)
    M = F'(x_0)
    Solve MΔx = r
    x_0 = x_0 − Δx
    if |Δx · r| < ε then
        break
    end if
end for
return x_0
```

An often used scheme is the trapezoidal rule, also called Crank-Nicolson method (CN)

$$\int_a^b f(x)\, dx \approx \frac{\tau}{2} \left(f(a) + f(b) \right) , \tag{5.55}$$

which has better properties in conserving the total energy than the explicit or implicit Euler scheme.

Only the pressure and the incompressible constraint are treated completely implicit. The arising scheme reads:

$$M(u^{n+1} - u^n) + \frac{\tau}{2} A(u^{n+1} + u^n) + \tau B p^{n+1} + \frac{\tau}{2}(C(u^{n+1}) + C(u^n)) - f^n = 0 \tag{5.56}$$

$$\tau B^T u^{n+1} = 0 \tag{5.57}$$

To solve this system with Newton's method is slower as an IMEX scheme, but the step size can be chosen larger, as the convection is treated also implicit. Another advantage

is the second order accuracy of the CN scheme.

5.15 Remark. *The CN method is not A-stable, so for large computation times oscillations may appear and the system can get unstable. Thus, the so-called shifted CN or one-step-theta scheme can be used with* $\theta := \frac{1}{2} + \varepsilon$.

Given the differential equation $b(u)\frac{\partial u}{\partial t} + Au = 0$ *it reads*

$$(\theta b(u^{n+1}) + (1-\theta)b(u^n))(u^{n+1} - u^n) + \tau\theta Au^{n+1} + \tau(1-\theta)Au^n = 0. \tag{5.58}$$

With this choice of θ *it is still of second order, but now also strictly A-stable.*

6 Discretization of the elastic wave equation

The discretization of the elastic wave equation is treated differently as the Navier-Stokes equations, due to the hyperbolic type of the equation. It can be written as a system of PDEs of first order

$$\frac{\partial d}{\partial t} = u, \tag{6.1a}$$

$$\rho \frac{\partial u}{\partial t} = f - K(d), \tag{6.1b}$$

with the displacement d, the velocity u and a nonlinear operator $K(\cdot)$.

Here, the time discretization influences the spatial one heavily, which will be seen later. We introduce two different methods for the time discretization. For the first one, we assume that the displacement and the velocity are both continuous and are approximated with H1-conforming elements. The displacement for the second method is also assumed to be in $H^1(\Omega)$, but the velocity gets approximated with H(curl)-conforming elements. This approach will be extended by the introduction of a new variable: the time derivative of the momentum which lives in the dual space of H(curl).

As for the Navier-Stokes equations we assume in the whole section a bounded domain $\Omega \subset \mathbb{R}^n$ with smooth boundary $\partial\Omega = \Gamma_N \dot{\cup} \Gamma_D$, divided into its Dirichlet and Neumann part. The triangulation of Ω is again denoted by $\mathcal{T}_h$.

6.1 Spatial discretization of the elasticity equation

As the natural space of the displacement d is $[H^1(\Omega)]^n$, we will treat first only the elasticity problem 4.9. As before, we start by considering the continuous problem, but specify immediately the according Sobolev spaces.

We multiply (4.25a) with a test function $w \in [H^1_{\Gamma_D}(\Omega)]^n$, integrate over Ω and use integration by parts on the left-hand side to obtain

$$-\int_\Omega \operatorname{div}(F\Sigma) \cdot w \, dx = \int_\Omega (F\Sigma) : \nabla w \, dx - \int_{\Gamma_N} (F\Sigma)_n \cdot w \, ds, \tag{6.2}$$

and the variational formulation reads:

6.1 Problem. *For a given $f \in L^2(\Omega)$ and $d_D \in H^{\frac{1}{2}}(\Gamma_D)$ find $d \in [H^1(\Omega)]^n$ such that*

$$\int_\Omega (F\Sigma) : \nabla w \, dx = \int_\Omega f \cdot w \, dx + \int_{\Gamma_N} (F\Sigma)_n \cdot w \, ds \quad \forall w \in [H^1_{\Gamma_D}(\Omega)]^n, \tag{6.3a}$$

$$d = d_D \text{ on } \Gamma_D. \tag{6.3b}$$

We define the nonlinear and nonsymmetric "bilinear from"

$$k(d, w) := \int_\Omega (F\Sigma) : \nabla w \, dx. \tag{6.4}$$

The existence and uniqueness of a solution of problem 6.1 is more advanced than for the Stokes problem. One can use the poly-convexity to minimize the energy functional (see [Tal94]), but with this approach the continuous dependency on the given data is missing.

Another possibility is to use the implicit function theorem (see [Cia94]), which has the disadvantage that very high regularity assumptions have to be made.

For a given triangulation $\mathcal{T}_h$ of Ω, we choose for the finite element space for the displacement

$$D_h := [\Pi^k(\mathcal{T}_h)]^n \cap [C^0(\Omega)]^n \tag{6.5}$$

and

$$D_{h,\Gamma_D} := \{d_h \in D_h : \, d_h = 0 \text{ on } \Gamma_D\}. \tag{6.6}$$

Hence, the discrete problem is:

6.2 Problem. *Find $d_h \in D_h$ such that*

$$k(d_h, w_h) = f(w_h) + \int_{\Gamma_N} \sigma_n \cdot w_h \, ds \quad \forall w_h \in D_{h,\Gamma_D}. \tag{6.7}$$

As already mentioned in the previous section, the remaining boundary term will play a crucial rule. Later on we will use the notation

$$\sigma^s := \sigma = F\Sigma \tag{6.8}$$

for the first Piola-Kirchhoff stress tensor.

We define the vector $K(d_h)$ and the operator $K(\cdot)$ as preparation for the time discretization

$$K_i(d_h) := \int_\Omega (F\Sigma) : \nabla \varphi_i \, dx \quad \forall i = 0, \ldots, N_D, \tag{6.9}$$

where $\{\varphi_i\}_{i=0}^{N_D}$ denote the shape functions of the space D_h.

6.2 H1-conforming time discretization

This method approximates both quantities with elements in $H^1(\Omega)$. For the linear wave equation

$$\frac{\partial^2 d}{\partial t^2} - \Delta d = f \tag{6.10}$$

two different methods with good properties were developed, symplectic Runge Kutta methods and the Newmark method (see [New59]). In this thesis, however, we will consider only the Newmark method as it fits better in the fluid-structure setting.

6.2.1 Newmark methods

Newmark methods were constructed for conserving the total energy in wave equations. For linear operators K one can show that the energy is preserved exactly and the implicit methods are unconditionally stable, whereas explicit ones are only conditionally stable. The dependency in the time parameter τ is only linear to the spatial discretization parameter h compared with parabolic equations with a dependency of h^2, which makes explicit methods a bit more popular for wave equations.

To use a kind of a Newmark scheme we start with (6.1). As in the last section, the interval $[0, T]$ is divided in equidistant steps with the step size τ. We integrate both equations with respect to time and use the midpoint rule

$$\int_{t_n}^{t_{n+1}} f(s)\, ds \approx \tau f\left(\frac{t_{n+1} + t_n}{2}\right) \tag{6.11}$$

as an integration scheme for the right-hand side of (6.1a) and for the operator $K(\cdot)$, whereas the explicit Euler scheme for the external forces f is used

$$d^{n+1} = d^n + \frac{\tau}{2}(u^{n+1} + u^n), \tag{6.12a}$$

$$u^{n+1} = u^n + \tau M^{-1}\left(f^n - K\left(\frac{d^{n+1} + d^n}{2}\right)\right). \tag{6.12b}$$

With the mass matrix M arising from the spatial discretization of $\rho\frac{\partial u}{\partial t}$

$$M_{ij} := \int_\Omega \rho\varphi_i \cdot \varphi_j\, dx \quad \forall i, j = 0, \ldots, N_D,$$

where $\{\varphi_i\}$ are again the shape functions of D_h.

We can eliminate the displacement by plugging the first into the second equation, which yields

$$u^{n+1} = u^n + \tau M^{-1}\left(f^n - K\left(d^n + \frac{\tau}{4}(u^{n+1} + u^n)\right)\right). \tag{6.13}$$

Here, only u^{n+1} is unknown and can be calculated. After the new velocity has been computed, the displacement for the next step can be reconstructed by (6.12a).

The drawback of this method is that for nonlinear solid mechanics a nonlinear system has to be solved in every step which is quite expensive and slow. On the other hand just using the explicit Euler scheme in (6.1) and solving the explicit system

$$d^{n+1} = d^n + \tau u^n, \tag{6.14a}$$

$$u^{n+1} = u^n + \tau M^{-1} \left(f^n - K \left(d^n + \frac{\tau}{2} u^n \right) \right), \tag{6.14b}$$

is cheap but rather unstable due to the nonlinearity of $K(\cdot)$ and therefore not suited for our needs.

6.2.2 Linear-implicit Runge-Kutta methods

A good compromise is to use so called linear-implicit Runge-Kutta methods. The idea is to construct a scheme which is implicit in the linear case, but explicit in the nonlinear terms, while guaranteeing stability. Such methods are also called Rosenbrock methods or Rosenbrock-Wanner-methods (short ROW-methods). For detailed informations to linear-implicit Runge-Kutta methods we refer to [DB13].

For a short derivation we assume an autonomous ordinary differential equation (ODE) with a nonlinear right-hand side $f \in C^1(\Omega, \mathbb{R}^n)$

$$x'(t) = f(x). \tag{6.15}$$

The idea is to add and subtract the gradient of f, $Jx = J(x) := Df(x)$, which is obviously linear

$$x'(t) = Jx(t) + (f(x(t)) - Jx(t)). \tag{6.16}$$

Now the first term is treated implicitly and the second and last one explicitly, which yields

$$\frac{x^{n+1} - x^n}{\tau} \approx Jx^{n+1} + (f(x^n) - Jx^n). \tag{6.17}$$

6.3 Remark. *If the right-hand side f is linear, then $J = Df(x) = f$ and the last two terms cancel. Then the equation is treated only implicit*

$$\frac{x^{n+1} - x^n}{\tau} \approx f(x^{n+1})$$

and thus the name linear-implicit.

More general, similar to Runge-Kutta methods, the discrete evolution can be described by the following system

$$x^{n+1} = x^n + \tau \sum_{j=1}^{s} b_j k_j, \tag{6.18a}$$

$$k_j = J(x + \tau \sum_{j=1}^{i} \beta_{ij} k_j) + (f(x + \tau \sum_{j=1}^{i-1} \alpha_{ii} k_j) - J(x + \tau \sum_{j=1}^{i-1} \beta_{ij} k_j)) \tag{6.18b}$$

which are called linear-implicit methods of order s.

We will use only the first-order ROW-method where we set

$$b_1 = 1,\ \beta_{11} = 1,\ \alpha_{11} = 0, \tag{6.19}$$

to obtain the following scheme

$$x^{n+1} = x^n + \tau(I - \tau J)^{-1} f(x^n). \tag{6.20}$$

6.4 Remark. *By adding the gradient evaluated at x^n we obtain a linear operator, which, if combined with an implicit term Jx^{n+1}, increases the region of absolute stability extremely.*

The ROW-method for the elastic wave equation (6.1) reads

$$J^n = K'(d^n), \tag{6.21a}$$

$$u^{n+1} = u^n + \tau \left(M + \frac{\tau^2}{2} J^n \right)^{-1} \left(f^n - K(d^n) - \tau J^n u^n \right), \tag{6.21b}$$

$$d^{n+1} = d^n + \frac{\tau}{2}(u^{n+1} + u^n). \tag{6.21c}$$

With this a linear system has to be solved at every time step, which is much more efficient and avoids Newton-like methods.

6.2.3 Crank-Nicolson method for the elastic wave equation

Again, like for the IMEX scheme for the Navier-Stokes equations, the ROW method is only of first order accuracy. It is also possible to use the Crank-Nicolson scheme directly for the elastic wave equation and use Newton's method (algorithm 5.1) to solve the nonlinear system, which is of second order and a bit simpler to implement. The arising system reads:

$$M(u^{n+1} - u^n) - \tau f^n + \tau K(d^n + \frac{\tau}{4}(u^{n+1} + u^n)) = 0, \tag{6.22a}$$

$$d^{n+1} = d^n + \frac{\tau}{2}(u^{n+1} + u^n), \tag{6.22b}$$

or, if everything is put into a huge bilinear form and use the trapezoidal rule

$$\begin{aligned} M_I(\frac{\tau}{2}(u^{n+1}+u^n) - d^{n+1} + d^n) + M(u^{n+1}-u^n) - \tau f^n + \\ \frac{\tau}{2}(K(d^{n+1}) + K(d^n)) = 0, \end{aligned} \tag{6.23}$$

with the according trivial mass bilinear form to the operator M_I

$$m_I(u,v) := \int_\Omega d \cdot w \, dx. \tag{6.24}$$

6.3 H(curl)-conforming time discretization

For the second method we use different spaces for the displacement and the velocity, which will be motivated in this section.

6.3.1 Motivation

The displacement is going to be in $[H^1(\Omega)]^n$ again, but the velocity lives now in the space $H(\mathrm{curl}, \Omega)$ defined as

$$H(\mathrm{curl}, \Omega) := \{u \in [L^2(\Omega)]^n : \mathrm{curl}(u) \in [L^2(\Omega)]^n\}. \tag{6.25}$$

Another huge difference is that the velocity is going to be treated in material coordinates and not in deformed coordinates, which can be seen as following. If the displacement of a material point $X \in \mathbb{R}^n$ is d_0 at time t_0 and d_1 at t_1 then the velocity in deformed coordinates is approximatively $\frac{d_1 - d_0}{t_1 - t_0} \approx u$.

For the situation in figure 6.1 on the facing page the velocity in the reference configuration points left, but in material coordinates it should point upwards, which can be reached by using the covariant transformation

$$u := F^{-T} u_R \tag{6.26}$$

with the deformation gradient F. Now, the material velocity u_R points in the correct direction in the reference configuration Ω_R.

The choice of H(curl)-conforming elements ensures that the material velocity u_R is in $H(\mathrm{curl}, \Omega_R)$ if and only if the global velocity u is in $H(\mathrm{curl}, \Omega)$, like the Piola transformation for H(div)-conforming elements.

Furthermore, the use of H(curl)-conforming elements yields to the exact conservation of rigid body rotations. Assume the deformation Φ is described by a rotation $R \in SO(2)$ in two dimensions

$$\Phi(x,y) = \begin{pmatrix} \cos(t) & \sin(t) \\ -\sin(t) & \cos(t) \end{pmatrix} \begin{pmatrix} x \\ y \end{pmatrix} =: R\vec{x}, \tag{6.27}$$

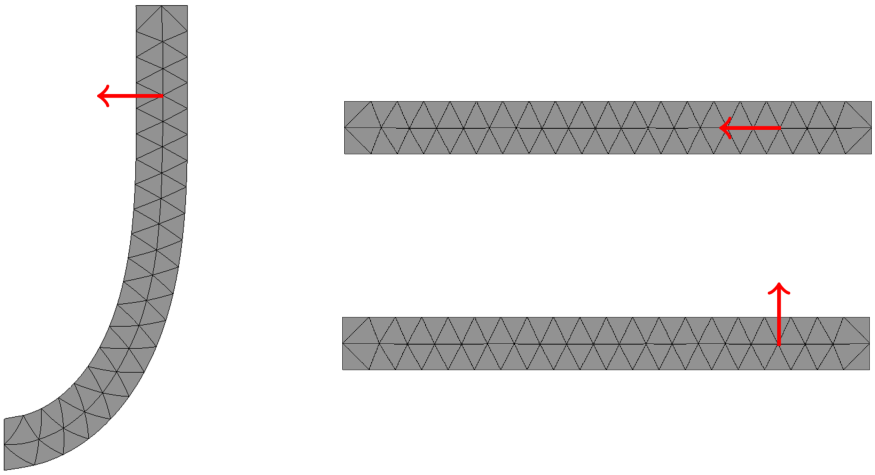

Figure 6.1: Left: global velocity in deformed configuration, right top: global velocity in reference configuration, right bottom: material velocity in reference configuration

with $t \in [0, 2\pi]$. Then the deformation gradient F is R. By defining the velocity as

$$u = \frac{\partial (R\vec{x})}{\partial t} = \dot{R}\vec{x}$$

and using the covariant transformation yields

$$u_R = F^T u = R^T \dot{R}\vec{x}. \tag{6.28}$$

By differentiating the identity $R^T R = I$ we immediately deduce that $R^T \dot{R} = -\dot{R}^T R$ is skew symmetric and thus, $R^T \dot{R}\vec{x}$ lies exactly in the lowest order Nédélec space of 1st-kind (see section below).

6.3.2 H(curl)-conforming elements

Like for $H(\text{div})$ we give a short overview about the Sobolev space $H(\text{curl})$.

To obtain a global function u_h in $H(\text{curl}, \Omega)$ the tangential component has to be continuous over the interfaces

$$N_h := \{u_h \in [\Pi^k(\mathcal{T}_h)]^2 : [\![u_h \cdot \tau]\!] = 0, \forall E \in \mathcal{F}_h\}, \tag{6.29}$$

where τ denotes the tangent vector in two dimensions. In three dimensions the tangential component of u_h has to be continuous over the faces.

6.5 Lemma. *Let $\mathcal{T}_h$ be a triangulation of a domain Ω. A function u is in $H(\mathrm{curl}, \Omega)$ if and only if $u \in H(\mathrm{curl}, T)$ for all triangles $T \in \mathcal{T}_h$ and the tangential jump $[\![u]\!]_\tau$ vanishes on all interior interfaces $\gamma_{ij} := \overline{T_i} \cap \overline{T_j}$, $i \neq j$.*

Similar to the H(div)-conforming elements there are two common H(curl)-conforming elements, the Nédélec elements of 1st- and 2nd-kind, see [Néd80] and [Néd86].

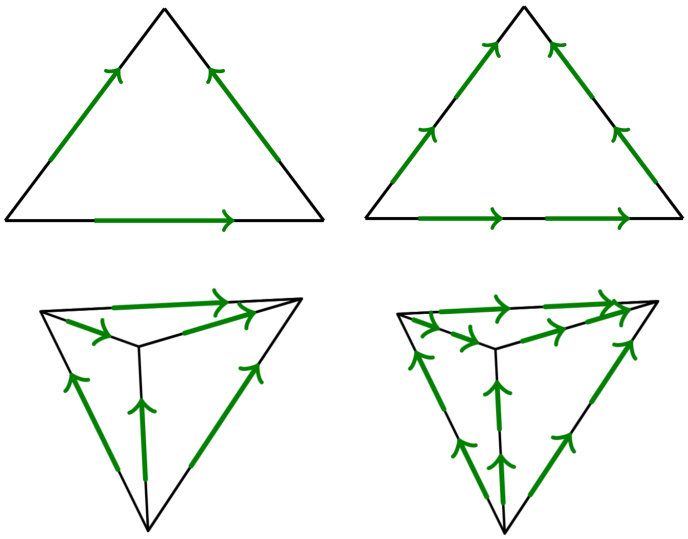

Figure 6.2: Lowest order Nédélec elements of 1st- and 2nd-kind in two and three dimensions

The Nédélec elements of 1st-kind of order k lie between the polynomial spaces of order $k-1$ and k, whereas the other uses the whole polynomial degree (see figure 6.2). For example the lowest order Nédélec space of 1st-kind in three dimensions is

$$\mathcal{N}_{1,0} = \{a + b \times x : a, b \in \mathbb{R}^3\}. \tag{6.30}$$

In two dimensions the Nédélec elements are the Raviart-Thomas and BDM-elements, only rotated by 90 degrees, but in three dimensions they are different (compare figure 5.2 and figure 6.2). For details about the construction of high order Nédélec elements we refer to [Zag06] and [SZ05].

As mentioned before the covariant transformation ensures the tangential continuity on physical elements. Moreover, the covariant transformation has the following properties:

6.6 Theorem (Covariant transformation). *Let $\Phi : \hat{T} \to T$ be a diffeomorphic mapping from the reference element $\hat{T}$ to a physical element T. Let $\hat{u} \in H(\mathrm{curl}, \hat{\Omega})$. Then, the covariant transformation defined by*

$$u := F^{-T}\hat{u} \circ \Phi^{-1}, \tag{6.31}$$

where F denotes the gradient of Φ and $J = \det F$, has the following properties:

1. *Let $\Omega \subset \mathbb{R}^3$. Then u is in $H(\mathrm{curl}, \Omega)$ with*

$$\mathrm{curl}_x(u) = P[\mathrm{curl}_{\hat{x}}(\hat{u})] = \frac{1}{J} F \mathrm{curl}_{\hat{x}}(\hat{u}) \circ \Phi^{-1}. \tag{6.32}$$

2. *Let $\Omega \subset \mathbb{R}^2$. Then u is in $H(\mathrm{curl}, \Omega)$ with*

$$\mathrm{curl}_x(u) = \frac{1}{J} \mathrm{curl}_{\hat{x}}(\hat{u}) \circ \Phi^{-1}. \tag{6.33}$$

3. *Let furthermore $\hat{e}$ be an edge of the reference element and $e = \Phi(\hat{e})$. Then*

$$\int_e u \cdot \tau_e \, ds = \int_{\hat{e}} \hat{u} \cdot \tau_{\hat{e}} \, d\hat{s}. \tag{6.34}$$

Proof. Direct calculations, see e.g. [Sch09a, p. 18 f]. □

6.7 Remark. *At first, the factor $\frac{1}{J}F$ in (6.32) seems strange, but with it the following identity holds*

$$\mathrm{div}(\mathrm{curl}(u)) = \mathrm{div}(P[\mathrm{curl}(\hat{u})]) = \frac{1}{J} \mathrm{div}(\mathrm{curl}(\hat{u})) \circ \Phi^{-1} = 0, \tag{6.35}$$

i.e. the exact sequence from the continuous level is inherited by the discrete one if the H(div)- and H(curl)-conforming elements are chosen. This is reflected in the de Rham complex in three dimensions:

$$\begin{array}{ccccccc} H^1 & \xrightarrow{\nabla} & H(\mathrm{curl}) & \xrightarrow{\mathrm{curl}} & H(\mathrm{div}) & \xrightarrow{\mathrm{div}} & L2 \\ \bigcup & & \bigcup & & \bigcup & & \bigcup \\ Q_h & \xrightarrow{\nabla_h} & V_h & \xrightarrow{\mathrm{curl}_h} & W_h & \xrightarrow{\mathrm{div}_h} & S_h \end{array}$$

6.3.3 Complete discretization

Let Ω_R be the reference configuration of the solid domain and $\Phi(\Omega_R) =: \Omega$ the deformed state. For simplicity we assume homogeneous Dirichlet and Neumann data. In this subsection we will write $\frac{D\cdot}{Dt}$ instead of $\frac{\partial\cdot}{\partial t}$ for the material time derivative (see remark

4.14).

The starting point is again (6.1), where we look for $d \in L^2((0,T), H^1(\Omega_R))$ and $u \in L^2((0,T), H(\mathrm{curl}, \Omega))$ such that

$$\frac{Dd}{Dt} = u, \tag{6.36a}$$

$$\rho \frac{Du}{Dt} = \mathrm{div}(F\Sigma). \tag{6.36b}$$

We differentiate the velocity in local body frame $u_R \in L^2((0,T), H(\mathrm{curl}, \Omega_R))$

$$u_R = F^T u \circ \Phi \tag{6.37}$$

with respect to time and obtain

$$\begin{aligned} \frac{Du_R}{Dt} &= \frac{DF^T}{Dt} u + F^T \frac{Du}{Dt} \\ \Leftrightarrow F^{-T} \frac{Du_R}{Dt} &= F^{-T} \frac{DF^T}{Dt} F^{-T} u_R + \frac{Du}{Dt} \end{aligned} \tag{6.38}$$

6.8 Remark. *We remember that there holds $u(x_R, t) = u(\Phi(x_R, t), t) = u(x, t)$ (see section 2).*

Now, we multiply the first equation (6.36a) with F^{-T} and the test function $v_R \in H(\mathrm{curl}, \Omega_R)$ and integrate over the domain Ω_R

$$\int_{\Omega_R} \frac{Dd}{Dt} F^{-T} v_R \, dx_R = \int_{\Omega_R} (F^{-T} u_R)(F^{-T} v_R) \, dx_R = \int_{\Omega_R} C^{-1} u_R v_R \, dx_R. \tag{6.39}$$

For the second equation (6.36b) we use (6.38), multiply with $w \in [H^1(\Omega_R)]^n$ and integrate over Ω_R

$$\int_{\Omega_R} \rho F^{-T} \frac{Du_R}{Dt} w \, dx_R = \int_{\Omega_R} \left(\rho F^{-T} \frac{DF^T}{Dt} F^{-T} u_R + \mathrm{div}(F\Sigma) \right) w \, dx_R \tag{6.40}$$

Summing up, the continuous problem reads:

6.9 Problem. *Find $d \in L^2((0,T),[H^1_{\Gamma_D}(\Omega_R)]^n)$ and $u_R \in L^2((0,T),H(\mathrm{curl},\Omega_R))$ such that for all $t \in [0,T]$*

$$\int_{\Omega_R} \frac{Dd}{Dt} F^{-T} v_R \, dx_R = \int_{\Omega_R} C^{-1} u_R v_R \, dx_R \qquad \forall v_R \in H(\mathrm{curl},\Omega_R), \tag{6.41a}$$

$$\int_{\Omega_R} \rho F^{-T} \frac{Du_R}{Dt} w \, dx_R = \int_{\Omega_R} (\rho F^{-T} \frac{DF^T}{Dt} F^{-T} u_R + \mathrm{div}(F\Sigma)) \, dx_R \qquad \forall w \in [H^1_{\Gamma_D}(\Omega_R)]^n. \tag{6.41b}$$

After the spatial discretization of (6.41) with the finite element spaces D and N for the displacement and velocity, respectively, the time discretization is done using a mix of the midpoint and trapezoidal rule. With the notation

$$f_{n+\frac{1}{2}}(x(t)) := f\left(\frac{x^{n+1}+x^n}{2}\right) \tag{6.42}$$

we obtain:

6.10 Problem. *Find $(d^{n+1}, u_R^{n+1}) \in D \times N$ such that*

$$\int_{\Omega_R} \frac{d^{n+1}-d^n}{\tau} F^{-T}_{n+\frac{1}{2}} v_R \, dx_R = \int_{\Omega_R} C^{-1}_{n+\frac{1}{2}} u_{R,n+\frac{1}{2}} v_R \, dx_R \qquad \forall v_R \in N, \tag{6.43a}$$

$$\int_{\Omega_R} \rho F^{-T}_{n+\frac{1}{2}} \frac{u_R^{n+1}-u_R^n}{\tau} w \, dx_R = \int_{\Omega_R} (\rho F^{-T}_{n+\frac{1}{2}} \frac{(F^T)^{n+1}-(F^T)^n}{\tau} F^{-T}_{n+\frac{1}{2}} u_{R,n+\frac{1}{2}} + \mathrm{div}(F_{n+\frac{1}{2}} \Sigma(C_{n+\frac{1}{2}}))) w \, dx_R \qquad \forall d \in D. \tag{6.43b}$$

6.11 Remark. *For a complete midpoint rule discretization we would obtain terms of the form*

$$F^T_{n+\frac{1}{2}} F_{n+\frac{1}{2}}$$

instead of

$$C_{n+\frac{1}{2}}.$$

This has the drawback that rigid body motions, which would lead to $C = 0$, are not discretized correctly. Using $C_{n+\frac{1}{2}}$ overcomes this problem as the rigid body motions then get interpolated.

6.3.4 Further discretization in 3d

Instead of discretizing $\frac{DF^T}{Dt}$ directly with the difference quotient, we can rewrite the term $F^{-T}\frac{DF^T}{Dt}F^{-T}u_R$ as following:

$$\begin{aligned} F^{-T}\frac{DF^T}{Dt}F^{-T}u_R &= F^{-T}\left(\nabla_{x_R}u\right)^T F^{-T}u_R \\ &= (\nabla_x u)^T u \\ &= \operatorname{sym}(\nabla_x u)u - \operatorname{skew}(\nabla_x u)u \\ &= \operatorname{sym}(\nabla_x u)u - \frac{1}{2}\operatorname{curl}_x(u)\times u \\ &\overset{(6.32)}{=} \operatorname{sym}(F^{-T}\dot{F}^T)F^{-T}u_R - \frac{1}{2}J^{-1}F\operatorname{curl}_{x_R}(u_R)\times F^{-T}u_R, \end{aligned}$$

where we used the transformation rule for gradients, i.e. $\nabla_{x_R}u = \nabla_x u F$, split $\nabla_x u$ into its symmetric and skew-symmetric part and used the following identity

$$\operatorname{skew}(\nabla_x u)v = \frac{1}{2}\begin{pmatrix} 0 & \frac{\partial u_1}{\partial y} - \frac{\partial u_2}{\partial x} & \frac{\partial u_1}{\partial z} - \frac{\partial u_3}{\partial x} \\ \frac{\partial u_2}{\partial x} - \frac{\partial u_1}{\partial y} & 0 & \frac{\partial u_2}{\partial z} - \frac{\partial u_3}{\partial y} \\ \frac{\partial u_3}{\partial x} - \frac{\partial u_1}{\partial z} & \frac{\partial u_3}{\partial y} - \frac{\partial u_2}{\partial z} & 0 \end{pmatrix} v = \frac{1}{2}\operatorname{curl}_x(u)\times v, \tag{6.44}$$

which holds for all $u \in C^1(\mathbb{R}^3,\mathbb{R}^3)$ and $v \in \mathbb{R}^3$. In the last step we used the property of the covariant transformation.

Thus, the new problem reads:

6.12 Problem (H(curl)-dynamics 3d). *For $\Omega \subset \mathbb{R}^3$, find $d \in L^2((0,T),[H^1_{\Gamma_D}(\Omega_R)]^n)$ and $u_R \in L^2((0,T),H(\operatorname{curl},\Omega_R))$ such that for all $t \in [0,T]$*

$$\int_{\Omega_R}\frac{Dd}{Dt}\cdot F^{-T}v_R\,dx_R = \int_{\Omega_R} C^{-1}u_R\cdot v_R\,dx_R \qquad \forall v_R \in H(\operatorname{curl},\Omega_R), \tag{6.45a}$$

$$\begin{aligned} \int_{\Omega_R}\rho F^{-T}\frac{Du_R}{Dt}\cdot w\,dx_R &= \int_{\Omega_R}\rho\operatorname{sym}(F^{-T}\dot{F}^T)F^{-T}u_R\cdot w\,dx_R \\ &\quad - \int_{\Omega_R}\frac{\rho}{2}J^{-1}F\operatorname{curl}_{x_R}(u_R)\times F^{-T}u_R\cdot w\,dx_R \\ &\quad - \int_{\Omega_R} F\Sigma : \nabla w\,dx_R \qquad \forall w \in [H^1_{\Gamma_D}(\Omega_R)]^n. \end{aligned} \tag{6.45b}$$

For this problem, a time discretization similar to (6.43) can be applied.

6.3.5 Further discretization in 2d

Identity (6.32) holds only if $\Omega \subset \mathbb{R}^3$, but in two dimensions (6.33) can be used instead. Relation (6.44) has to be replaced by

$$\begin{aligned}\operatorname{skew}(\nabla_x u)v &= \frac{1}{2}\begin{pmatrix} 0 & \frac{\partial u_1}{\partial y} - \frac{\partial u_2}{\partial x} \\ \frac{\partial u_2}{\partial x} - \frac{\partial u_1}{\partial y} & 0 \end{pmatrix} v \\ &= \frac{1}{2}(\frac{\partial u_1}{\partial y} - \frac{\partial u_2}{\partial x})\begin{pmatrix} v_2 \\ -v_1 \end{pmatrix} \\ &= -\frac{1}{2}\operatorname{curl}_x(u)\begin{pmatrix} v_2 \\ -v_1 \end{pmatrix} \\ &= -\frac{1}{2}\operatorname{curl}_x(u)\operatorname{rot}(v).\end{aligned} \tag{6.46}$$

We compute $\operatorname{rot}(u) = \operatorname{rot}(F^{-T}u_R)$

$$\begin{aligned}\operatorname{rot}(F^{-T}u_R) &= \frac{1}{J}\operatorname{rot}(\begin{pmatrix} F_{22} & -F_{21} \\ -F_{12} & F_{11} \end{pmatrix}\begin{pmatrix} u_{R1} \\ u_{R2} \end{pmatrix}) \\ &= \frac{1}{J}\operatorname{rot}(\begin{pmatrix} F_{22}u_{R1} - F_{21}u_{R2} \\ -F_{12}u_{R1} + F_{11}u_{R2} \end{pmatrix}) \\ &= \frac{1}{J}\begin{pmatrix} F_{11}u_{R2} - F_{12}u_{R1} \\ F_{21}u_{R2} - F_{22}u_{R1} \end{pmatrix} \\ &= \frac{1}{J}F\operatorname{rot}(u_R),\end{aligned} \tag{6.47}$$

which yields

$$\begin{aligned}F^{-T}\frac{DF^T}{Dt}F^{-T}u_R &= \operatorname{sym}(\nabla_x u)u - \operatorname{skew}(\nabla_x u)u \\ &= \operatorname{sym}(F^{-T}\dot{F}^T)F^{-T}u_R + \frac{1}{2}\operatorname{curl}_x(u)\operatorname{rot}(u) \\ &\overset{(6.33)}{=} \operatorname{sym}(F^{-T}\dot{F}^T)F^{-T}u_R + \frac{1}{2J}\operatorname{curl}_{x_R}(u_R)\operatorname{rot}(F^{-T}u_R) \\ &\overset{(6.47)}{=} \operatorname{sym}(F^{-T}\dot{F}^T)F^{-T}u_R + \frac{1}{2J^2}\operatorname{curl}_{x_R}(u_R)(F\operatorname{rot}(u_R)).\end{aligned}$$

6.13 Remark. *Note that there holds*

$$J^2 = \det(F)\det(F) = \det(F^TF) = \det(C) \tag{6.48}$$

and thus, it can be discretized with $\det(C_{n+\frac{1}{2}})$.

6.14 Problem (H(curl)-dynamics 2d). *For $\Omega \subset \mathbb{R}^2$, find $d \in L^2((0,T), [H^1_{\Gamma_D}(\Omega_R)]^n)$ and $u_R \in L^2((0,T), H(\mathrm{curl}, \Omega_R))$ such that for all $t \in [0,T]$*

$$\int_{\Omega_R} \frac{Dd}{Dt} \cdot F^{-T} v_R \, dx_R = \int_{\Omega_R} C^{-1} u_R \cdot v_R \, dx_R \qquad \forall v_R \in H(\mathrm{curl}, \Omega_R), \tag{6.49a}$$

$$\begin{aligned} \int_{\Omega_R} \rho F^{-T} \frac{Du_R}{Dt} \cdot w \, dx_R = & \int_{\Omega_R} \rho \, \mathrm{sym}(F^{-T} \dot{F}^T) F^{-T} u_R \cdot w \, dx_R \\ & - \int_{\Omega_R} \frac{\rho}{2J^2} \mathrm{curl}_{x_R}(u_R)(F \mathrm{rot}(u_R)) \cdot w \, dx_R \\ & - \int_{\Omega_R} F\Sigma : \nabla w \, dx_R \qquad \forall w \in [H^1_{\Gamma_D}(\Omega_R)]^n. \end{aligned} \tag{6.49b}$$

6.4 H(curl)-velocity-momentum discretization

The discretization method from above works well for pure solid problems, but the coupling with the fluid does not work in this way (see section 8.4.2). Thus, we will introduce another method, where a new variable is used: the time derivative of the momentum. For the sake of simplifying the presentation we assume homogeneous Dirichlet data on the whole boundary $\partial\Omega_R$.

6.4.1 Appropriate space for the time derivative of the momentum

System (6.36) can be rewritten as

$$\frac{Dd}{Dt} = u, \tag{6.50a}$$

$$\rho \frac{Du}{Dt} = p, \tag{6.50b}$$

$$p = \mathrm{div}(F\Sigma). \tag{6.50c}$$

The according weak formulation reads:

6.15 Problem. *Find* $(d, u, p) \in L^2((0,T), D) \times L^2((0,T), N) \times L^2((0,T), H)$ *such that for all* $t \in [0,T]$

$$\int_{\Omega_R} \frac{Dd}{Dt} \cdot q \, dx_R = \int_{\Omega_R} u \cdot q \, dx_R \qquad \forall q \in H, \tag{6.51a}$$

$$\int_{\Omega_R} \rho \frac{Du}{Dt} \cdot v \, dx_R = \int_{\Omega_R} \frac{Dp}{Dt} \cdot v \, dx_R \qquad \forall v \in N, \tag{6.51b}$$

$$\int_{\Omega_R} \frac{Dp}{Dt} \cdot w \, dx_R = -\int_{\Omega_R} F\Sigma : \nabla w \, dx_R \qquad \forall w \in D, \tag{6.51c}$$

with the $[H^1_{\Gamma_D}(\Omega)]^n$ *and* $H(\mathrm{curl}, \Omega)$ *finite element spaces for* D *and* N*, respectively.*

The question now is what finite element space H should be used for the new unknown p, which can physically be interpreted as the time derivative of the momentum?

We make the ansatz of choosing the finite element space for p in such a way that it is bi-orthogonal to the H(curl)-space. If we take a closer look to the variational formulation (6.51), we recognize that with the choice of these spaces the right-hand sides of the first and second equation become block diagonal matrices after the spatial discretization.

This motivates us to use the topological dual space of H(curl) as the appropriate space for the variable p, $H := H(\mathrm{curl})^*$.

The dual space consists for example of functionals of the form

$$\begin{aligned} f : H &\to \mathbb{R} \\ u &\mapsto \int_E u \cdot \tau \, ds, \end{aligned} \tag{6.52}$$

i.e. the evaluation of the tangential component of u over an edge E. Nevertheless, by using Riesz's representation theorem we can identify the dual space with H(curl) again.

6.16 Remark. *Moreover, by using complete discontinuous elements for the velocity and the time derivative of the momentum, we can apply static condensation to eliminate both of them, such that a small system involving only the displacement has to be solved, like for the Newmark method* (6.13)*.*

Next, we discuss the time discretization of system (6.51). Again, we use the covariant transformation to obtain the material velocity and also the variable p gets transformed in material coordinates. As it is dual to the velocity the appropriate transformation is given by

$$p = F p_R. \tag{6.53}$$

6.17 Remark. *With these transformation rules there holds*

$$u \cdot p = (F^{-T} u_R) \cdot (F p_R) = u_R^T F^{-1} F p_R = u_R \cdot p_R. \tag{6.54}$$

6.18 Lemma. *Let $A, B, C \in GL(n)$ and C differentiable. Then there holds*

a) $\operatorname{skew}(ABA^T) = A \operatorname{skew}(B) A^T$.

b) $\frac{\partial C^{-1}}{\partial t} = -C^{-1} \frac{\partial C}{\partial t} C^{-1}$.

Proof. a) Direct calculation shows

$$\operatorname{skew}(ABA^T) = \frac{1}{2}\left(ABA^T - AB^TA^T\right) = \frac{1}{2}A\left(B - B^T\right)A^T = A\operatorname{skew}(B)A^T.$$

b) Differentiating the identity $C^{-1}C = I$ yields

$$\frac{\partial C^{-1}}{\partial t} C + C^{-1}\frac{\partial C}{\partial t} = 0.$$

□

We start with the first equation of (6.51) using the notation from above and (6.54)

$$\int_{\Omega_R} \frac{Dd}{Dt} F q_R \, dx_R = \int_{\Omega_R} u_R q_R \, dx_R. \tag{6.55}$$

The third equation is also easy to transform

$$\int_{\Omega_R} F p_R \cdot w \, dx_R = -\int_{\Omega_R} F\Sigma : \nabla w \, dx_R. \tag{6.56}$$

For the second one we use (6.38) and (6.18b)

$$\int_{\Omega_R} \rho(F^{-T}\frac{Du_R}{Dt} + \frac{DF^{-T}}{Dt}u_R) \cdot F^{-T} v_R \, dx_R = \int_{\Omega_R} p_R \cdot v_R \, dx_R. \tag{6.57}$$

The left-hand side can be rewritten with

$$\begin{aligned}
(\dot{F}^{-T}u_R) \cdot (F^{-T}v_R) &= (F^{-1}\dot{F}^{-T}u_R) \cdot v_R \\
&= ((\operatorname{sym}(F^{-1}\dot{F}^{-T}) + \operatorname{skew}(F^{-1}\dot{F}^{-T}))u_R) \cdot v_R \\
&\overset{(6.18b)}{=} ((\operatorname{sym}(F^{-1}\dot{F}^{-T}) - \operatorname{skew}(F^{-1}F^{-T}\dot{F}^T F^{-T}))u_R) \cdot v_R \\
&= ((\operatorname{sym}(F^{-1}\dot{F}^{-T}) - \operatorname{skew}(F^{-1}\underbrace{F^{-T}F^T}_{=I}(\nabla_x u)^T F^{-T}))u_R) \cdot v_R \\
&\overset{(6.18a)}{=} ((\frac{1}{2}\dot{C}^{-1} - F^{-1}\operatorname{skew}((\nabla_x u)^T)F^{-T})u_R) \cdot v_R \\
&= ((\frac{1}{2}\dot{C}^{-1} + F^{-1}\operatorname{skew}(\nabla_x u)F^{-T})u_R) \cdot v_R.
\end{aligned}$$

6.4.2 Further discretization in 3d

The left part of the scalar product can be further simplified

$$\begin{aligned}\frac{1}{2}\dot{C}^{-1}u_R + F^{-1}\mathrm{skew}(\nabla_x u)F^{-T}u_R &\overset{(6.18a)}{=} -\frac{1}{2}C^{-1}\dot{C}C^{-1}u_R + F^{-1}\mathrm{skew}(\nabla_x u)F^{-T}u_R \\ &\overset{(6.44)}{=} -\frac{1}{2}C^{-1}\dot{C}C^{-1}u_R + \frac{1}{2}F^{-1}\mathrm{curl}_x(u)\times F^{-T}u_R \\ &\overset{(6.32)}{=} -\frac{1}{2}C^{-1}\dot{C}C^{-1}u_R + \frac{1}{2}F^{-1}J^{-1}F\mathrm{curl}_{x_R}(u_R)\times F^{-T}u_R \\ &= -\frac{1}{2}C^{-1}\dot{C}C^{-1}u_R + \frac{1}{2}J^{-1}\mathrm{curl}_{x_R}(u_R)\times F^{-T}u_R.\end{aligned}$$

All together, we obtain the following problem:

6.19 Problem (velocity-momentum method 3d). *For $\Omega\subset\mathbb{R}^3$, find $(d,u,p)\in L^2((0,T),D)\times L^2((0,T),N)\times L^2((0,T),H)$ such that for all $t\in[0,T]$*

$$\int_{\Omega_R}\frac{Dd}{Dt}Fq_R\,dx_R = \int_\Omega u_Rq_R\,dx_R \qquad \forall q\in H, \tag{6.58a}$$

$$\begin{aligned}\int_{\Omega_R}\rho(F^{-T}\frac{Du_R}{Dt}F^{-T}v_R &- \frac{1}{2}C^{-1}\dot{C}C^{-1}u_R \\ &+ \frac{1}{2}J^{-1}\mathrm{curl}_{x_R}(u_R)\times F^{-T}u_R)v_R\,dx_R = \int_{\Omega_R}p_R\cdot v_R\,dx_R \quad \forall v\in N,\end{aligned} \tag{6.58b}$$

$$\int_{\Omega_R}Fp_R\cdot w\,dx_R = -\int_{\Omega_R}F\Sigma:\nabla w \quad \forall w\in D. \tag{6.58c}$$

6.4.3 Further discretization in 2d

In two dimensions, the curl operator and the cross product have to be replaced by (6.33) and (6.46), respectively, to obtain

$$\begin{aligned}\frac{1}{2}\dot{C}^{-1}u_R + F^{-1}\mathrm{skew}(\nabla_x u)F^{-T}u_R &\overset{(6.18a)}{=} -\frac{1}{2}C^{-1}\dot{C}C^{-1}u_R + F^{-1}\mathrm{skew}(\nabla_x u)F^{-T}u_R \\ &\overset{(6.46)}{=} -\frac{1}{2}C^{-1}\dot{C}C^{-1}u_R - \frac{1}{2}F^{-1}\mathrm{curl}_x(u)\mathrm{rot}(F^{-T}u_R) \\ &\overset{(6.47)}{=} -\frac{1}{2}C^{-1}\dot{C}C^{-1}u_R - \frac{1}{2J}F^{-1}F\mathrm{curl}_x(u)\mathrm{rot}(u_R) \\ &\overset{(6.33)}{=} -\frac{1}{2}C^{-1}\dot{C}C^{-1}u_R - \frac{1}{2J^2}\mathrm{curl}_{x_R}(u_R)\mathrm{rot}(u_R)\end{aligned}$$

and the according problem:

6.20 Problem (velocity-momentum method 2d). *For $\Omega \subset \mathbb{R}^2$, find $(d, u, p) \in L^2((0,T), D) \times L^2((0,T), N) \times L^2((0,T), H)$ such that for all $t \in [0,T]$*

$$\int_{\Omega_R} \frac{Dd}{Dt} F q_R \, dx_R = \int_{\Omega} u_R q_R \, dx_R \qquad \forall q \in H, \tag{6.59a}$$

$$\int_{\Omega_R} \rho(F^{-T} \frac{Du_R}{Dt} F^{-T} v_R - \frac{1}{2} C^{-1} \dot{C} C^{-1} u_R - \frac{1}{2J^2} \mathrm{curl}_{x_R}(u_R) \mathrm{rot}(u_R)) v_R \, dx_R = \int_{\Omega_R} p_R \cdot v_R \, dx_R \quad \forall v \in N, \tag{6.59b}$$

$$\int_{\Omega_R} F p_R \cdot w \, dx_R = -\int_{\Omega_R} F\Sigma : \nabla w \quad \forall w \in D. \tag{6.59c}$$

6.5 Numerical example

To compare the Newmark, velocity-dynamics and velocity-momentum method, we give a numerical example in this section.

Parameter	Value
ρ	1
E	2000
ν	0.2
f_g	-5

Table 6.1: Parameters for the elastic wave example

We assume an elastic beam in two dimensions with a length of 10 units and a height of 1 unit. The according physical quantities can be seen in table 6.1.

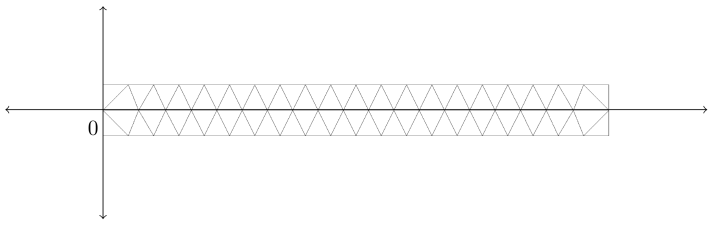

Figure 6.3: Initial mesh with coordinate system

On the left side we prescribe homogeneous Dirichlet data, $d_D = 0$, and on the remaining boundaries the do-nothing condition, $\sigma_n^s = 0$. The right-hand side will be a constant force f_g to simulate gravity and we use the material law of Neo-Hook (4.21), as the deformations are expected to be critical.

We fix the triangulation $\mathcal{T}_h$ of the mesh (see figure 6.3 on the preceding page), use the polynomial order $k = 2$ for all finite element spaces and compute until $T = 10$.

For the Newmark scheme we use (6.22), whereas for the H(curl)-dynamics method (6.41), which we will name dynamicsstart (see figure 6.4 on the following page and figure 6.5 on page 57), and (6.49), which is called just dynamics, are used to show the differences between numerical differentiation and further discretization. The velocity-momentum scheme is (6.59) and the complete discretization for one time step reads reads:

6.21 Problem. *Find* $(d^{n+1}, u_R^{n+1}, p_R^{n+1}) \in (D, N, H)$ *such that*

$$\int_{\Omega^s} \frac{d^{n+1} - d^n}{\tau} F_{n+\frac{1}{2}} q_R \, dx = \int_{\Omega^s} u_{R,n+\frac{1}{2}} q_R \, dx \quad \forall q_R \in H, \tag{6.60a}$$

$$\int_{\Omega^s} \rho(F_{n+\frac{1}{2}}^{-T} \frac{u_R^{n+1} - u_R^n}{\tau} v_R - \frac{1}{2} C_{n+\frac{1}{2}}^{-1} \frac{C^{n+1} - C^n}{\tau} C_{n+\frac{1}{2}}^{-1} - \frac{1}{2\det(C_{n+\frac{1}{2}})} \mathrm{curl}(u_{R,n+\frac{1}{2}}) \mathrm{rot}(u_{R,n+\frac{1}{2}})) v_R \, dx = \int_{\Omega^s} p_{R,n+\frac{1}{2}} v \, dx \quad \forall v_R \in N, \tag{6.60b}$$

$$\int_{\Omega^s} F_{n+\frac{1}{2}} p_{R,n+\frac{1}{2}} w \, dx + \int_{\Omega^s} F_{n+\frac{1}{2}} \Sigma(C_{n+\frac{1}{2}}) : \nabla w \, dx = 0 \quad \forall w \in D. \tag{6.60c}$$

6.22 Remark. *In numerical experiments we did not find any differences, if we use the implicit Euler instead of the midpoint scheme for the variable p in* (6.60).

The first quantity of comparison is the displacement of the beam over time. Therefore, we use the following discrete norm

$$||d||_B^2 := \tau \sum_{i=1}^{n} \left(\int_{\mathcal{T}_h} |\frac{1}{2} \left(d(x, t_i) + d(x, t_{i-1}) \right)|^2 \, dx \right), \tag{6.61}$$

which is a discretization of the following norm

$$||d||_{L^2(0,T;L^2(\Omega))}^2 := \int_0^T ||d(\cdot, t)||_{L^2(\Omega)}^2 \, dt. \tag{6.62}$$

This is a Lebesgue integral of functions that take values in a Banach space (in our case $L^2(\Omega)$). For more details we refer to the theory of Bochner integrals.

Additionally, we compare the property of conserving the total energy

$$E_{tot} = E_{kin} + E_{pot}, \tag{6.63}$$

with the kinetic energy measured over time is given by

$$E_{kin} := \tau \sum_{i=1}^{n} \int_{\mathcal{T}_h} \frac{\rho}{2} |u(x,t_i)|^2 \, dx = \tau \sum_{i=1}^{n} \int_{\mathcal{T}_h} \frac{\rho}{2} |F^{-T} u_R(x,t_i)|^2 \, dx \tag{6.64}$$

and

$$E_{pot} := \tau \sum_{i=1}^{n} \left(\int_{\mathcal{T}_h} N(C(d(x,t_i))) \, dx + \int_{\mathcal{T}_h} d(x,t_i) \cdot \begin{pmatrix} 0 \\ -f_g \end{pmatrix} dx \right) \tag{6.65}$$

the potential energy, which is the sum of the internal stresses of the beam and the effect of the position in the gravity field.

6.23 Remark. *With* (6.65) *as the definition for the potential energy and the chosen coordinate system in figure 6.3 on page 54 the beam has zero energy at the beginning* $t = 0$. *Thus, we can calculate the exact energy error as the norm of the total energy* $|E_{tot}|$.

For the computation of the displacement error we need a reference solution. Unfortunately, there does not exist an analytical solution for this problem, so we use a solution of the Newmark method with a smaller time step as an approximative reference solution d_{ref}. This yields the error estimator

$$e(d) := ||d - d_{ref}||_B. \tag{6.66}$$

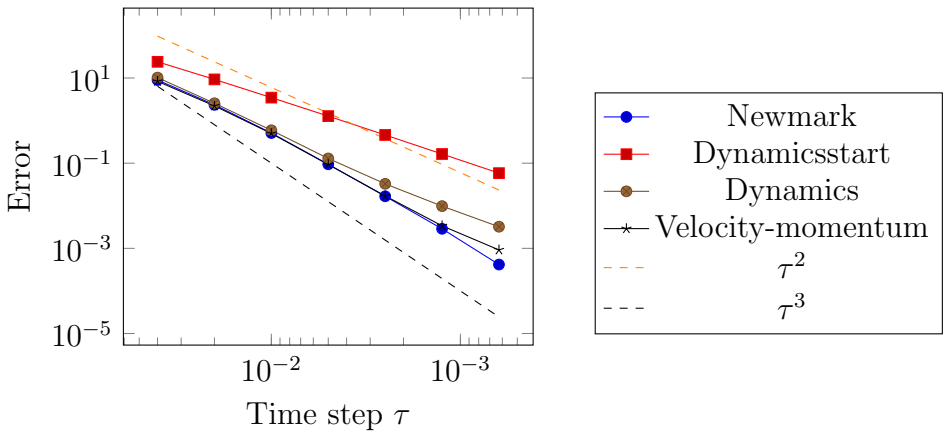

Figure 6.4: Displacement error

As can be seen in figure 6.4 and in table 6.2 on the facing page and 6.3 on page 58 all methods converge to the same solution, where the convergence rate of the dynamicsstart method is the slowest with an order a bit less than 1.5. The dynamics method has an improved second order convergence rate and the velocity-momentum and Newmark

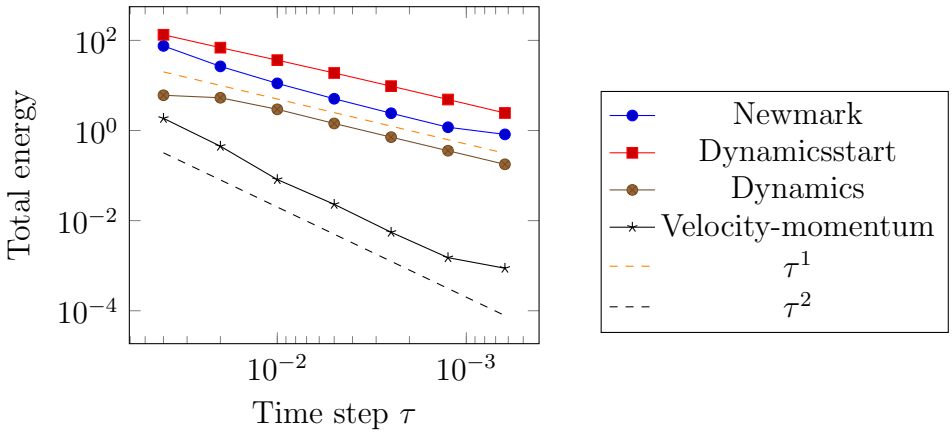

Figure 6.5: Energy error

Timestep	k	error	order
4.00e-2	2	8.99	-
2.00e-2		2.35	3.83
1.00e-2		5.11e-1	4.59
5.00e-3		9.42e-2	5.42
2.50e-3		1.67e-2	5.63
1.25e-3		2.88e-3	5.81
6.25e-4		4.16e-4	6.91

Timestep	k	error	order
4.00e-2	2	24.03	-
2.00e-2		9.28	2.59
1.00e-2		3.46	2.68
5.00e-3		1.27	2.72
2.50e-3		4.60e-1	2.77
1.25e-3		1.64e-1	2.80
6.25e-4		5.84e-2	2.81

Table 6.2: Displacement error of the Newmark and dynamicsstart method

method are the fastest with a rate about 2.5.

For the property of conserving the total energy E_{tot} listed in table 6.4 on the following page and 6.5 on the next page the dynamicsstart method is again worse than all other methods and has a linear convergence rate. The Newmark method provides a linear order in conserving the energy, but starts with a lower error as dynamicsstart. The dynamics method gives a little improvement, but the velocity momentum method has obviously the best conservation property as it is of second order accuracy in time.

Timestep	k	error	order
4.00e-2	2	10.23	-
2.00e-2		2.35	4.01
1.00e-2		5.93e-1	4.31
5.00e-3		1.29e-1	4.59
2.50e-3		3.27e-2	3.95
1.25e-3		9.80e-3	3.34
6.25e-4		3.22e-3	3.05

Timestep	k	error	order
4.00e-2	2	8.35	-
2.00e-2		2.21	3.77
1.00e-2		4.98e-1	4.44
5.00e-3		9.29e-2	5.36
2.50e-3		1.70e-2	5.46
1.25e-3		3.38e-3	5.03
6.25e-4		9.17e-4	3.69

Table 6.3: Displacement error of the dynamics and velocity-momentum method

Time step	k	error	order
4.00e-2	2	75.36	-
2.00e-2		26.51	2.84
1.00e-2		11.12	2.38
5.00e-3		5.07	2.19
2.50e-3		2.42	2.10
1.25e-3		1.18	2.05
6.25e-4		8.21e-1	1.44

Time step	k	error	order
4.00e-2	2	133.20	-
2.00e-2		68.96	1.93
1.00e-2		36.44	1.89
5.00e-3		18.93	1.93
2.50e-3		9.65	1.96
1.25e-3		4.87	1.98
6.25e-4		2.45	1.99

Table 6.4: Energy error of the Newmark and dynamicsstart method

Time step	k	error	order
4.00e-2	2	6.06	-
2.00e-2		5.33	1.14
1.00e-2		2.95	1.81
5.00e-3		1.43	2.06
2.50e-3		7.13e-1	2.01
1.25e-3		3.56e-1	2.00
6.25e-4		1.78e-1	2.00

Time step	k	error	order
4.00e-2	2	1.86	-
2.00e-2		4.48e-1	4.16
1.00e-2		8.17e-2	5.48
5.00e-3		2.30e-2	3.54
2.50e-3		5.52e-3	4.17
1.25e-3		1.51e-3	3.66
6.25e-4		8.78e-4	1.72

Table 6.5: Energy error of the dynamics and velocity-momentum method

7 Arbitrary Lagrangian Eulerian description

As mentioned at the start of this thesis, the problems in fluid dynamics and nonlinear solid mechanics require different descriptions of the motion of the particles. We discuss the advantages and drawbacks of these forms and motivate the usage of a new form, which combines the advantages of both and gives more freedom. For a detailed introduction we refer to [DHPRF04] and [DH03].

7.1 Introduction into ALE

In Lagrangian form each mesh node is identified with a material particle. Using this, the history of a particle can easily be reconstructed. A problem that appears is the instability of the mesh if the deformation is huge as the elements can get extremely stretched, rotated and pressed. Mostly, two domains are used, the material domain $\hat{\Omega}$ which describes the reference domain corresponding to the initial configuration, and the spatial domain Ω corresponding to the current configuration. The deformation function

$$\begin{aligned} &\Phi : \hat{\Omega} \times [0,T] \to \Omega \times [0,T] \\ &(X,t) \mapsto \Phi(X,t) = (x,t) \end{aligned} \tag{7.1}$$

establishes the relation between the material particles X and the spatial points x.
The gradient of Φ with respect to space and time of Φ reads in matrix form

$$\frac{\partial \Phi}{\partial (X,t)} = \begin{pmatrix} \frac{\partial x}{\partial X} & u \\ 0^T & 1 \end{pmatrix}, \tag{7.2}$$

with the material velocity u

$$u(X,t) = \frac{\partial x}{\partial t}\Big|_{X=\text{const}}, \tag{7.3}$$

where the material coordinate X is fixed.

With the Eulerian description the problems are overcome when large deformations occur. Here, the mesh is fixed and the nodes describe the velocity without any reference to the initial state of the continuum

$$u = u(x,t). \tag{7.4}$$

The drawback of the separation of the nodes and the particles is that convective effects appear due to the relative motion of the grid and the material points and thus, the equations become non symmetric and more difficult to solve. Another difficulty occurs if more than one material with different behaviour is used, e.g. a solid beam in a fluid. With a fixed mesh it is nearly impossible to resolve the interface.

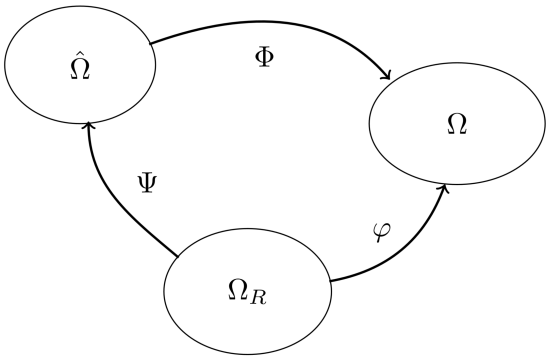

Figure 7.1: ALE domains with the corresponding mappings

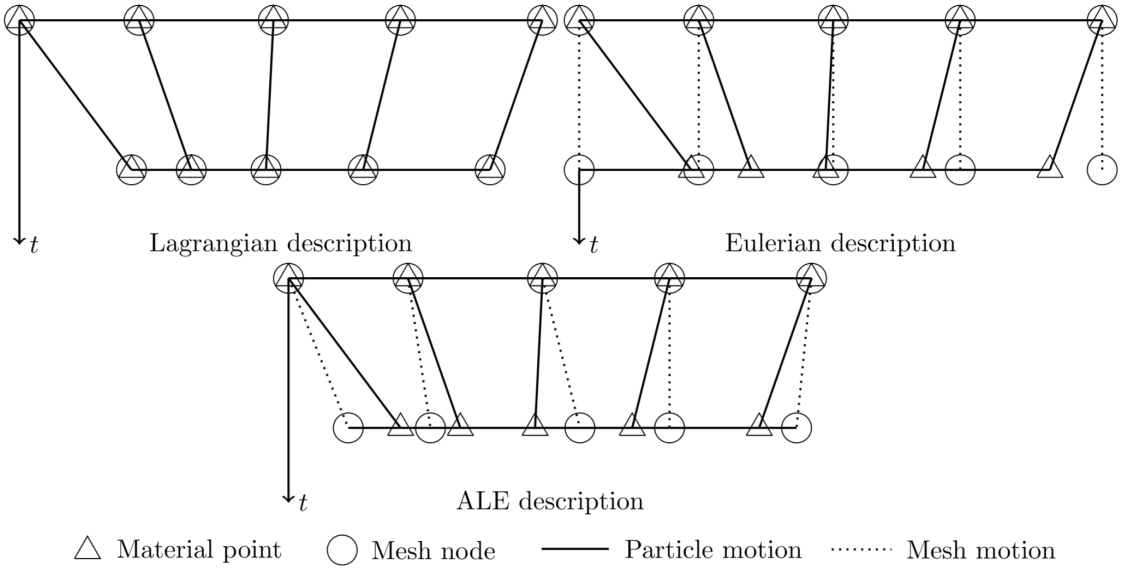

Figure 7.2: Lagrangian, Eulerian and ALE description

The Arbitrary Lagrangian Eulerian (ALE) description is a kind of generalization of the descriptions above. Here, neither the material configuration $\hat{\Omega}$ nor the spatial configuration Ω is taken as the reference configuration. Therefore, a new reference domain Ω_R is introduced where the reference coordinates are identified with the mesh nodes. Now we have three transformations connecting the different configurations. The mapping φ from the reference to the spatial domain is defined by

$$\begin{aligned} &\varphi : \Omega_R \times [0,T] \to \Omega \times [0,T] \\ &(X_R, t) \mapsto \varphi(X_R, t) = (x, t) \end{aligned} \tag{7.5}$$

with the gradient

$$\frac{\partial \varphi}{\partial (X_R, t)} = \begin{pmatrix} \frac{\partial x}{\partial X_R} & \hat{u} \\ 0^T & 1 \end{pmatrix} \tag{7.6}$$

where $\hat{u}$ denotes the mesh velocity

$$\hat{u}(X_R, t) = \frac{\partial x}{\partial t}\Big|_{X_R=\text{const}}. \tag{7.7}$$

Instead of Ψ, the inverse mapping Ψ^{-1} from the material to the reference domain (see figure 7.1)

$$\begin{aligned} &\Psi^{-1} : \hat{\Omega} \times [0,T] \to \Omega_R \times [0,T] \\ &(X,t) \mapsto \Psi^{-1}(X,t) = (X_R, t) \end{aligned} \tag{7.8}$$

is used with its gradient

$$\frac{\partial \Psi^{-1}}{\partial (X,t)} = \begin{pmatrix} \frac{\partial X_R}{\partial X} & w \\ 0^T & 1 \end{pmatrix}. \tag{7.9}$$

Here the velocity w is

$$w = \frac{\partial X_R}{\partial t}\Big|_{X_R=\text{const}}. \tag{7.10}$$

To obtain a relation between the velocities u, $\hat{u}$ and w we differentiate $\Phi = \varphi \circ \Psi^{-1}$

$$\begin{aligned} \frac{\partial \Phi}{\partial (X,t)}(X,t) &= \frac{\partial \varphi}{\partial (X_R,t)}(\Psi^{-1}(X,t)) \frac{\partial \Psi^{-1}}{\partial (X,t)}(X,t) \\ &= \frac{\partial \varphi}{\partial (X_R,t)}(X_R,t) \frac{\partial \Psi^{-1}}{\partial (X,t)}(X,t). \end{aligned} \tag{7.11}$$

The according matrix equation is

$$\begin{pmatrix} \frac{\partial x}{\partial X} & u \\ 0^T & 1 \end{pmatrix} = \begin{pmatrix} \frac{\partial x}{\partial X_R} & \hat{u} \\ 0^T & 1 \end{pmatrix} \begin{pmatrix} \frac{\partial X_R}{\partial X} & w \\ 0^T & 1 \end{pmatrix}, \tag{7.12}$$

which yields the relation

$$u = \hat{u} + \frac{\partial x}{\partial X_R} w \tag{7.13}$$

or by defining the convective velocity c

$$c := u - \hat{u} = \frac{\partial x}{\partial X_R} w \tag{7.14}$$

which gives the relative velocity between the continuum and the mesh.

We note that the Eulerian and Lagrangian description can both be obtained from the ALE formulation by selecting $\Psi = \text{id}$ and $\Phi = \text{id}$, respectively.

The obtained freedom of moving the mesh independently of the particles is not without costs. The mesh deformation must be included in the equations and discretizations, which will be the topic of the rest of this chapter.

7.2 Relations between the different forms of description

A physical quantity can be described in the reference, material and spatial domain:

$$f(x,t),\ f_R(X_R,t),\ \hat{f}(X,t).$$

With the mappings defined above we can relate these quantities. We start with the material and spatial description

$$\hat{f} = f \circ \Phi. \tag{7.15}$$

By differentiating both sides with respect to (X,t) we obtain the following two equations

$$\frac{\partial \hat{f}}{\partial t} = \frac{\partial f}{\partial t} + \frac{\partial f}{\partial x} \cdot u, \tag{7.16a}$$

$$\frac{\partial \hat{f}}{\partial X} = \frac{\partial f}{\partial x}\frac{\partial x}{\partial X}, \tag{7.16b}$$

where (7.16a) is exactly the equation (2.9) from section 2, connecting the material and spatial time derivative. By dropping the different indications for f and using the material and spatial time derivation introduced in section (2.9) we get

$$\frac{Df}{Dt} = \frac{\partial f}{\partial t} + (u \cdot \nabla) f. \tag{7.17}$$

Next, we investigate the relation between the reference and material configuration. There holds

$$\hat{f} = f_R \circ \Psi^{-1} \tag{7.18}$$

and with (7.9) and similar calculations as before we obtain

$$\frac{\partial \hat{f}}{\partial t} = \frac{\partial f_R}{\partial t} + \frac{\partial f_R}{\partial X_R} \cdot w, \tag{7.19a}$$

$$\frac{\partial \hat{f}}{\partial X} = \frac{\partial f_R}{\partial X_R}\frac{\partial X_R}{\partial X}. \tag{7.19b}$$

Working with (7.19) requires the computation of the gradient $\frac{\partial f_R}{\partial X_R}$ in the reference domain, but it is easier to work in the other domains (spatial or material). By using (7.14) and the chain rule equation (7.19a) can be rewritten as

$$\frac{\partial \hat{f}}{\partial t} = \frac{\partial f_R}{\partial t} + \frac{\partial f}{\partial x} \cdot c. \tag{7.20}$$

The third pairing involve the spatial and reference configuration by

$$f_R = f \circ \varphi, \tag{7.21}$$

and differentiating both sides yields

$$\frac{\partial f_R}{\partial t} = \frac{\partial f}{\partial t} + \frac{\partial f}{\partial x}\hat{u}, \tag{7.22a}$$

$$\frac{\partial f_R}{\partial X_R} = \frac{\partial f}{\partial x}\frac{\partial x}{\partial X_R}. \tag{7.22b}$$

7.3 ALE for H1-conforming discretization

For applying the techniques above to the FSI problem we first have to specify the functions between the different configurations. In our case, we identify the reference and material state of the solid domain, $\Psi = \mathrm{id}$, as the deformation is expected to be small enough for a pure Lagrangian description. Thus, only the fluid domain with the Navier-Stokes equations has to be adjusted in this setting.

7.1 Remark. *To avoid misunderstandings: we will always work on a fixed initial mesh, which does not move during the computations. Thus, only the Eulerian description must be adjusted.*

If we choose the Taylor-Hood discretization for the Navier-Stokes equations, the results can be employed without bigger changes. As in the Navier-Stokes equations a physical quantity representing the deformation or displacement does not appear, we have to add an artificial displacement in the fluid domain, which we will denote, as for the solid, with d. In literature the artificial deformation function is often denoted by $\mathcal{A}$. The displacement d will also be discretized with H1-conforming elements.

We start by integrating the weak formulation of the Navier-Stokes equations on the spatial domain over Ω. For simplicity we set $f \equiv 0$ and $\nu = 1$.

$$\begin{aligned}&\int_\Omega \frac{\partial u}{\partial t} \cdot v + (u \cdot \nabla)u \cdot v + \nabla u : \nabla v - \mathrm{div}(v)p \, dx = 0,\\ &-\int_\Omega \mathrm{div}(u)q \, dx = 0\end{aligned}$$

We use the integral transformation theorem and (7.22b) to transform the equations to the reference domain

$$\begin{aligned}&\int_{\Omega_R} J(\frac{\partial u}{\partial t} \circ \varphi \cdot v_R + (\nabla u_R F^{-1} u_R) \cdot v_R + \nabla u_R F^{-1} : \nabla v_R F^{-1} - \mathrm{tr}(\nabla v_R F^{-1}) p_R) \, dx_R = 0,\\ &-\int_{\Omega_R} \mathrm{tr}(\nabla u_R F^{-1}) q_R \, dx_R = 0,\end{aligned}$$

with $F = \nabla\varphi = \frac{\partial x}{\partial X_R}$, $J = \det(F)$, $v_R = v \circ \varphi$, $p_R = p \circ \varphi$, $q_R = q \circ \varphi$ and $u_R = u \circ \varphi$, and use (7.22a) to obtain the ALE description for the fluid part

$$\begin{aligned}&\int_{\Omega_R} J(\frac{\partial u_R}{\partial t} \cdot v_R + \nabla u_R F^{-1}(u_R - \hat{u}) \cdot v_R + \nabla u_R F^{-1} : \nabla v_R F^{-1}\\ &\qquad - \mathrm{tr}(\nabla v_R F^{-1}) p_R) \, dx_R = 0, \qquad (7.23a)\\ &-\int_{\Omega_R} \mathrm{tr}(\nabla u_R F^{-1}) q_R \, dx_R = 0. \qquad (7.23b)\end{aligned}$$

7.2 Remark. *We will denote the mesh velocity $\hat{u}$ in the following with $\frac{\partial d}{\partial t}$ or, more shortly, with $\dot{d}$, where the mapping φ is of the form $\varphi = \mathrm{id} + d$, which helps simplifying*

the notation in section 8.

Therefore, we define the following forms for the Navier-Stokes equations

$$a(d,u,v) := \int_{\Omega_R} \nu J \nabla u_R F^{-1} : \nabla v_R F^{-1} \, dx_R \tag{7.24a}$$

$$c(d,u,v) := \int_{\Omega_R} J \left(\nabla u_R F^{-1} (u_R - \dot{d}) \right) \cdot v_R \, dx_R \tag{7.24b}$$

$$b(d,u,q) := -\int_{\Omega_R} J \mathrm{tr}(\nabla u_R F^{-1}) q_R \, dx_R \tag{7.24c}$$

$$m(d,u,v) := \int_{\Omega_R} J \frac{\partial u_R}{\partial t} \cdot v_R \, dx_R \tag{7.24d}$$

and the according discrete forms for the Taylor-Hood discretization on the triangulation $\mathcal{T}_h$.

7.3 Remark. *We derived the ALE description of the Navier-Stokes equations by using the weak form. It is also possible to deduce them in strong form by using appropriate transformation rules, which yields to the same result.*

We again interpret the forms in (7.24) as the operators M, A, B and C introduced in section 5.4 by adding the additional nonlinear dependency on the artificial displacement

$$\begin{aligned} &M(d)\frac{\partial u}{\partial t} + A(d)u + C(d,\dot{d},u) + B(d)p = 0, \\ &B^T(d)u = 0. \end{aligned} \tag{7.25}$$

To use standard (IMEX) Runge-Kutta methods, the ODE has to be of the following form

$$u'(t) = f(u(t),t)\,. \tag{7.26}$$

Unfortunately, the mass matrix M is now also time-dependent. One possibility is to invert it and define $M^{-1}(t)f(u(t),t) =: F(u(t),t)$ as a new right-hand side. With this method the discretization does have the disadvantage of inverting more than one matrix, which we would like to avoid.

Another idea is to define $M(t)u(t) = y(t)$ as a new unknown y and use the product rule to rewrite (7.26) as

$$(M(t)u(t))' - M'(t)u(t) = f(u(t),t). \tag{7.27}$$

With this substitution we obtain

$$y'(t) - M'(t)M^{-1}(t)y(t) = f(M^{-1}(t)y(t),t)$$

and with a new right-hand side the ODE

$$y'(t) = F(y(t), t) := f(M^{-1}(t)y(t), t) + M'(t)M^{-1}(t)y(t), \tag{7.28}$$

where we can apply the Runge-Kutta methods and, after that, we replace $y(t)$ with $M(t)u(t)$ again.

As before, the stiffness matrix and the pressure terms are treated implicitly and the convection explicitly. The additional term $M'M^{-1}y$ will be discretized later.

To simplify the notation we write a subscript on the operator which refers to the displacement dependency, e.g. $A_{n+1} \hat{=} A(d^{n+1})$, and we will neglect the pressure variable p. Additionally, we use the Stokes operator D from (5.54). This yields

$$\frac{y^{n+1} - y^n}{\tau} = \frac{1}{\tau} \int M'M^{-1}y \, dt - D_{n+1}(M_{n+1}^{-1}y^{n+1}) - C_n(M_n^{-1}y^n). \tag{7.29}$$

After substituting back we get

$$\frac{M_{n+1}u^{n+1} - M_n u^n}{\tau} = \frac{1}{\tau} \int M'u \, dt - D_{n+1}u^{n+1} - C_n(u^n), \tag{7.30}$$

and simple rearranging yields

$$(M_{n+1} + \tau D_{n+1})(u^{n+1} - u^n) = (M_n - M_{n+1})u^n + \int M'u \, dt - \tau \left(D_{n+1}u^n + C_n(u^n)\right). \tag{7.31}$$

In a last step we have to approximate the integral $\int_{t_n}^{t_{n+1}} M'u \, dt$. The derivative can be approximated with the forward, backwards or central differential quotient and u explicitly or implicitly, where every choice leads to a bit different discretization. We list three combinations below with the resulting systems:

- Forward difference quotient $M' \approx \frac{M_{n+1} - M_n}{\tau}$ and explicit $\int u \, dt \approx \tau u^n$

$$(M_{n+1} + \tau D_{n+1})(u^{n+1} - u^n) = -\tau \left(D_{n+1}u^n + C_n(u^n)\right) \tag{7.32}$$

- Forward difference quotient $M' \approx \frac{M_{n+1} - M_n}{\tau}$ and implicit $\int u \, dt \approx \tau u^{n+1}$

$$(M_n + \tau D_{n+1})(u^{n+1} - u^n) = -\tau \left(D_{n+1}u^n + C_n(u^n)\right) \tag{7.33}$$

- Central difference quotient $M' \approx \frac{M_{n+1} - M_{n-1}}{2\tau}$ and explicit $\int u \, dt \approx \tau u^n$

$$(M_{n+1} + \tau D_{n+1})(u^{n+1} - u^n) = \frac{-M_{n+1} + 2M_n - M_{n-1}}{2} u^n - \tau \left(D_{n+1}u^n + C_n(u^n)\right) \tag{7.34}$$

The first approach simplifies the equation as some terms cancel out. If u is treated implicitly also some terms cancel. Note that on the left-hand side now the term M_n appears instead of M_{n+1} and thus, the mass matrix is completely explicit. By using the central difference quotient the mass matrix must be known also from the last step. The fraction remembers on the second derivative of M: $\frac{1}{2}(-M_{n+1} + 2M_n - M_{n-1}) \approx -M''$.

7.4 Remark. *The convection part depends also on the mesh velocity $\dot{d}$. As the convection is treated explicitly, we will approximate the mesh velocity with the backward difference quotient*

$$\dot{d}^n \approx \frac{d^n - d^{n-1}}{\tau}. \tag{7.35}$$

7.5 Remark. *To obtain a second order scheme a second order IMEX method and the central difference quotient* (7.34) *must be used.*

7.4 ALE for H(div)-conforming discretization

For the H(div)-conforming elements the situation is a bit more tangled. The velocity gets transformed with the Piola-transformation (5.34), which depends also on time t. Therefore, we have to calculate the ALE transformation precisely.

With the notation of this section, we relate the velocities u and u_R by

$$u \circ \varphi = P[u_R] := \frac{1}{J} F u_R. \tag{7.36}$$

The time derivative of the determinant $J = \det(F) = \det(\nabla_{x_R}\varphi) = \det(\frac{\partial x}{\partial X_R})$ can be calculated elementary, which is

$$\dot{J} = J\mathrm{div}_x(\dot{\varphi}) = J\mathrm{div}_x(\dot{d}). \tag{7.37}$$

Note that the divergence is taken with respect to the spatial derivative x and not to the reference coordinates x_R.

We differentiate both sides of (7.36) with respect to time t and use the product and chain rule

$$\begin{aligned}
(\nabla_x u) \circ \varphi\, \dot{d} + \frac{\partial u}{\partial t} \circ \varphi &= -\frac{\dot{J}}{J^2} + \frac{1}{J}\dot{F} u_R + P[\dot{u_R}] \\
\overset{(7.37)}{\Leftrightarrow} (\nabla_x u) \circ \varphi\, \dot{d} + \frac{\partial u}{\partial t} \circ \varphi &= \frac{1}{J}\left(\nabla_{x_R}\dot{d}\, u_R - \mathrm{div}_x(\dot{d})\right) + P[\dot{u_R}],
\end{aligned}$$

where we used the Schwarz theorem

$$\frac{\partial F}{\partial t} = \frac{\partial \nabla_{x_R}\varphi}{\partial t} = \nabla_{x_R}\dot{\varphi} = \nabla_{x_R}\dot{d}.$$

With this and the transformation rule for gradients $\nabla_x b = \nabla_{x_R} b F^{-1}$ we obtain

$$\begin{aligned}\frac{\partial u}{\partial t} \circ \varphi &= \frac{1}{J}\left(\nabla_{x_R}\dot{d} - \mathrm{div}_x(\dot{d})F\right) u_R + P[\dot{u_R}] - (\nabla_{x_R} u)F^{-1}\dot{d} \\ &\overset{(7.36)}{=} \frac{1}{J}\left(\nabla_{x_R}\dot{d} - \mathrm{div}_x(\dot{d})F\right) u_R + P[\dot{u_R}] - (\nabla_{x_R} P[u_R])F^{-1}\dot{d}. \end{aligned} \tag{7.38}$$

Now we integrate over the spatial domain Ω, multiply with a test function v, use the integral transformation theorem, plug in (7.38) and note that $v \circ \varphi = P[v_R]$:

$$\begin{aligned}\int_\Omega \dot{u} v \, dx &= \int_{\Omega_R} J\dot{u} \circ \varphi \cdot v \circ \varphi \, dx_R \\ &= \int_{\Omega_R} J(\frac{1}{J}(\nabla_{x_R}\dot{d} - \mathrm{div}_x(\dot{d})F) \underbrace{F^{-1}F}_{=I} u_R + P[\dot{u_R}] - \nabla_{x_R} P[u_R]F^{-1}\dot{d})P[v_R] \, dx_R \\ &= \int_{\Omega_R} J((\nabla_{x_R}\dot{d}F^{-1} - \mathrm{div}_x(\dot{d}))P[u_R] + P[\dot{u_R}] - \nabla_{x_R} P[u_R]F^{-1}\dot{d})P[v_R] \, dx_R. \end{aligned}$$

Note that for the numerical implementations all derivatives with respect to x have to be rewritten as derivatives with respect to x_R. For the divergence the following relation holds

$$\mathrm{div}_x(\dot{d}) = \mathrm{tr}(\nabla_{x_R}\dot{d}F^{-1}). \tag{7.39}$$

For the derivation of the convection part (5.47) integration by parts and the divergence-freeness of the velocity and the wind were used. Now the wind is the convective velocity $u - \dot{d}$, which is not divergence-free, as d is only in $H^1(\Omega)$ and not a $H(\mathrm{div}, \Omega)$ function. Thus, we get the additional term

$$\mathrm{tr}(\nabla_{x_R}\dot{d}F^{-1})P[u]P[v], \tag{7.40}$$

which cancels with (7.39).

The transformation of the other terms of the H(div)-conforming HDG formulation of the Navier-Stokes equations can be calculated in a straight-forward fashion using the integral transformation theorem and the transformation rule for gradients and the divergence rule for H(div)-conforming elements (5.35).

The facet variables $\hat{u}$ do not get transformed with the Piola-transformation, as they live in another finite element space. This vector-facet space can be interpreted as an H(curl)-space without its inner degrees of freedom. Thus, to preserve the tangential continuity, we use the covariant transformation (6.31), i.e. $\hat{u} \circ \varphi = F^{-T}\hat{u}_R$, and the same holds for the according test function $\hat{v}$.

7.6 Remark. *In the following we will neglect x_R and the subscripts R to simplify the notation.*

As before, we define the following forms on the triangulation $\mathcal{T}_h$ on the reference domain Ω, where k denotes the polynomial order and u^{up} the upwind function defined in (5.45):

$$\begin{aligned} a(d,\bar{u},\bar{v}) := &\sum_{T\in\mathcal{T}_h}\int_T J\nabla P[u]F^{-1} : \nabla P[v]F^{-1}\,dx + \int_{\partial T} J\frac{\partial P[u]}{\partial n}(F^{-T}\hat{v} - P[v])_\tau\,ds \\ &+ \int_{\partial T} J\frac{\partial v}{\partial n}(F^{-T}\hat{u} - P[u])_\tau + \frac{\alpha k^2}{h}J(F^{-T}\hat{u} - P[u])_\tau(F^{-T}\hat{v} - P[v])_\tau\,ds \end{aligned} \tag{7.41a}$$

$$\begin{aligned} c(d,\bar{u},\bar{v}) := &-\sum_{T\in\mathcal{T}_h}\int_T J\left(\nabla P[v]F^{-1}(P[u] - \dot{d})\right)\cdot P[u]\,dx + \int_{\partial T} P[u]_n u^{up} P[v]\,ds \\ &+ \int_{\partial T_{out}} P[u]_n(F^{-T}\hat{u} - P[u])_\tau(F^{-T}\hat{v})_\tau\,ds \end{aligned} \tag{7.41b}$$

$$b(d,\bar{u},q) := -\int_{\mathcal{T}_h}\operatorname{div}(u)q\,dx \tag{7.41c}$$

$$m(d,\bar{u},\bar{v}) := \int_{\mathcal{T}_h} JP[\dot{u}]\cdot P[v]\,dx \tag{7.41d}$$

$$r(d,\bar{u},\bar{v}) := \int_{\mathcal{T}_h} J\nabla\dot{d}F^{-1}P[u]\cdot P[v]\,dx \tag{7.41e}$$

Like in the case of continuous elements, the mesh velocity part appears and is put into the convection (7.41b), as the terms fit good together. We mention that due to (5.35) the Piola-transformation of u vanishes in (7.41c). A huge difference to the Taylor-Hood discretization is the additional form (7.41e) which appears due to the time dependency of the Piola-transformation.

For the time discretization we will approximate again the mesh velocity with a difference quotient (see (7.35)). To calculate the gradient of it, we will take the difference quotient of the gradients

$$\nabla\dot{d}^n \approx \frac{1}{\tau}\left(\nabla d^n - \nabla d^{n-1}\right). \tag{7.42}$$

7.7 Remark. *Due to* (5.37) *the compositions of Piola-transformations is a Piola-transformation again. Thus the normal continuity of the velocity is ensured.*

7.5 Numerical experiment of the additional term

To discuss the additional term (7.41e) from the H(div)-conforming ALE formulation, we will prepare a simple numerical experiment.

We consider a rectangular channel with a parabolic inflow, $u = u_D$, on the left side and the outflow boundary on the right with the do-nothing condition, $\sigma_n^f = 0$. On the top and bottom wall we prescribe homogeneous Dirichlet data $u = 0$.

By setting the height to 1 and the width to 2 and the maximal inflow velocity to 0.25 the exact solution for the velocity u is given by

$$u(x, y, t) = \begin{pmatrix} y(1-y) \\ 0 \end{pmatrix}$$

in the whole channel.

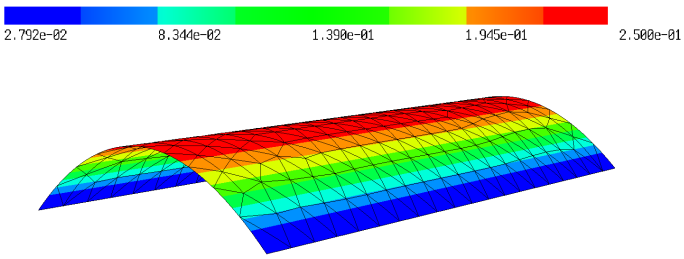

Figure 7.3: Exact solution $u(x, y, t)$

The deformation is given by the following function

$$d(x, y, t) := \begin{pmatrix} 0 \\ t \sin(\pi t) x(2-x) y(1-y) \sin(\frac{5\pi x}{2}) \end{pmatrix}, \tag{7.43}$$

which produces quite strong oscillations. These cannot be resolved exactly with a polynomial spatial discretization.

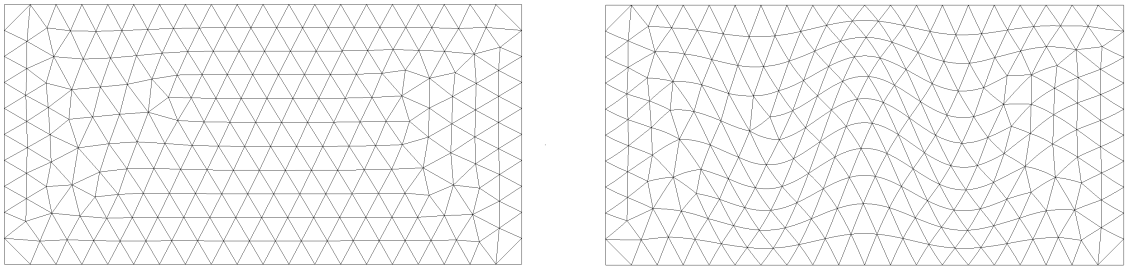

Figure 7.4: Reference and deformed mesh at $t = 0.4$

We use (7.41) once with (7.41e), which solution will be denoted by u_1, and one time without the additional term, u_2. For the time discretization we will take (7.33) and the backward difference quotient (7.42) and thus, the method should be of first order accuracy in time.

τ	$\|\|u - u_1\|\|_{L^2(\Omega)}$	order	$\|\|u - u_2\|\|_{L^2(\Omega)}$	order
0.02	6.69e-3	-	8.77e-2	-
0.01	3.31e-3	2.02	8.72e-2	1.01
0.005	1.64e-3	2.02	8.70e-2	1.00
0.0025	8.21e-4	1.99	8.69e-2	1.00
0.00125	4.09e-4	2.00	8.69e-2	1.00

Table 7.1: L2-error of the solutions at $t = 0.4$

The comparison between the two solutions u_1, u_2 is done at time $t = 0.4$, where the L^2-error is measured

$$e_i := ||u(x, y, 0.4) - u_i(x, y, 0.4)||_{L^2(\Omega)} \quad i = 1, 2. \tag{7.44}$$

In table 7.1 the results are listed for different time steps τ and, as already can be seen in figure 7.5, the method u_2 without the additional term (7.41e) fails completely, as the artificial deformation can directly be seen. Thus, it cannot be neglected and must be implemented to achieve good results.

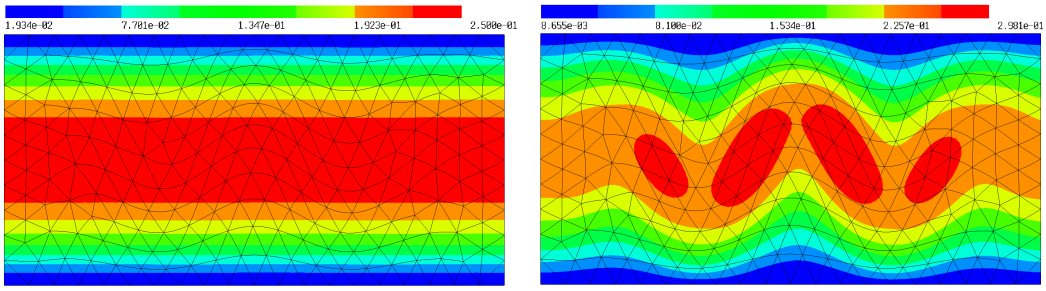

Figure 7.5: Correct solution u_1 and incorrect solution u_2 at $t = 0.4$

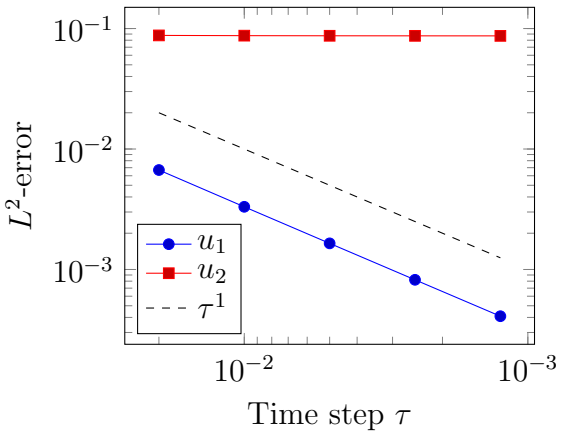

Figure 7.6: L^2-error of the solutions at $t = 0.4$

8 Fluid-structure interaction formulation

After the Navier-Stokes and the elastic wave equations have been prepared and the ALE description has been introduced, we are now able to start deriving the complete FSI description.

We start by discussing the interface conditions between the fluid and solid domain and how the quantities are coupled. Another important topic is the uniform description of the equations and how they can be solved sufficiently and efficiently. First, a general approach will be introduced and then we specialize to two different discretization techniques, one consisting of completely H1-conforming elements and the other using H(div)-conforming elements for the fluid part and the mixed version of the elastic wave equation with elements in $H^1(\Omega)$ for the displacement, H(curl)-conforming elements for the velocity and the dual space $H(\text{curl})^*$ for the time derivative of the momentum.

8.1 General description

There are two different general approaches for describing FSI problems, the monolithic and the partitioned approach.

- For a monolithic approach the equations for the fluid and solid are solved together at once with a single solver. Therefore, the arising system is larger and the solver must be able to handle both types of equations. An advantage is that the interface conditions can be treated quite easy in a natural way.
- The partitioned approach uses two different solvers and the equations are split to solve them separately. Here, the solver can be optimized for each equation or existing solvers can be used. The drawback of these methods is that the interface conditions must be treated also separately which can be complicated.

In this thesis, however, only the monolithic description is used and thus, we build a huge system which is then solved at once.

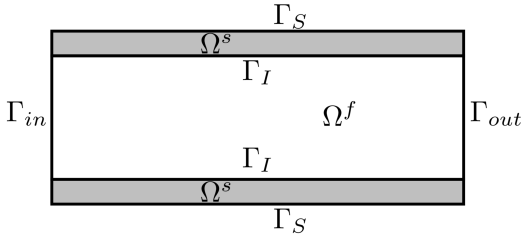

Figure 8.1: FSI model problem

As a model problem, we assume a bounded domain Ω which is divided into two disjoint subdomains: $\Omega^f \subset \Omega$, which is occupied by the fluid, and the solid domain $\Omega^s \subset \Omega$,

$\Omega^f \cap \Omega^s = \emptyset$ (see figure 8.1 on the preceding page). We denote with $\Gamma_{\text{in}} \subset \partial\Omega$ and $\Gamma_{\text{out}} \subset \partial\Omega$ the inflow and outflow boundary of the fluid domain, respectively. The interface boundary Γ_{I}, where the fluid and solid interact with each other, is defined by

$$\Gamma_{\text{I}} := \overline{\Omega}^f \cap \overline{\Omega}^s. \tag{8.1}$$

For the remaining fluid boundaries we write Γ_{F} and for the solid boundaries Γ_{S}.

The two main quantities are the displacement and the velocity, which appear in both domains. Therefore, we split the global displacement d into the solid and fluid displacement and use the following notation

$$d^s : \Omega^s \times [0,T] \to \mathbb{R}^3, \tag{8.2a}$$
$$d^f : \Omega^f \times [0,T] \to \mathbb{R}^3, \tag{8.2b}$$

for the solid and fluid, respectively.

The global velocity u is split in the same way

$$u^s : \Omega^s \times [0,T] \to \mathbb{R}^3, \tag{8.3a}$$
$$u^f : \Omega^f \times [0,T] \to \mathbb{R}^3. \tag{8.3b}$$

We will always construct the displacement in such a way that it is globally continuous and thus, it is in $[H^1(\Omega)]^n$. Then we are able to define the deformation gradient and its determinant globally:

$$F = I + \nabla d, \qquad J = \det F. \tag{8.4}$$

The boundary conditions for the boundaries involving only one of the domains are handled in the usual way. For the inflow boundary Γ_{in} the inflow velocity, which can depend on time t, is prescribed and we use the do-nothing condition for the outflow boundary Γ_{out}. On the remaining fluid boundaries the no-slip condition is prescribed

$$u^f = u_D(t) \text{ on } \Gamma_{\text{in}}, \qquad \sigma_n^f = 0 \text{ on } \Gamma_{\text{out}}, \qquad u^f = 0 \text{ on } \Gamma_{\text{F}}. \tag{8.5}$$

We remember that σ^f denotes the fluid stress tensor and n the outer normal vector.

The solid boundaries which are not part of the interface can be set to be fixed, i.e. homogeneous Dirichlet data is prescribed for the displacement, or they should be stress free, which is exactly the do-nothing condition

$$d^s = 0 \text{ or } \sigma_n^s = 0 \text{ on } \Gamma_{\text{S}}. \tag{8.6}$$

Here, σ^s is the first Piola-Kirchhoff stress tensor.

For the interface boundary Γ_I the situation is a bit more involved. First, the velocity of the fluid and solid has to be continuous on the interface, otherwise the domain would break up. In other words, a no-slip condition for the fluid is prescribed on the interface. With this the fluid velocity is the same as the solid one. Another important thing is the transportation of the forces between the two domains, as the interface is the only possibility to exchange information from the fluid to the solid and vice versa in a monolithic sense

$$\sigma_n^f = \sigma_n^s \text{ and } u^f = u^s \text{ on } \Gamma_\mathrm{I}. \tag{8.7}$$

8.2 Deformation extension

Until now, the displacement of the fluid domain has not been mentioned, which plays a crucial role in FSI. The deformation d is only calculated directly in the solid part, as it appears in the elastic wave equation and the interface conditions ensure just the continuity of the velocity u. Thus, a method has to be used to "extend" the information of the deformation of the solid to the whole domain Ω. For different approaches we refer to [Wic11].

A first simple approach is to solve a Poisson problem in the fluid domain with the Dirichlet data as the deformation of the solid on the interface and homogeneous Dirichlet data on all other fluid boundaries:

8.1 Problem (Poisson extension). *Find d^f such that*

$$-\Delta d^f = 0 \quad \text{in } \Omega^f, \tag{8.8a}$$
$$d^f = d^s \quad \text{on } \Gamma_I, \tag{8.8b}$$
$$d^f = 0 \quad \text{on } \partial\Omega^f \backslash \Gamma_I. \tag{8.8c}$$

This works fine as long as the deformation is small because the values of the solution of the Poisson problem decrease very fast. If large deformations occur, it is possible that elements are pressed through others, which is neither realistic nor desirable and the system can become unstable (see figure 8.2 on the next page).

Solving a biharmonic instead of a Poisson problem improves the situation as it is a stiffer problem, but with large deformations also this approach fails without further treatment.

To avoid such effects we can add a kind of penalty term to the problem, more precisely we divide through the determinant J of the deformation gradient (see (8.4)), which gets small if a volume element gets pressed and compressed:

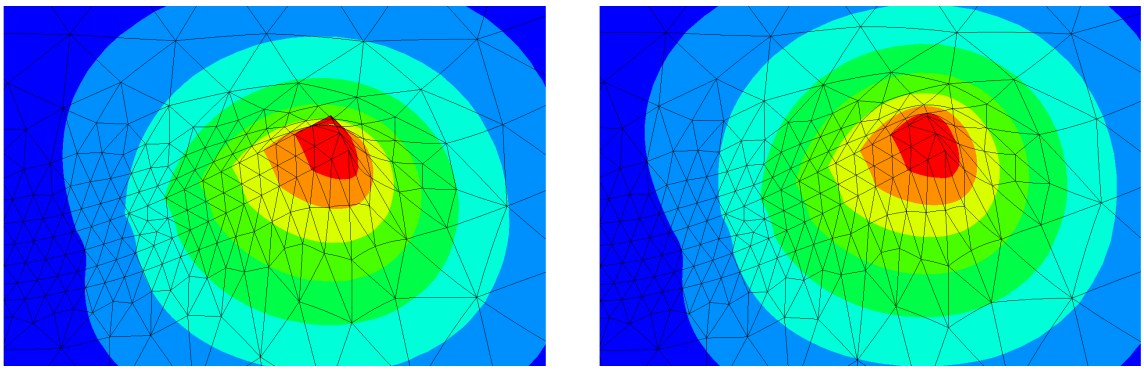

Figure 8.2: Left side: Poisson extension, right side: Poisson extension with determinant as penalty term

8.2 Problem (Poisson extension with penalty term). *Find* d^f *such that*

$$-\frac{1}{J}\Delta d^f = 0 \qquad \text{in } \Omega^f, \tag{8.9a}$$

$$d^f = d^s \qquad \text{on } \Gamma_I, \tag{8.9b}$$

$$d^f = 0 \qquad \text{on } \partial\Omega^f \backslash \Gamma_I. \tag{8.9c}$$

This ensures the stability of the solution in the sense that elements are not pressed so their volume gets zero, but now the problem is nonlinear. Treating it explicitly is not recommended as it can get unstable and therefore an implicit system has to be solved in every time step, for example with Newton's method.

There are two possible ways to include the deformation extension to an existing FSI problem. One is to solve the system first without it and thus, the new deformation is only known in the solid part. If information of the deformation is needed in the fluid equations, e.g. they are treated implicitly, an extrapolated deformation has to be used. Then (8.9) is solved alone on the fluid domain. The drawback of the extrapolation in the fluid domain gets balanced by the advantage that the FSI system can be solved without a Newton's method, if the discretization method of the other equations allow this, and the smaller nonlinear system involving only the displacement must be calculated in such a way, which is more efficient and faster.

However, if the original system is already solved as a nonlinear problem, then adding (8.9) to it is a more natural way. A subtle detail has then to be considered. The weak form of (8.9) reads:

8.3 Problem. *Find* $d \in [H^1_{\partial\Omega^f \setminus \Gamma_I}(\Omega^f)]^n$ *such that*

$$\int_{\Omega^f} \frac{1}{J} \nabla d : \nabla w \, dx - \int_{\Gamma_I} \frac{1}{J} \nabla d_n \cdot w \, ds = 0 \quad \forall w \in [H^1_{\partial\Omega^f \setminus \Gamma_I}(\Omega^f)]^n, \tag{8.10}$$

where the test function w only vanishes on the outer boundary $\partial\Omega^f \setminus \Gamma_\mathrm{I}$, but not on the interface. We would like to just neglect the additional boundary integral, but this would effect the solid displacement. A compromise is to multiply (8.10) with a small factor ε which reduces this effect, but not the stability as the factor $\frac{1}{J}$ dominates for strong compressions of the elements.

8.4 Problem. *Find* $d \in [H^1_{\partial\Omega^f \setminus \Gamma_I}(\Omega^f)]^n$ *such that*

$$\int_{\Omega^f} \frac{\varepsilon}{J} \nabla d : \nabla w \, dx - \underbrace{\int_{\Gamma_I} \frac{\varepsilon}{J} \nabla d_n \cdot w \, ds}_{\approx 0} = 0 \quad \forall w \in [H^1_{\partial\Omega^f \setminus \Gamma_I}(\Omega^f)]^n. \tag{8.11}$$

8.5 Remark. *The argument that the boundary term in* (8.11) *can be neglected if* ε *is chosen small enough, requires that the term* $\frac{1}{J}$ *is bounded from below for all* $t \in [0, T]$ *on* Γ_I*. This holds as we always assume that the edges on* Γ_I *connecting the fluid and solid domain do not get strongly compressed.*

Although (8.11) does a good job, the elements can get deformed quite heavily, which can have poor consequences for the stability.

Using an elasticity problem instead of the Poisson problem helps, as the elements rotate more to preserve the triangle structure. Another approach is to use position-dependent coefficients to increase the stiffness, e.g. near edges where the deformation is expected to be high. We combine all three methods, which yields the material law of Neo-Hook (4.21) with a position-dependent function $h(x)$, which must be chosen appropriate to the actual problem (see e.g. section 9).

The new method can be described by the following minimization problem:

8.6 Problem (Neo-Hook extension with position-weighted function). *Find* $d \in [H^1_{\partial\Omega^f \setminus \Gamma_I}(\Omega^f)]^n$ *such that*

$$N(C(d)) := \int_\Omega h(x) \frac{\mu}{2} \left(\mathrm{tr}(C - I) + \frac{2\mu}{\lambda} (\det(C))^{-\frac{\lambda}{2\mu}} - 1 \right) dx \to \min!, \tag{8.12}$$

where C denotes the Cauchy-Green strain tensor (4.4) and μ and λ the Lamé-constants (see (4.26)).

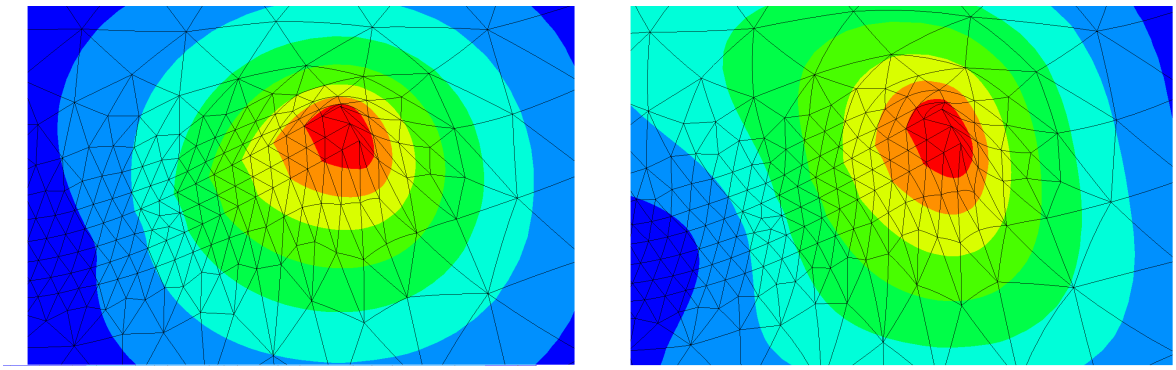

Figure 8.3: Left side: Poisson with determinant, right side: Neo-Hook with position-weighted function

This energy functional induces the following variational formulation, where again the small parameter ε is used, if the big solving is solved at once.

8.7 Problem. *Find* $d \in [H^1_{\partial\Omega^f \setminus \Gamma_I}(\Omega^f)]^n$ *such that*

$$nh_\varepsilon(d, w) := \int_\Omega \varepsilon h(x) \mu F(I - \det(C)^{-\frac{\lambda}{2\mu}} C^{-1}) : \nabla w \, dx = 0 \quad \forall w \in [H^1_{\partial\Omega^f \setminus \Gamma_I}(\Omega^f)]^n. \tag{8.13}$$

In figure 8.3 the different extensions between (8.11) and (8.12) can be seen.

8.3 FSI description for H1-conforming discretization

We use the Taylor-Hood discretization for the Navier-Stokes equations in the ALE setting (7.24) together with the H1-conforming discretization of the elastic wave equation. As both of them use continuous elements, we can combine them to a FSI description without bigger changes. We recall the two equations

$$m^f(\frac{\partial u^f}{\partial t}, v) + a(u^f, v) + b(v, p) + b(u^f, q) + c(u^f, u^f, v) = \int_{\Gamma_I} \sigma_n^f v \, ds, \tag{8.14}$$

$$m^s(\frac{\partial^2 d^s}{\partial t^2}, w) + k^s(d^s, w) = \int_{\Gamma_I} \sigma_n^s w \, ds. \tag{8.15}$$

Due to the continuity of all quantities and the interface conditions (8.7) we can add both equations and the boundary integrals cancel out, because the outer normal vector n has a different sign on the fluid and solid domain. This yields in operator form

$$M^f \frac{\partial u^f}{\partial t} + D^f u^f + C^f(u^f) + M^s \frac{\partial u^s}{\partial t} + K(d^s) = 0, \tag{8.16}$$

where D denotes again the Stokes operator and the (nonlinear) dependency of the displacement d^f and the pressure p^f have been neglected. The superscripts on the operators help to remember on which domains they are defined, but sometimes we neglect them for ease of presentation. The same holds for the superscripts for the velocity u and displacement d.

For the spatial discretization an IMEX scheme can be used. Another approach is to use the Crank-Nicolson method, write everything into a huge bilinear form and use Newton's method to solve the resulting system (see section (8.3.2)), which is done for example in [HT06]. A different approach is used in [Wic13], where the Rothe method is used, discretizing first in time and then in space.

8.3.1 IMEX scheme for H1-conforming FSI

Here, we combine the results from the ALE time discretization of the Navier-Stokes equations in section 7.3 and the time discretization of the elastic wave equation in section 6.2.2. This leads to the following IMEX time discretization for the FSI problem:

$$(M^s + M^f_{n+1} + \tau D_{n+1})(u^{n+1} - u^n) = -\tau \left(D_{n+1}u^n + C_n(u^n) + \frac{\tau}{2}K'_n(u^n + u^{n+1}) + K_n \right).$$

8.8 Remark. *The dependency on the displacement will be denoted by a subscript again, e.g.* $D_{n+1} \hat{=} D(d^{n+1})$.

We bring all terms with u^{n+1} on the left-hand side and add terms such that the equation is again in update form

$$(M^s + M^f_{n+1} + \tau D_{n+1} + \frac{\tau^2}{2}K'_n)(u^{n+1} - u^n) = -\tau \left(D_{n+1}u^n + C_n(u^n) + \tau K'_n u^n + K_n \right). \tag{8.17}$$

8.9 Remark. *For the Navier-Stokes equations we used* (7.32)*, but* (7.33) *or* (7.34) *can also be taken. In the numerical experiments we did not find significant differences between these schemes.*

We note that K_n *depend only on* d^n *and not on the velocity* u*. Thus, it appears on right-hand side.*

As mentioned before, we have to decide if we calculate the deformation extension after the system has been solved or at the same time. In (8.17), all the nonlinear terms, despite the displacement in M^f_{n+1} and D_{n+1}, are treated explicitly and so, we can avoid solving a nonlinear system if we extrapolate the needed displacement at least linearly and expand the deformation afterwards.

The FSI algorithm for one time step with H1-conforming elements in pseudo code reads:

Algorithm 8.1 FSI-IMEX-H1(u^n, p^n, d^n)

1: Extrapolate d^n
2: Calculate K_n'
3: Solve the linear system (8.17) $\rightarrow u^{n+1}$, p^{n+1}
4: Use (6.21c) $\rightarrow d_s^{n+1}$
5: Expand the deformation by solving (8.12) with Newton's method $\rightarrow d^{n+1}$

8.3.2 Crank-Nicolson method for H1-conforming FSI

To use Crank-Nicolson we combine the time discretization in section 5.4.2 for the Navier-Stokes equations and (6.23) for the elastic wave equation. These can be added together without any changes.

Now, we take (8.13) for the deformation extension and the arising system for one time step is:

8.10 Problem. *Find* (u^{n+1}, d^{n+1}) *such that*

$$\begin{aligned}\frac{1}{2}(M_{n+1}^f + M_n^f)(u^{n+1} - u^n) + \frac{\tau}{2}(A_{n+1}u^{n+1} + A_n u^n) + \tau(B_{n+1}p^{n+1} + B_{n+1}^T u^{n+1}) + \\ \frac{\tau}{2}(C_{n+1}(u^{n+1}) + C_n(u^n)) + M^s(u^{n+1} - u^n) + \frac{\tau}{2}(K(d^{n+1}) + K(d^n)) + \\ M_I^s(\frac{\tau}{2}(u^{n+1} + u^n) - d^{n+1} + d^n) + NH_\varepsilon(d^{n+1}) = 0,\end{aligned} \tag{8.18}$$

where NH_ε is the operator according to (8.13).

8.4 FSI description for H(div)- and H(curl)-conforming discretization

For the second pairing we use the H(div)-conforming HDG method from section 5.3 for the Navier-Stokes equations and the new discretization method for the elastic wave equation derived in section 6.3. Now, the continuity of the velocity in the fluid domain Ω^f is split into the normal continuous H(div)-conforming elements u and the facet variables $\hat{u}$, which consider only the tangential part. The velocity of the solid gets approximated by H(curl)-conforming elements and thus, is only tangential continuous. Therefore, the implementation of the interface conditions need more treatment than for the first pairing. The displacement d is continuous again, so that the deformation extension into the fluid domain can be handled in the same manner as before.

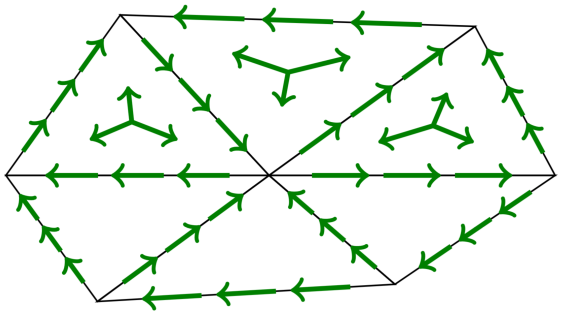

Figure 8.4: H(curl) and vector-facet combined

8.4.1 General approach

First, the facet variables which live only on the skeleton of the triangulation $\mathcal{T}_h$ can be interpreted as $H(\text{curl})$ elements without the inner degrees of freedom. Exploiting this we can define a global $H(\text{curl})$ finite element space where the inner degrees of freedom are only used on the solid domain (see figure 8.4).

Now the interface condition for the velocity is split into its tangential and normal components

$$u_\tau^s = u_\tau^f \text{ and } u_n^s = u_n^f \text{ on } \Gamma_\text{I}. \tag{8.19}$$

Due to the tangential continuity of the facet variables and the solid velocity the first equation is already fulfilled. Unfortunately, for the normal component we have to use a new approach as the normal trace of the solid velocity is not well-defined on the interface Γ_I, as it is in $H(\text{curl})$.

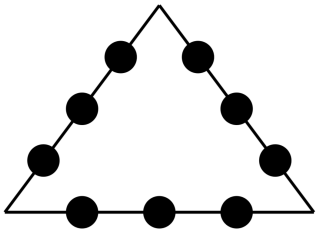

Figure 8.5: L^2-surface element

Therefore, we introduce a new unknown $\lambda \in L^2(\mathcal{F})$ and the corresponding test function $\mu \in L^2(\mathcal{F})$ as a Lagrange parameter for the normal velocity. The L2-surface finite element space consists of polynomials, which live only on the skeleton of the triangulation $\mathcal{T}_h$ (see figure 8.5). To enforce the normal continuity of the velocity on the interface

we define

$$s(d^s, u^f, \mu) := \int_{\Gamma_I} \left(\dot{d}^s - u^f\right)_n \mu \, ds. \tag{8.20}$$

The velocity $\dot{d}^s$ will be approximated by the difference quotient $\dot{d}^s \approx \frac{d^{n+1}-d^n}{\tau}$. By using λ as a Lagrange parameter, the following term is added to the existing forms

$$\int_{\Gamma_I} (w - v^f)_n \lambda \, ds, \tag{8.21}$$

where $w \in [H^1_{\Gamma_D}(\Omega)]^n$ denotes the test function corresponding to the displacement d and v the test function to the velocity u living in $H(\mathrm{div}, \Omega_f)$.

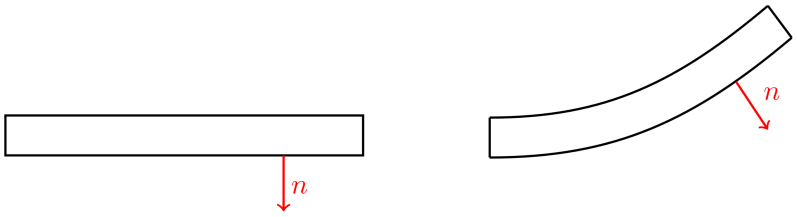

Figure 8.6: Rotated outer normal vector

The outer normal vector n and thus the coupling of the normal component of the velocity changes, if the solid gets transformed (see figure 8.6). To enforce the correct continuity condition we have to transform also (8.20) and (8.21):

$$\int_{\Gamma_I} \left(\dot{d}^s - P[u^f]\right) (F^{-T} n) \mu \, ds, \tag{8.22a}$$

$$\int_{\Gamma_I} (w - v^f)(F^{-T} n) \lambda \, ds, \tag{8.22b}$$

where $P[\cdot]$ denotes the Piola-Transformation (5.34).

For the time discretization we use the Crank-Nicolson method as it gives a bit more freedom than the implicit Euler scheme

$$\frac{1}{2} \int_{\Gamma_I} (\frac{d^{n+1} - d^n}{\tau} - P[u^f_{n+1}])(F^{-T}_{n+1} n) \mu \, ds + \frac{1}{2} \int_{\Gamma_I} (\frac{d^{n+1} - d^n}{\tau} - P[u^f_n])(F^{-T}_n n) \mu \, ds, \tag{8.23a}$$

$$\frac{1}{2} \int_{\Gamma_I} (w - v^f)(F^{-T}_{n+1} n) \lambda^{n+1} \, ds + \frac{1}{2} \int_{\Gamma_I} (w - v^f)(F^{-T}_n n) \lambda^n \, ds. \tag{8.23b}$$

After the global continuity of the velocity is recovered, the boundary integrals

$$\int_{\Gamma_I} \sigma_n^f \, ds \quad \text{and} \quad \int_{\Gamma_I} \sigma_n^s \, ds$$

cancel out again, when we add both equations.

8.4.2 H(div)-conforming HDG with H(curl)-dynamics

The first approach is to couple the H(div)-conforming HDG method from section 5.3 with the H(curl)-dynamics method (6.45) or (6.49). Unfortunately, this does not work appropriately, which can be seen as following.

The first equation in (6.45) enforces the coupling of the time derivative of the displacement with the velocity

$$\int_{\Omega^s} (F^{-1}\dot{d} - C^{-1}\hat{u}) \cdot \hat{v} \, dx = 0. \tag{8.24}$$

The velocity test function $\hat{v}$ appears also on the fluid domain in the Navier-Stokes equations

$$\int_{\partial T^f} \nu^f (\frac{\partial u}{\partial n} + \frac{\alpha k^2}{h}(\hat{u} - u)_\tau) \cdot \hat{v}_\tau \, ds = 0, \tag{8.25}$$

where k denotes the polynomial degree, h the mesh size and α the stability parameter.

Thus, if we add both equations, they interact on the interface Γ_I. If we look on the physical quantities on the left side, we obtain with $[\hat{u}] = [\hat{v}] = \frac{m}{s}$, $[C^{-1}] = [F^{-1}] = 1$ and $[\int_{\Omega^s} \cdot \, dx] = m^2$

$$[\int_{\Omega^s} (F^{-1}\dot{d} - C^{-1}\hat{u}) \cdot \hat{v} \, dx] = \frac{m^4}{s^2}, \tag{8.26}$$

but on the left side with $[\nu^f] = \frac{m^2}{s}$, $[\frac{\partial u}{\partial n}] = \frac{1}{s}$ and $[\frac{1}{h}] = \frac{1}{m}$

$$[\int_{\Gamma_I} \nu^f (\frac{\partial u}{\partial n} + \frac{\alpha k^2}{h}(\hat{u} - u)_\tau) \cdot \hat{v}_\tau \, ds] = \frac{m^4}{s^3}, \tag{8.27}$$

e.i, the quantities (8.26) and (8.27) do not fit together.

8.11 Remark. *Another problem is that on the interface Γ_I we cannot ensure that the time derivative of the displacement coincides with the velocity in the solid anymore.*

8.4.3 H(div)-conforming HDG with velocity-momentum method

In this section we try to couple the H(div)-conforming HDG method with the velocity-momentum method (6.59) (or (6.58) in three dimensions) instead of the H(curl)-dynamics method. Now, the test function of the equation coupling the time derivative of the displacement with the velocity of the solid is in the dual space $H = H(\text{curl}, \Omega^s)^*$, which does not appear in the Navier-Stokes equations

$$\int_{\Omega^s} (\dot{d} - \hat{u}) \cdot q \, dx = 0. \tag{8.28}$$

The H(curl) test function $\hat{v}$ appears in the second equation of the velocity-momentum method

$$\int_{\Omega^s} (\rho^s \frac{\partial}{\partial t}(F^{-T}\hat{u}) - p) \cdot \hat{v} \, dx = 0, \tag{8.29}$$

which has the physical quantity

$$[\int_{\Omega^s} (\rho^s \frac{\partial}{\partial t}(F^{-T}\hat{u}) - p) \cdot \hat{v} \, dx] = [\rho^s]\frac{m^4}{s^3} = \frac{kg\,m}{s^3}. \tag{8.30}$$

The units fit together with (8.27) if we add ρ^f to it, which is done in section 9, or divide (8.30) through ρ^s. This makes also physically sense, as the forces get exchanged over the interface Γ_I.

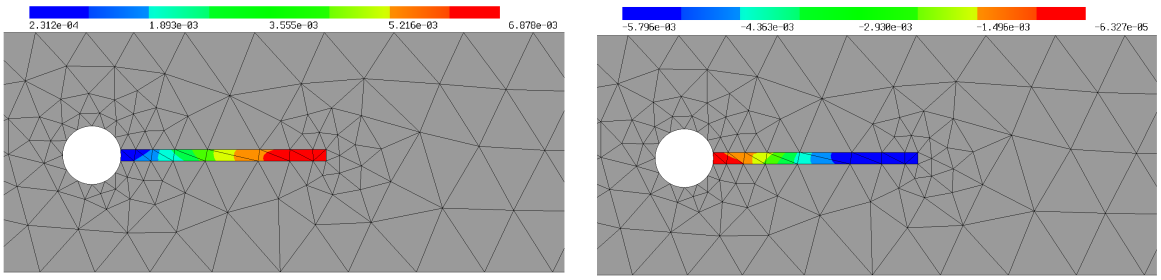

Figure 8.7: Correct and wrong force coupling

We have to be careful when adding the two equations. If we change the sign in (8.29), the equation itself is still fulfilled, but the forces might get transported in the wrong way in the tangential direction (see figure 8.7).

In our case we want the time derivative of the momentum in the solid and the forces in the fluid domain to have the same sign

$$p \cdot \hat{v} + \cdots = \frac{\partial u}{\partial n} \cdot \hat{v} + \cdots, \tag{8.31}$$

to enforce the correct coupling.

8.4.4 Complete discretization

Now, we are able to finish the discretization for the H(div)-conforming HDG coupled with the velocity-momentum method.

We use (7.41) for the Navier-Stokes equations and the discretization (6.59) in two dimensions, with its complete discretization (6.60). For ease of presentation we will set all appearing parameters to 1.

For the Navier-Stokes equations we use the Crank-Nicolson method for the time discretization, only the pressure and incompressibility constraint are treated completely implicit, and for the elasticity part a mix of the midpoint and CN scheme (see remark 6.11). The deformation extension into the fluid domain is done again with (8.13).

Note that we used the variable p for the pressure in the fluid domain and the time derivative of the momentum in the solid domain, which live in different spaces. This should not yield into confusion as in the context of the bilinear forms the appropriate variable, and thus the appropriate space should be obvious.

Altogether, the huge bilinear form F reads:

$$
\begin{aligned}
F(\begin{pmatrix}\bar{u}\\ d\\ p\\ \lambda\end{pmatrix}, \begin{pmatrix}\bar{v}\\ w\\ q\\ \mu\end{pmatrix}) :=& \frac{1}{2}\big(a(d^{n+1},\bar{u}^{n+1},\bar{v}) + a(d^n,\bar{u}^n,\bar{v}) + m(d^{n+1},\bar{u}^{n+1},\bar{v}) + m(d^n,\bar{u}^n,\bar{v}) + \\
& c(d^{n+1},\bar{u}^{n+1},\bar{v}) + c(d^n,\bar{u}^n,\bar{v}) + r(d^{n+1},\bar{u}^{n+1},\bar{v}) + r(d^n,\bar{u}^n,\bar{v})\big) + \\
& b(d^{n+1},\bar{u}^{n+1},q) + b(d^{n+1},\bar{v},p^{n+1}) + nh_\varepsilon(d^{n+1},w) + \\
& \int_{\Omega^s} \frac{d^{n+1}-d^n}{\tau} F_{n+\frac{1}{2}} q - \hat{u}_{n+\frac{1}{2}} q - p_{n+\frac{1}{2}}\hat{v} + F^{-T}_{n+\frac{1}{2}} \frac{\hat{u}^{n+1}-u^n}{\tau}\hat{v} - \\
& \frac{1}{2} C^{-1}_{n+\frac{1}{2}} \frac{C^{n+1}-C^n}{\tau} C^{-1}_{n+\frac{1}{2}} - \frac{1}{2\det(C_{n+\frac{1}{2}})}\mathrm{curl}(\hat{u}_{n+\frac{1}{2}})\mathrm{rot}(\hat{u}_{n+\frac{1}{2}})\hat{v} + \\
& F_{n+\frac{1}{2}} p_{n+\frac{1}{2}} w + F_{n+\frac{1}{2}} \Sigma(C_{n+\frac{1}{2}}) : \nabla w \, dx + \\
& \frac{1}{2}\int_{\Gamma_I} (\frac{d^{n+1}-d^n}{\tau} - P[u^f_{n+1}]) F^{-T}_{n+1} n\mu + (\frac{d^{n+1}-d^n}{\tau} - P[u^f_n]) F^{-T}_n n\mu + \\
& (w - v^f)(F^{-T}_{n+1} n)\lambda^{n+1} + (w - v^f)(F^{-T}_n n)\lambda^n \, ds.
\end{aligned}
\tag{8.32}
$$

8.12 Remark. *In the bilinear forms* (7.41) *some time derivatives appear, which are replaced by the backwards difference quotient*

$$
\dot{d} \approx \frac{d^{n+1}-d^n}{\tau} \quad \text{and} \quad \dot{u} \approx \frac{u^{n+1}-u^n}{\tau}. \tag{8.33}
$$

9 Numerical examples

The following benchmark was purposed by Turek and Hron in [TH06] and [THM+10], which is based on the configurations of the classical flow around cylinder CFD benchmark in [STD+96].

9.1 Equations and geometry

As in the last chapter, the domain Ω consists of the fluid Ω^f and the solid domain Ω^s. The interface boundary is again denoted by $\Gamma_{\mathrm{I}} = \overline{\Omega}^f \cap \overline{\Omega}^s$.

The incompressible Newtonian fluid is described by the Navier-Stokes equations (similar to (3.22)):

$$\rho^f \frac{\partial u^f}{\partial t} + \rho^f (u^f \cdot \nabla) u^f - \rho^f \nu^f \operatorname{div}(\nabla u^f + \nabla u^T) + \nabla p^f = 0, \tag{9.1a}$$

$$\operatorname{div}(u^f) = 0, \tag{9.1b}$$

with the fluid density ρ^f and the dynamic viscosity ν^f.

The constitutive equation for the elastic solid is (see (4.32))

$$\rho^s \frac{\partial^2 d^s}{\partial t^2} - \operatorname{div}(F\Sigma^s) = 0, \tag{9.2}$$

where ρ^s denotes the solid density. We assume the constitutive law of the St. Venant-Kirchhoff material

$$\Sigma^s = \lambda^s \operatorname{tr}(E) I + 2\mu^s E,$$

with the Lamé coefficients λ^s and μ^s. As in section 4, we will also use the Poisson's ratio ν^s.

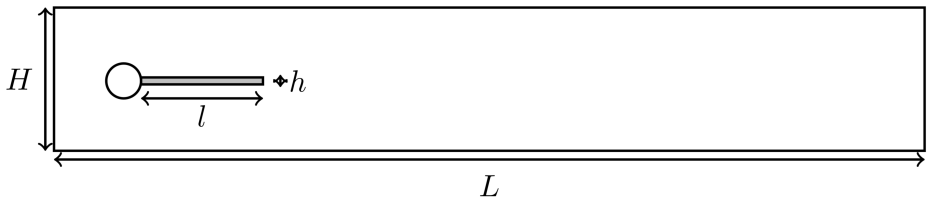

Figure 9.1: Complete channel

The configuration is based on the CFD benchmark in [STD+96], which consists of a channel with a cylinder, which is set non-symmetric. For the FSI benchmark there is

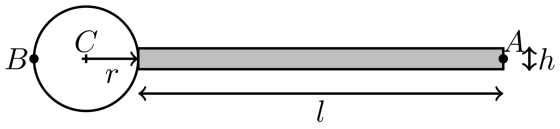

Figure 9.2: Cylinder and structure part

additionally an elastic flag attached at the end of this cylinder (see figure 9.1 on the previous page). The exact values of the channel, cylinder and elastic structure can be seen in table 9.1.

Parameter		value [m]
channel length	L	2.5
channel width	H	0.41
cylinder position	C	$(0.2, 0.2)$
cylinder radius	r	0.05
solid structure length	l	0.35
solid structure height	h	0.02
reference point (at $t = 0$)	A	$(0.6, 0.2)$
reference point	B	$(0.15, 0.2)$

Table 9.1: Geometry parameters

9.2 Boundary data, initial condition and quantities of interest

We prescribe a parabolic inflow profile at the left channel by the function

$$u^f(0, y) = 1.5\overline{U}\frac{y(H-y)}{\left(\frac{H}{2}\right)^2} = 1.5\overline{U}\frac{4}{0.1681}y(0.41-y), \tag{9.3}$$

which is chosen in such a way that $\overline{U}$ is the mean value of the velocity and the maximal velocity is $1.5\overline{U}$. Together with the geometry data, the Reynolds number is then defined by $Re = \frac{2r\overline{U}}{\nu^f}$.

For the outflow boundary we choose the do-nothing condition, $\sigma_n^f = 0$, and on the other boundaries the no-slip condition, $u_D^f = 0$, is prescribed for the fluid.

The following smooth function is used as inflow data for the non-steady tests

$$u^f(0, y, t) = \begin{cases} u^f(0, y)\frac{1-\cos(\frac{\pi}{2}t)}{2} & \text{if } t < 2, \\ u^f(0, y) & \text{otherwise,} \end{cases} \tag{9.4}$$

with the velocity profile $u^f(0, y)$ from (9.3).

The most reasonable quantity for comparison is the displacement of the beam which is measured at the point $A(t)$ on the right end at the middle of the flag (see figure 9.2 on the preceding page).

In the non-steady cases the frequency of the oscillation can also be computed.

Parameter	FSI1	FSI2	FSI3
$\rho^s\,[10^3]$	1	10	1
ν^s	0.4	0.4	0.4
$\mu^s\,[10^3]$	0.5	0.5	2
$\rho^f\,[10^3]$	1	1	1
$\nu^f\,[10^{-3}]$	1	1	1
$\overline{U}$	0.2	1	2

Table 9.2: Parameters for the FSI tests

For the tests three different configurations of the parameters are used, which are listed in table 9.2. The first one leads to a steady solution, while for the others the beam starts bending periodically. We mention that in all cases we are in the situation of a laminar flow without turbulences.

9.3 Mesh and used methods

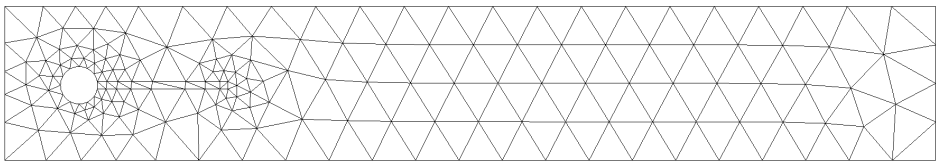

Figure 9.3: Mesh on the coarsest level

level	k	TH-H1	HDG-VM
0	3	3980	7698
	4	7668	11840
	5	12527	16966

Table 9.3: Total number of degree of freedom for H1-conforming and H(div)-conforming HDG-velocity-momentum FSI method

For the computations the mesh in figure 9.3 is used, which represents the coarsest level. Normally, the mesh gets refined to increase the number of degrees of freedom

and to obtain a better spatial accuracy. In this thesis, however, we choose a different approach and increase the polynomial degree k for the velocity and displacement from three to five. We remember that for Taylor-Hood elements the pressure has one polynomial degree less as the velocity, whereas the polynomial degree of the pressure in the H(div)-conforming HDG setting can be set to zero, if all basis functions Ψ, which are not divergence free, $\mathrm{div}(\Psi) \neq 0$, are neglected (see reduced spaces in [LS16]). The total amount of degrees of freedom at each polynomial level is listed in table 9.3 on the preceding page.

The linear system arising in Newton's method or directly from the equations in the case an IMEX scheme is used, is solved directly. For symmetric and positive definite (spd) matrices a Sparse Cholesky solver is used, whereas for non spd matrices we use the direct solver UMFPACK[3].

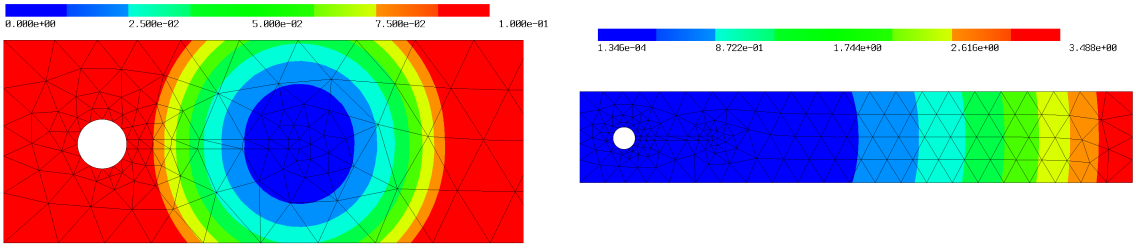

Figure 9.4: Position-dependent function $\mathrm{dist}(x)$

For the deformation extension (8.13) we need to specify the position-dependent function $h(x)$. As the beam will bend up and down, we expect very strong deformations of the mesh triangulation $\mathcal{T}_h$ near the corners on the right of the flag. Thus, we define the function as

$$h(x) := \frac{1}{\sqrt{|\mathrm{dist}(x)|^2 + \bar{\varepsilon}}}, \tag{9.5}$$

with

$$\mathrm{dist}(x) := \min\left(|x - p_1|^2, |x - p_2|^2\right), \qquad p_1 = \begin{pmatrix} 0.6 \\ 0.19 \end{pmatrix}, \; p_2 = \begin{pmatrix} 0.6 \\ 0.21 \end{pmatrix}, \tag{9.6}$$

where p_1 and p_2 are the corners and $\bar{\varepsilon}$ a small regularisation parameter to avoid singularities. This will make the elements stiffer, if they are near the corners (see figure 9.4).

For the material law of Neo-Hook in (8.13) we will set the parameters μ and λ simply to one.

We will use two different discretization schemes for this benchmark. The first one is the H1-conforming FSI method (8.18), where we use the CN method and Newton's

[3] http://faculty.cse.tamu.edu/davis/suitesparse.html

method to solve the huge arising system. For the second one, the H(div)-conforming HDG combined with the velocity-momentum method (8.32) is used, which is also solved by CN and Newton's method.

9.1 Remark. *For the H1-conforming method, also the FSI problem involving the IMEX scheme (algorithm* (8.1)*) could be used. With it one time step is faster as one with the CN method, but the time step τ must be chosen smaller, as the convection is treated only explicitly. Thus, for easier comparison to the H(div)-conforming HDG velocity-momentum method, we use* (8.18)*.*

9.4 Numerical results

In the following tables the displacement of the control point A in the stationary solution for the FSI 1 benchmark and the maximal/minimal displacement of A in the FSI 2 and FSI 3 examples are given.

We can observe that both discretization schemes give the same qualitative results for all benchmark problems, which coincide also with the qualitative observation in [Wic13] and [TH06].

level	k	ux $[10^{-5}]$	uy $[10^{-4}]$
0	3	2.296	8.22
	4	2.294	8.16
	5	2.290	8.21

Table 9.4: FSI 1 with H(div)-conforming HDG velocity-momentum method and time step $\tau = 0.001$

level	k	ux $[10^{-5}]$	uy $[10^{-4}]$
0	3	2.269	8.17
	4	2.269	8.14
	5	2.270	8.18

Table 9.5: FSI 1 with Taylor-Hood-H1 method and time step $\tau = 0.001$

For a quantitative comparison of the H(div)-conforming HDG velocity-momentum with the H1-conforming method the number of degrees of freedom is too little and thus, the spatial accuracy is not high enough.

level	k	ux $[10^{-2}]$	uy $[10^{-2}]$
0	3	-1.39±1.18	0.15±7.97
	4	-1.42±1.22	0.11±8.00
	5	-1.46±1.26	0.12±8.11

Table 9.6: FSI 2 with H(div)-conforming HDG velocity-momentum method and time step $\tau = 0.002$

level	k	ux $[10^{-2}]$	uy $[10^{-2}]$
0	3	-1.44±1.28	0.15±8.25
	4	-1.51±1.26	0.12±8.13
	5	-1.52±1.27	0.12±8.22

Table 9.7: FSI 2 with Taylor-Hood-H1 method and time step $\tau = 0.002$

level	k	ux $[10^{-3}]$	uy $[10^{-2}]$
0	3	-2.28±2.16	0.03±3.20
	4	-2.87±2.68	0.09±3.75
	5	-3.29±3.11	0.13±3.53

Table 9.8: FSI 3 with H(div)-conforming HDG velocity-momentum method and time step $\tau = 0.0005$

level	k	ux $[10^{-3}]$	uy $[10^{-2}]$
0	3	-1.95±1.83	0.13±3.02
	4	-3.30±3.15	0.12±3.78
	5	-3.10±2.94	0.14±3.63

Table 9.9: FSI 3 with Taylor-Hood-H1 method and time step $\tau = 0.0005$

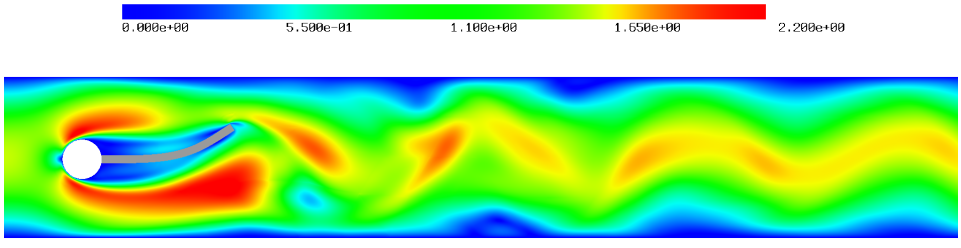

Figure 9.5: FSI 2 with H(div)-conforming HDG velocity-momentum method

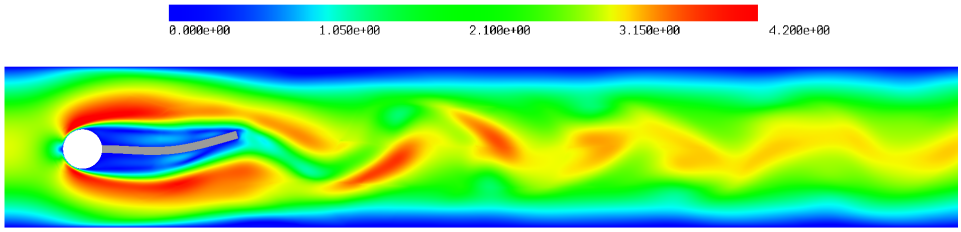

Figure 9.6: FSI 3 with H(div)-conforming HDG velocity-momentum method

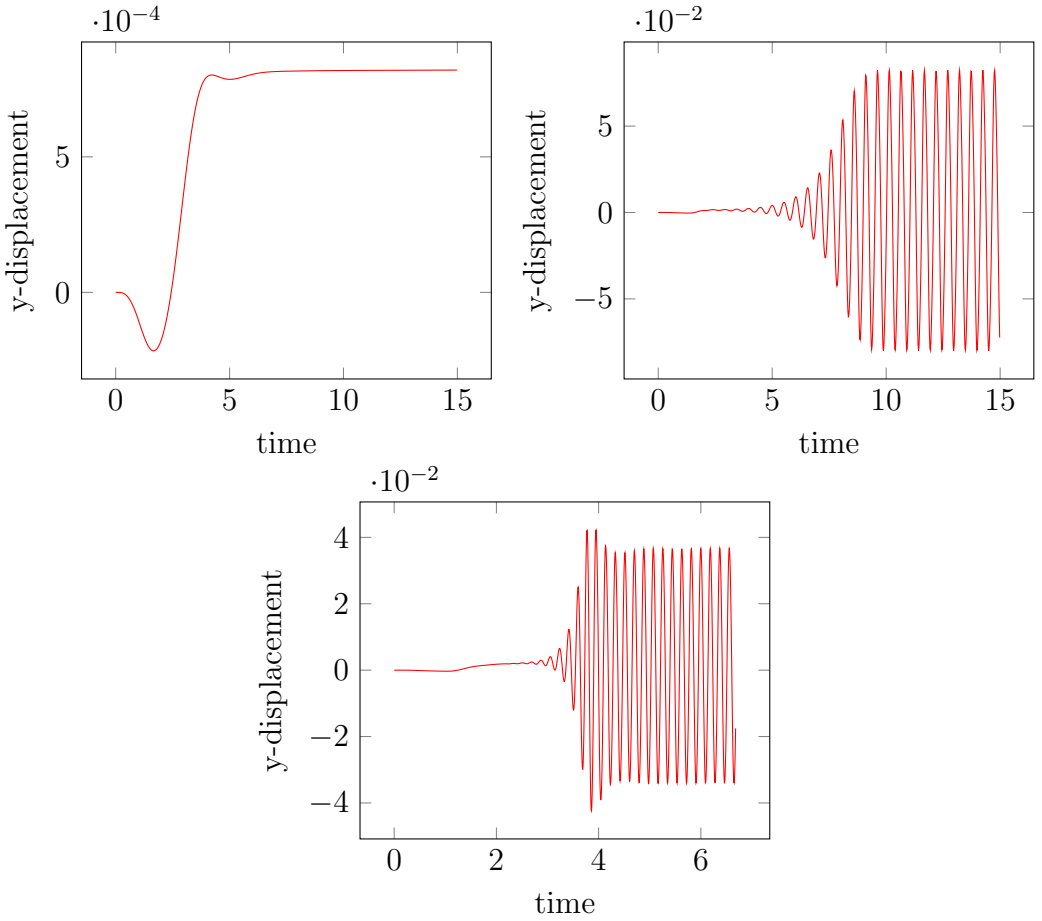

Figure 9.7: Y-displacement of control point A with H(div)-conforming HDG velocity-momentum method for FSI 1, 2 and 3

10 Conclusion

10.1 Summary

In this thesis we presented a new discretization method for the elastic wave equation, where the velocity is in H(curl) and the time derivative of the momentum, which lives in the topological dual space H(curl)*, was introduced. With this scheme the total energy is conserved in space.

Together with the H(div)-conforming HDG method for the Navier-Stokes equations, which ensures exact divergence-free and more robust solutions as for the Taylor-Hood elements, a new discretization scheme for fluid-structure interaction was introduced. This method combines the advantages of the discretizations on the fluid and solid part. Numerical experiments showed that the method works well and produces qualitatively very similar results as the standard method consisting of Taylor-Hood and H1-conforming elements for the Navier-Stokes equations and the elastic wave equation, respectively. For a quantitative comparison of the methods a higher spatial resolution is needed.

10.2 Future work

The presented spatial discretization for the elastic wave equation has very good properties in conserving the total energy, but the time discretization with the Crank-Nicolson scheme or the midpoint rule does not preserve the energy exactly. Thus, a new time discretization, motivated by the Discrete Gradient method and Poisson Systems (see [HLW13]), is needed to guarantee the conservation of the total energy also in time.

The system of equations arising in the fluid-structure interaction problem is now quite large. By using static condensation the size could be reduced, which needs more treatment. Another improvement in computational time would be to use appropriate preconditioners, which have to be developed.

IMEX schemes avoid solving a nonlinear system, which is much cheaper and well understood for the Navier-Stokes equations, but the time step is very restrictive. With more advanced spitting methods this problem can be overcome. Furthermore, the new discretization of the elastic wave equation must be adjusted in this setting.

List of Figures

List of Tables

References

[ARS97] Ascher, Uri M. ; Ruuth, Steven J. ; Spiteri, Raymond J.: Implicit-explicit Runge-Kutta methods for time-dependent partial differential equations. In: *Applied Numerical Mathematics* 25 (1997), Nr. 2, S. 151–167

[BDM85] Brezzi, Franco ; Douglas, Jim ; Marini, L. D.: Two families of mixed finite elements for second order elliptic problems. In: *Numerische Mathematik* 47 (1985), Nr. 2, S. 217–235

[Bra13] Braess, Dietrich: *Finite Elemente - Theorie, schnelle Löser und Anwendungen in der Elastizitätstheorie*. 5. Berlin Heidelberg New York : Springer-Verlag, 2013. – ISBN 978–3–642–34796–2

[Bra16] Braun, Stefan: *Strömungslehre für Technische Physiker*. Wien : Institut für Strömungsmechanik und Wärmeübertragung E322, 2016

[CCNP13] Cesmelioglu, Aycil ; Cockburn, Bernardo ; Nguyen, Ngoc C. ; Peraire, Jaume: Analysis of HDG Methods for Oseen Equations. In: *Journal of Scientific Computing* 55 (2013), Nr. 2, S. 392–431

[Cia94] Ciarlet, Philippe G.: *Mathematical Elasticity - Three-dimensional elasticity*. Reprint. Amsterdam : Elsevier, 1994. – ISBN 978–0–444–81776–1

[CKS05] Cockburn, Bernardo ; Kanschat, Guido ; Schötzau, Dominik: A locally conservative LDG method for the incompressible Navier-Stokes equations. In: *Mathematics of Computation* 74 (2005), S. 1067–1095

[CKS07] Cockburn, Bernardo ; Kanschat, Guido ; Schötzau, Dominik: A Note on Discontinuous Galerkin Divergence-free Solutions of the Navier–Stokes Equations. In: *Journal of Scientific Computing* 31 (2007), Nr. 1, S. 61–73

[CM13] Chorin, Alexandre J. ; Marsden, J.E.: *A Mathematical Introduction to Fluid Mechanics*. Berlin Heidelberg : Springer Science & Business Media, 2013. – ISBN 978–1–461–20883–9

[DB13] Deuflhard, Peter ; Bornemann, Folkmar: *Gewöhnliche Differentialgleichungen*. Berlin : Walter de Gruyter, 2013. – ISBN 978–3–11–031636–0

[DH03] Donea, Jean ; Huerta, Antonio: *Finite Element Methods for Flow Problems*. New. New York : John Wiley & Sons, 2003. – ISBN 978–0–471–49666–3

[DHPRF04] *Kapitel* 1.14. In: Donea, Jean ; Huerta, Antonio ; Ponthot, J.-Ph. ; Rodriguez-Ferran, A.: *Arbitrary Lagrangian-Eulerian Methods*. John Wiley & Sons, 2004

[HLW13] Hairer, Ernst ; Lubich, Christian ; Wanner, Gerhard: *Geometric Numerical Integration - Structure-Preserving Algorithms for Ordinary Differential Equations*. Berlin Heidelberg : Springer Science & Business Media, 2013. – ISBN 978–3–662–05018–7

[HT73] Hood, P. ; Taylor, C.: Numerical solution of the Navier-Stokes equations using the finite element technique. In: *Computer & Fluids* 1 (1973), S. 73–100

[HT06] Hron, Jaroslav ; Turek, Stefan: A Monolithic FEM/Multigrid Solver for an ALE Formulation of Fluid-Structure Interaction with Applications in Biomechanics. (2006), S. 146–170

[Led16] Lederer, Philip: *Pressure Robust Discretizations for Navier Stokes Equations: Divergence-free Reconstruction for Taylor-Hood Elements and High Order Hybrid Discontinuous Galerkin Methods*, Technische Universität Wien, Diplomarbeit, 2016

[Leh10] Lehrenfeld, Christoph: *Hybrid Discontinuous Galerkin methods for solving incompressible flow problems*, Rheinisch-Westfälischen Technischen Hochschule Aachen, Diplomarbeit, 2010

[LLMS17] Lederer, Philip L. ; Linke, Alexander ; Merdon, Christian ; Schöberl, Joachim: Divergence-free Reconstruction Operators for Pressure-Robust Stokes Discretizations with Continuous Pressure Finite Elements. In: *SIAM Journal on Numerical Analysis* 55 (2017), Nr. 3, S. 1291–1314

[LS16] Lehrenfeld, Christoph ; Schöberl, Joachim: High order exactly divergence-free Hybrid Discontinuous Galerkin Methods for unsteady incompressible flows. In: *Computer Methods in Applied Mechanics and Engineering* 307 (2016), S. 339 – 361

[MH12] Marsden, Jerrold E. ; Hughes, Thomas J. R.: *Mathematical Foundations of Elasticity*. Reprint. New York : Courier Corporation, 2012. – ISBN 978–0–486–14227–2

[MSW13] Mardal, Kent-Andre ; Schöberl, Joachim ; Winther, Ragnar: A uniformly stable Fortin operator for the Taylor-Hood element. In: *Numerische Mathematik* 123 (2013), Nr. 3, S. 537–551

[Néd80] Nédélec, J. C.: Mixed finite elements in R3. In: *Numerische Mathematik* 35 (1980), Nr. 3, S. 315–341

[Néd86] Nédélec, J. C.: A new family of mixed finite elements in R3. In: *Numerische Mathematik* 50 (1986), Nr. 1, S. 57–81

[New59] Newmark, Nathan M.: A Method of Computation for Structural Dynamics. In: *Journal of the Engineering Mechanics Division* 85 (1959), S. 67–94

[RT77] In: Raviart, P. A. ; Thomas, J. M.: *A mixed finite element method for 2-nd order elliptic problems*. Berlin, Heidelberg : Springer Berlin Heidelberg, 1977, S. 292–315

[Sch97] Schöberl, Joachim: NETGEN An advancing front 2D/3D-mesh generator based on abstract rules. In: *Computing and Visualization in Science* 1 (1997), Nr. 1, S. 41–52

[Sch09a] Schöberl, Joachim: *Numerical Methods for Maxwell Equations*. 2009 `http://www.asc.tuwien.ac.at/ schoeberl/wiki/lva/notes/maxwell.pdf`

[Sch09b] Schöberl, Joachim: *Numerical Methods for Partial Differential Equations*. 2009 `http://www.asc.tuwien.ac.at/ schoeberl/wiki/lva/notes/numpde.pdf`

[Sch14] Schöberl, Joachim: C++11 Implementation of Finite Elements in NGSolve. In: *Institute for Analysis and Scientic Computing, Vienna University of Technology* (2014)

[STD+96] Schäfer, M. ; Turek, S. ; Durst, F. ; Krause, E. ; Rannacher, R.: Benchmark Computations of Laminar Flow Around a Cylinder. (1996), S. 547–566

[SZ05] Schöberl, Joachim ; Zaglmayr, Sabine: High Order Nédélec Elements with local complete sequence properties. In: *Int. J for Computation and Maths in Electrical and Electronic Eng COMPEL*, 2005, S. 374–384

[Tal94] Tallec, Patrick L.: Numerical methods for nonlinear three-dimensional elasticity. In: *Handbook of Numerical Analysis* 3 (1994), S. 465 – 622. – ISSN 1570–8659

[TH06] Turek, Stefan ; Hron, Jaroslav: Proposal for Numerical Benchmarking of Fluid-Structure Interaction between an Elastic Object and Laminar Incompressible Flow. (2006), S. 371–385

[THM+10] In: Turek, S. ; Hron, J. ; Mádlík, M. ; Razzaq, M. ; Wobker, H. ; Acker, J. F.: *Numerical Simulation and Benchmarking of a Monolithic Multigrid Solver for Fluid-Structure Interaction Problems with Application to Hemodynamics*. Berlin, Heidelberg : Springer Berlin Heidelberg, 2010, S. 193–220

[Wic11] Wick, Thomas: Fluid-structure Interactions Using Different Mesh Motion Techniques. In: *Comput. Struct.* 89 (2011), Nr. 13-14, S. 1456–1467

[Wic13] Wick, Thomas: Solving Monolithic Fluid-Structure Interaction Problems in Arbitrary Lagrangian Eulerian Coordinates with the deal.II Library. 1 (2013)

[Wri13] Wriggers, Peter: *Nichtlineare Finite-Element-Methoden*. Berlin Heidelberg New York : Springer-Verlag, 2013. – ISBN 978–3–642–56865–7

[Zag06] Zaglmayr, Sabine: *High Order Finite Element Methods for Electromagnetic Field Computation*, Johannes Kepler Universität Linz, Diss., 2006